INVESTIGATION OF MHD HYBRID NANOFLUID FLOW OVER AN INCLINED SURFACE IN A POROUS MEDIUM

By

Zarka Razzaq

DEPARTMENT OF MATHEMATICS

NATIONAL UNIVERSITY OF MODERN LANGUAGES

ISLAMABAD

July, 2025

Investigation of MHD Hybrid Nanofluid Flow over an Inclined Surface in a Porous Medium

By

Zarka Razzaq

Supervised By

Dr. Anum Naseem

MS Mathematics, National University of Modern Languages, Islamabad, 2025

A THESIS SUBMITTED IN PARTIAL FULFILMENT OF
THE REQUIREMENTS FOR THE DEGREE OF

MASTER OF SCIENCE

Mathematics

To

DEPARTMENT OF MATHEMATICS

FACULTY OF ENGINEERING & COMPUTING

NATIONAL UNIVERSITY OF MODERN LANGUAGES ISLAMABAD

THESIS AND DEFENSE APPROVAL FORM

The undersigned certify that they have read the following thesis, examined the defense, are satisfied with overall exam performance, and recommend the thesis to the Faculty of Engineering and Computing for acceptance.

Thesis Title: Investigation of MHD Hybrid Nanofluid Flow over an Inclined Surface in a Porous Medium

Submitted By: Zarka Razzaq **Registration #:** 80 MS/Math/S23

Master of Science in Mathematics (MS Math)
Title of the Degree

Mathematics
Name of Discipline

Dr. Anum Naseem _____
Name of Research Supervisor Signature of Research Supervisor

Dr. Sadia Riaz _____
Name of HOD (Math) Signature of HOD (Math)

Dr. Noman Malik _____
Name of Dean (FEC) Signature of Dean (FEC)

July 7, 2025

AUTHOR'S DECLARATION

I Zarka Razzaq

Daughter of Razzaq Hussain

Registration # 80 MS/Math/S23

Discipline Mathematics

Candidate of **Master of Science in Mathematics (MS Math)** at the National University of Modern Languages do hereby declare that the thesis **Investigation of MHD Hybrid Nanofluid Flow over an Inclined Surface in a Porous Medium** submitted by me in partial fulfillment of MS Mathematics degree, is my original work, and has not been submitted or published earlier. I also solemnly declare that it shall not, in future, be submitted by me for obtaining any other degree from this or any other university or institution. I also understand that if evidence of plagiarism is found in my thesis/dissertation at any stage, even after the award of a degree, the work may be cancelled and the degree revoked.

Signature of Candidate

Zarka Razzaq

Name of Candidate

July 7, 2025

Date

ABSTRACT

Title: Investigation of MHD Hybrid Nanofluid Flow over an Inclined Surface in a Porous Medium

This study analyzes the hybrid nanofluid flow, which is a mixture of copper (*Cu*) and aluminum oxide (Al_2O_3) nanoparticles suspended in water (H_2O). The hybrid nanofluids are crucial for optimizing thermal management systems, such as heat exchangers, cooling devices, car engines, and electronics, where efficient heat transfer is a dominant feature. The considered fluid flows over an inclined surface within a porous medium. The impact of several physical phenomena on the heat transfer and flow characteristics of this nanofluid is examined. The fluid model involves mixed convection, where both forced and natural convection contribute to the heat transfer process. It also investigates the effects of magnetohydrodynamics, thermal radiation, Joule heating and non-uniform heat source/sink on the considered flow. To model this complex system, a set of partial differential equations (PDEs) is formulated. These PDEs are typically challenging to solve directly due to their complexity, so the similarity transformations are employed. These similarity transformations simplify the PDEs by reducing them to a set of ordinary differential equations (ODEs), making the problem more manageable and solvable. To solve the reduced system of ODEs, a MATLAB's bvp4c function, is utilized to handle the boundary value problem. This function helps in obtaining numerical solutions for the velocity and temperature profiles of the fluid under the specified conditions. The results from this numerical analysis provide insights into the velocity distribution, temperature profile, skin friction coefficient, which quantifies the drag force exerted by the fluid on the surface, and the Nusselt number, which is a dimensionless measure of the convective heat transfer rate, The velocity profile experiences an upsurge for the rise in stretching parameter and inclination angle. The temperature of the hybrid nanofluid is improved by the Biot number, heat source/sink parameters and Eckert number.

TABLE OF CONTENTS

LIST OF TABLES

LIST OF FIGURES

LIST OF ABBREVIATIONS

Acronyms

MHD	Magnetohydrodynamics
EMHD	Electromagnetohydrodynamics
PDEs	Partial differential equations
ODEs	Ordinary differential equations
Cu	Copper
Al_2O_3	Alumina/Aluminum oxide
MATLAB	Matrix Laboratory
Bvp4c	Boundary Value Problem for 4th Order Colocation
Nu_x	Local Nusselt Number
C_f	Skin Friction Coefficient
H_2O	Water

LIST OF SYMBOLS

x, y	Cartesian coordinates
u, v	Velocity components
T	Temperature
T_w	Temperature of the wall
T_∞	Ambient temperature of the hybrid nanofluid
θ_w	Ratio of temperature
ϕ_1	Concentration 1st nano-particle
ϕ_2	Concentration 2nd nano-particle
α	Inclination Angle
σ	Electrical conductivity
σ_{nf}	Electrical conductivity of nanofluid
σ_{hnf}	Electrical conductivity of hybrid nanofluid
ν	Kinematic viscosity
k	Thermal Conductivity
k_{nf}	Thermal Conductivity nanofluid
k_{hnf}	Thermal Conductivity hybrid nanofluid
C_p	Fluid heat capacity
$(C_p)_{nf}$	Specific heat capacity of nanofluid
$(C_p)_{hnf}$	Specific heat capacity of hybrid nanofluid
ρ	Density
ρ_{nf}	Density of nanofluid
ρ_{hnf}	Density of hybrid nanofluid
μ	Dynamic Viscosity

μ_{nf}	Dynamic viscosity nanofluid
μ_{hnf}	Dynamic viscosity hybrid nanofluid
β_T	Thermal expansion
$(\beta_T)_{nf}$	Thermal expansion of nanofluid
$(\beta_T)_{hnf}$	Thermal expansion hybrid nanofluid
Pr	Prandtl number
Re_x	Reynolds number
Ec	Eckert number
Nu_x	Nusselt number
Gr	Grashof number
q_r	Radiative heat flux
K	Porosity parameter
R	Thermal radiation
M	Magnetic field parameter
q'''	Nonuniform Heat generation/absorption parameter
λ	Mixed convection parameter
ϵ	Stretching and shrinking parameter
ζ_1	Space Dependent Heat source and sink
ζ_2	Temperature Dependent Heat source and sink

ACKNOWLEDGMENT

I am thankful to Almighty ALLAH who has enabled me to learn and to achieve milestones towards my destination and His beloved Prophet Hazrat Muhammad (PBUH) who is forever a constant source of guidance, a source of knowledge and blessing for the entire creation. His teaching shows us a way to live with dignity, stand with honor and learn to be humble.

My acknowledgment is to my kind, diligent and highly zealous supervisor, Dr. Anum Naseem who supported me with her valued opinions and inspirational discussions. Her expertise, suggestions, comments and instructions greatly improved the worth of this research work. I am placing my earnest thanks to Dr. Anum Naseem. I am so grateful to work under the supervision of such a great person. My gratitude is to my honorable supervisor who took me to the apex of my academia with their guidance. In particular, Dr. Anum Naseem has always been supportive during all of my course work and kept encouraging me throughout the session at the National University of Modern Languages.

My strong gratitude is to my parents and my adored siblings who have been always real pillars for my encouragement and showered their everlasting love, care and support throughout my life. Humble prayers, continuing support and encouragement from my family are always highly appreciated.

Consequently, my plea is to Allah, the Almighty, the beneficial to keep showering His blessings upon me and strengthen my wisdom and knowledge

DEDICATION

I dedicate this thesis to my parents and teachers, who have been my greatest source of inspiration and support throughout my life. Their unwavering encouragement, love and sacrifices have made this journey possible

CHAPTER 1

Introduction and Literature Review

1.1 Hybrid Nanofluid

The idea of manufacturing nanofluids by mixing nanoparticles with a base fluid was perceived by Choi [1]. The term "nano" has Latin roots and denotes a scale of 10^{-9} meters. The thermal conduction attributes of nanofluids are dependent on the form, and concentration of the nanoparticles and size as well as the aspects of the conventional fluid. The basefluid includes water, oils and lubricants, polymeric solutions, bio-fluids, organic liquids (such ethylene, tri-ethylene glycols, refrigerants, etc.), and other common liquids. The materials used to create the nanoparticles include chemically inert metals, oxide compounds (like alumina), oxide refractory materials (like *CuO*), metal carbides (like *SiC*), metallic nitrides (like *AIN*) and carbon in different forms (like fullerene) [2]. Electronics, solar energy, automotive industry, medical applications, food industry, machining processes, and building heating/cooling systems, nuclear reactors and pool boiling are a few commercial applications for nanofluids. When compared to conventional fluids, they show better thermal characteristics [3].

Hybrids are the most developed kind of nanofluids and are created by combining two distinct kinds of nanoparticles in a basefluid. The goal of this combination is to get better thermal properties and performance than single-nanoparticle fluids. Since hybrid nanofluids have good thermal properties, they improve heat transfer efficiency in thermal energy storage systems and heat pipes, heat exchangers, boiling processes and cooling applications.

Additionally, they function well in solar thermal and refrigerated systems, all of which contribute to lower energy consumption and higher cooling efficiency. All things considered, hybrid nanofluids are effective and practical for managing heat efficiency in many different sectors of the economy [4].Yang *et al*. [5] addressed the study on thermal convective coefficient of several nanoparticles in a tube- shaped flat heat exchanger with laminar conditions of flow. The heat transfer coefficient in laminar flow is increased by adding nanoparticles, based to the experimental data. Suresh *et al.* [6] examined the pressure drop and fully developed laminar flow and transfer of heat (convective) in a circular tube with water and Al_2O_3 hybrid nanofluid. The results of the study further showed that 0.1% friction aspects of Al_2O_3–Cu/water composite nanofluids is significantly larger than that of 0.1% Al_2O_3/H_20 nanofluid. Sarkar *et al*. [7] considered the characteristics of pressure loss, heat transfer, thermodynamic parameters, formulation, and difficulties associated with hybrid nanofluids. Results indicated that such nanofluids contain great ability to enhance heat transfer if the hybridization process is successful. Shoaib *et al*. [8] employed Lobatto IIIA method's computational method to look into the heat transfer in a hybrid nanofluid (Al_2O_3–Ag/H_20) flowing over a linearly stretched surface with the impact of radiation. Hussain *et al*. [9] analyzed the thermodynamic traits of magnetohydrodynamic and also mixed flow of nanofluid with thermal radiation. MATLAB software was implemented to solve the complicated differential equation system by employing the Bvp4c strategy. Basavarajappa *et al*. [10] looked into the problem of impulsive movement for nonlinear convective flow of nanoparticle based fluid across a plate. They availed central response surface method (RSM) and central composite design (CCD) for the simultaneous optimization of the thermal heat flux rate and drag coefficient. It was found that the flow fields are significantly affected by the density's quadratic fluctuation with temperature. Sneha *et al.* [11] analyzed the effect of an inclined MHD for hybrid nanofluid ($Cu–Al_2O_3/ H_20$) fluid flow as a result of stretching/shrinking sheet using and a mixed convection and thermal radiation effects. Mahesh [12] studied the impact of thermal radiation on hybrid nanofluid ($TiO_2–Ag/H_2O$) across a porous sheet with MHD. Hussein *et al*. [13] addressed the impacts of combining photovoltaic energy systems with hybrid nanofluids for water productivity. The important elements including system design, and concentration were also examined.Mahmood *et al*. [14] work examined thermal radiation and magnetohydrodynamic (MHD) influence on hybrid nanofluid flowing through a vertically stretching permeable surface near stagnation point. The understanding of these factors in relation to the stretching surface dynamics was the aim of the study. The effects of magnetohydrodynamic (MHD) on the hybrid nanofluid over a stretched sheet that was permeable was examined by Mahmood *et al.* [15]. Using Mathematica,

numerical solutions were derived for the coupled system with the help of Runge-Kutta (RK-IV) approach. Mahmood *et al*. [16] considered hybrid nanofluid (Al_2O_3–Cu/water) and its flow on a moving surface. The study also looked at how thermal and velocity slip conditions affect the flow phenomenon. Ali *et al.* [17] assessed the magnetohydrodynamic laminar fluid motion of Casson hybrid nanofluid (*Ag–Au*/blood) over an oscillating surface by combining thermal radiation effect with porous medium. It was illustrated the advantages of hybrid nanofluid which contained several nanoparticles in a conventional fluid have improved thermal conductivity and heat transfer as compared to single nanoparticle suspensions. Khalil *et al.* [18] considered temperature dependent viscosity and thermal conductivity while examining the flow and thermal conduction of a hybrid nanofluid across a linearly stretching surface. The investigation also revealed that the complex relationships such as the dynamics of porous media, slip boundary effects, variation in viscosity, and magnetohydrodynamic effects and their influence on the flow. The magnetohydrodynamic, 2D, unsteady flow of a hybrid nanofluid (Al_2O_3–Cu/water) inside a Darcy-Forchheimer media was looked at by Lund *et al.* [19]. The numerical study by Abd-Elmonem *et al.* [20] looked at how different governing parameters influence the hybrid nanofluid's (Al_2O_3–Cu/H_20) flow through a Darcy porous media. Molla, *et al.* [21] work on non-Newtonian hybrid nanofluids (Al_2O_3–$Cu/C_2H_6O_2$) in a two dimensional cavity with a thermal flate plate at its core. Raza *et al*. [22] explored the dispersion of various nanoparticles in liquid bases such as water (H_2O) including molybdenum disulfide (MoS_2) and graphene oxide (*GO*). The framework also incorporated permeability and the impact of magnetic field to provide a comprehensive evaluation.

1.2 Magnetohydrodynamics (MHD)

Magnetohydrodynamics or MHD for short is the analysis of electrically conductive fluids in the presence of magnetic field. These fluids include electrolytes, salt water, liquid metals, and plasmas. Magnetohydrodynamics was first established for electrically conducting fluids in a 1942 and studied by Hannes Alfvén as mentioned in "Existence of Electromagnetic–Hydrodynamic Waves" [23]. The fundamental idea of MHD is that conductive fluids in motion may generate electric current through magnetic fields, which can change the magnetic field and exert forces on the fluid. The electromagnetic equations and the Navier-Stokes equations for fluid dynamics make up the set of equations that define MHD. Applications of

magnetohydrodynamics (MHD) may be found in several technical domains. Among the notable uses of magnetohydrodynamic (MHD) are boundary layer control, controlled thermonuclear reactors, metallic plate cooling, oil recovery techniques, crystal growth, magnetic devices for cell separation, geothermal energy extraction, MHD generators, magnetic endoscopy, and controlling blood circulation during surgery. Many scholars have studied magnetohydrodynamics (MHD) in connection with the previously listed applications in different fluid mechanics problems. Magnetohydrodynamics (MHD) has been studied in many different contexts by researchers because of its numerous applicability in fluid mechanics problems [24]. The engineering applications such as liquid metal cooling systems in nuclear reactors and astronomy, helps to explain that solar flares and stellar winds, both depend on MHD. Jang *et al*. [25] presented a novel micropump that operated on the principles of magnetohydrodynamics (MHD). Wu [26] studied the generalized MHD (GMHD) equations. In particular, he investigated the evaluations of various parameters on the regularity of solutions. Raptis and Perdikis [27] looked at a consequence of a chemical reaction on the fluid flow across a semi-infinite stretched sheet. The sheet was stretched non-linearly (quadratically) in the vicinity of an orthogonal field of magnetism. The implications of varying heat conductivity and viscosity on hydromagnetic flow and heat transfer due to a non-linearly stretching surface were looked at by Prasad *et al*. [28]. In the subsistence of a magnetic field, Hamad [29] assessed the heat transfer as well as convective flow of a viscous nano particle fluid via partially-infinite upright stretched surface. Jalilpour *et al.* [30] studied the stagnation point, MHD of a nanofluid flow through heated permeable surface. Thermophoresis accompanied with Brownian motion effects were also included in the governing equations. The coupled partial differential equations were non-dimensionalized and analytically which applied the Padé technique. Hayat *et al.* [31] looked at how a field of magnetism influenced the peristaltic flow of a constant density fluid called Williamson in an inclined medium. Convective conditions for mass and heat transmission were also applied. Abbas *et al*. [32] discussed the hybrid nanofluid (*Ni-Ag/H_20*) flow at the stagnation point over a non-uniform cylinder and the magnetic field was also applied. A mathematical model of hybrid nanofluid flow was generated under certain flow assumptions. The effects of Joule heating and dissipative viscous were also taken into account. Dadheech *et al*. [33] examined a comparative analysis of linear viscosity fluids and non-linear viscosity fluids. Using non-uniform heat source along with heat sink, thermal radiation, heat transfer analysis was performed. Furthermore, a magnetic field was applied and the surface was assumed to be porous. Soomro [34] discussed a hybrid nanofluid (*Al_2O_3-Cu/H_20)* flow past an inclined surface and studied the effects of magnetohydrodynamics on the flow. A permeable

stretched sheet was considered by Khazayinejad [35] and the flow was assumed under the effect of the magnetohydrodynamics which was applied perpendicular to the flow. The influence of magnetohydrodynamics on the hybrid nanofluid flow (Al_2O_3-Cu/H_20) via stretched/shrinked sheet was looked into by Sneha *et al.* [36]. The investigation of hybrid nanofluid (Ag-CuO/H_20) flow above a nonlinear stretching surface was done by Algehyne [37]. The Brownian motion and thermophoresis variables was applied in the fluid problem. Using the effect of magnetohydrodynamics, Yasin *et al.* [38] exhibited the flow pattern at various inclination angles. This study employed blood as a medium of transport in a symmetric channel in order to study the hybrid nanofluid and its peristaltic flow with (Cu) and (Ag) nanoparticles. Galal *et al.* [39] had the main target to examine the impact of magnetohydrodynamics on the rate of heat as well as mass transfer for three-dimensional nanoliquid flow between two stretchable surfaces in the presence of chemical reaction and thermal radiation. Kirusakthika [40] investigated heat flux of a hybrid nanofluid (Fe_3O_4-$Al_2O_3/C_2H_6O_2$–H_2O) based on a 50:50 mixture, for a laminar, MHD, natural-convective boundary layer flow across an angled needle. Along with the influence of an applied Lorentz force, the inquiry also examined the implications of nonunifrom viscous dissipation and thermal radiation. Jeelani *et al.* [41] analyzed mass with also heat transfer for hybrid nanofluid flowing past an angled linearly stretched sheet using the Maxwell fluid model. The sheet was embedded in a porous medium, and it was linearly stretched to create a fluid flow. The results clearly showed that the hybrid nanofluid's thermal performance was improved by increasing the volume percentage of nanoparticles. Mahabaleshwar *et al.* [42] investigated how thermal radiation and MHD affected the biviscous Bingham hybrid nanofluid(GO $MoS_2/C_2H_6O_2$) and its flow over a permeable stretched surface. The results of the experiment show that skin friction was increased when the magnetic field was increased. Yadav *et al.* [43] considered the slip boundary condition for analyzing the thermally radiative, magnetohydrodynamic, mixed convection hybrid nanofluid flow across an inclined shrinking permeable plate.

1.3 Thermal Radiation

Thermal radiation is the term for electromagnetic waves that are released by an object as its temperature rises above absolute zero. These waves are mostly in the infrared spectrum. This radiation arises from the thermal motion of particles and is best described by the concept of blackbody radiation, which holds that a perfect blackbody absorbs all incident radiation and

emits energy in line with its temperature as indicated by Planck's equation [44]. In several areas, including heat transport, energy efficiency, and the greenhouse impact, thermal radiation is significant. The sun's warming beams and the radiation from it are two instances of thermal radiation in operation. Mohammadein *et al.* [45] observed that how the mixed convective, non-Newtonian fluid flow over a flat, horizontal plate placed in a porous medium was affected by thermal radiation. The non-Newtonian fluid dynamics was characterized by the Ostwald-de Waele model. Basu *et al*. [46] covered the fundamentals of thermal radiation and described the most recent advancements in the area. The thermal radiation application in near-field thermophotovoltaic systems was also discussed. Haile *et al.* [47] considered the boundary-layer nanofluid flow with the effect of thermal radiation, chemical reaction and viscous dissipation over a moving surface. The influence of a continuous, incompressible water-based MHD nanoparticle fluid flow through two stretchy or shrinkable walls with heat radiation from a source or outlet was studied by Dogonchi *et al.* [48]. Hakeem *et al.* [49] discussed impact of a thermal radiation on a multiple-dimensional, magnetohydrodynamic flow with a slip boundary condition of order 2 over a sheet using both analytical and numerical approaches. Hayat *et al.* [50] investigated a 3D model with the influence of chemical reactions and thermal radiation, for a flow over a linearly stretched surface when rotation was included Daniel *et al.* [51] looked into the non-uniform combination of convection movement of an electrical carrying nanofluid and heat transfer triggered by a permeable linear stretched surface together with thermal radiation. Using the mutual factors of MHD, and chemical reaction, the analysis was done. Iqbal *et al*. [52] looked at the effect of Hall currents on hybrid nanofluid (Cu-CuO/H_2O) flow in a circulating channel, with the effect of thermal radiation. After completing the required analysis and simplification, closed form solutions were found. Shoaib *et al.* [53] presented the numerical modelling of a hybrid nanofluid (Al_2O_3-Ag/H_2O) magnetohydrodynamic flow above a stretchable sheet in three dimensions with the aspects of the effects of thermal radiation. The objective of Yashkun *et al.* [54] research was to examine the thermal properties of a hybrid nanofluid flowing across a linearly stretchy and shrinkable surface while factoring in the influence of thermal radiation and magnetohydrodynamics. Basir *et al.* [55] done analysis on the two possible mixtures for the flow in stagnation point in a hybrid nanofluid (Co-$CeO_2/C_{12}H_{26}$-$C_{15}H_{32}$) which included melting heat transfer. It was demonstrated that because of thermal radiation and melting heat transfer, the drag force and rate of heat transfer were frequently much greater in hybrid nanofluids. Waini *et al.* [56] examined hybrid nanofluid steady flow and thermal conduction characteristics that was nonlinearly stretching and shrinking while accounting for suction, thermal radiation, and magnetohydrodynamics (MHD).

Waqas *et al*. [57] explored hybrid nanofluid (Al_2O_3-$CU/C_{22}H_6O$) flow on a stretching surface with heat source interacting with heat sink, in addition to thermal radiation effects. The findings were intended to improve engineering system efficiency and further the understanding of thermal management. The conduct of thermal radiation on the 3D flow characteristics of magnetized and rotating hybrid nanofluid (Al_2O_3-CU/H_2O) was examined by Asghar *et al*. [58] through the application of numerical methods. The understanding influences of thermal radiation and procedures of heat transfer on fluid dynamics was the aim of this research. Utilizing hybrid nanofluids, Khan *et al.* [59] studied the 2D magnetohydrodynamic flow inside the boundary layer in a surface that had pores, over a stretchable sheet. It was found out that how both mass and heat transfer was influenced by thermal radiation and varied slip conditions. The findings demonstrated that these factors changed flow dynamics and enhanced heat transfer, offering useful information for engineers. In order to analyze, entropy generation for a hybrid nanofluid *(*Gu-Fe_3O_4/H_2O*)* flow, Naqvi *et al*. [60] looked at a mathematical framework for magnetohydrodynamic flow across stretching and shrinking surfaces. The flow dynamics were affected by thermal radiation (nonlinear) and MHD. The behavior displayed by a hybrid nanofluid through a stretched surface that was influenced by thermal radiation and magnetohydrodynamic (MHD) was investigated by Asghar [61].

1.4 Joule Heating

The mechanism that produces heat when electric current passes across a conducting substance is described as the process of Joule heating. Ohmic heating is another term used in place of Joule heating. The power produced when an electrical conductor is heated is equal to the product of the resistance and the square of the current, according to Joule's first law. The phenomena of Joule heating may be used to build a variety of useful gadgets, such as electric fuses, electronic cigarettes, electric stoves, and cartridge warmers that employ Joule heating to vaporise vegetable glycerin and propylene glycol. Resistance thermometers and thermistors are also the uses of it. [62]. Xuan *et al*. [63] developed a computational model that takes temperature-dependent material properties and thermal boundary effects into account. The study was performed in the existence of ohmic heating. Tang *et al*. [64] made the use of numerical simulations to look into the combined impacts of Joule heating and temperature dependent features on electro-osmotic flow. Kates [65] introduced two numerical models to study heat transfer in diverging microchannels containing both stationary and flowing liquids.

The heat exchange using a magnetohydrodynamic nanofluid flow in a semiporous curved channel was studied by Sajid *et al.* [66]. The energy equation took into account the Joule heating effects. The conduct of an instigated magnetic field on the stagnation hybrid nanofluid flow (TiO_2-Cu/H_2O) via stretched sheet was examined by Ghadikolaei *et al*. [67]. Their research focused at the ways in which magnetic fields impact thermal behavior with flow characteristics of nanofluids. Xia *et al*. [68] presented a 3D flow of a viscous hybrid (Cu-$Ag/C_2H_6O_2$) nanofluid and its flow with Joule heating. The fluid was flowing between two parallel surfaces, the bottom surface was stretching linearly. Mahanthesh *et al*. [69] researched influence of Joule heating on the movement and thermal conduction for magneto-composite nanofluid through an isothermal wedge. It centered on a Newtonian composite nanomaterial with an exponential heat source, assuming an incompressible and electrically conducting fluid Khashi'ie *et al.* [70] attempted to explore the characteristics of a (Cu-Al_2O_3/H_2O) fluid for an axially stretching/shrinking surface with the simultaneous influence of MHD combined with Joule heating. Observing duality of solutions and examining the hybrid nanofluid, properties of flow and heat transfer of (Cu-Al_2O_3/H_2O) flowing through a narrowing cylinder with the impact of Ohmic heating was the goal of Khashi'ie *et al*. [71] work. Yashkun *et al*. [72] looked into flow and heat transfer of a hybrid nanofluid (Cu-Al_2O_3/H_2O) using a stretching/shrinking sheet with mixed convection and Joule heating. A computational investigation took place for the flow of a two-dimensional hybrid nanofluid (Cu-Al_2O_3/H_2O) across the sheet. The main goal of Teh *et al*. [73] study was to find out how the electromagnetic field and Joule heating altered the temperature and velocity characteristics of the hybrid nanofluid (Cu-Al_2O_3/H_2O). The magentohydrodynamic, hybrid nanofluid (Cu-Al_2O_3/H_2O) from the surface under the influence of Ohmic heating was objective of Khashi'ie *et al*. [74] work. Ramesh *et al.* [75] examined the mixed convection nanofluid flow through narrow channels (HNF-MC) employing the numerical determining system MATHEMATICA. The velocity slip, magnetohydrodynamics, and viscous dissipation effects were all taken into account. The heat transfer characteristics of a magnetized Casson hybrid nanofluid (Al_2O_3–$Cu/NaCl$) through porous surface were looked into by Lund et *al*. [76]. The effects of Joule heating with electromagnetic radiation were examined in the study. Investigating the mixed convective and magnetohydrodynamic (MHD) flow over a stretching surface with infrared effects using non-similar modelling of a hybrid nanofluid was the objective of Razzaq *et al*. [77] work. The effects of exposure to Joule heating, viscous dissipation and radiation on thermodynamic equation supported the flow in the investigation. In Mishra *et al*. [78] research, the flow of a hybrid nanofluid ($Ti02$–Fe_2O_3/H_2O) along effects of Joule heating, suction/injection and magnetohydrodynamics was examined. Gul *et al*. [79]

examined an annular flow of hybrid nanofluid(Al_2O_3–Ag/H_2O) flowing between two discs that was both electricity conducting and magnetically driven. The research took into account the mixed convection, and ohmic heating effects. The fluid flow of a hybrid nanofluid (Al_2O_3–Ag/H_2O) flowing over a linearly stretched cylinder immersed in a liquid were observed by Nabwey *et al*. [80] using magnetohydrodynamcis and Joule heating.

1.5 Contributions to the Thesis

In this thesis, the review work of Wahid *et al*. [85] is referenced and the flow analysis is expanded to investigate the impact of non-uniform heat source and heat sink on hybrid nanofluid flow under certain boundary conditions. This numerical study's goal is to examine magnetohydrodynamic hybrid nanofluid flow above a linearly extending surface while taking Joule heating into account. A set of ordinary differential equations (ODEs) is created which are derived through the nonlinear partial differential equations (PDEs) by using similarity transformations. MATLAB software is used to formulate the tables and graphs that display numerical findings. The conduct of dimensionless factors for $f'(\eta)$, $\theta(\eta)$, Nu_x, and C_f are explored in depth, and graphs and tables display the results with clarity.

1.6 Thesis Organization

The thesis is segmented into six chapters.

Chapter 1 comprises an introduction to numerous concepts and an in-depth literature assessment based on the current study.

Chapter 2 summarizes the fundamental words and ideas employed in the study. This chapter provides the crucial laws that are to be used to assess upcoming chapters.

Chapter 3 investigates the two-dimensional flow brought about an inclined shrinking sheet using a hybrid nanofluid. The mechanisms of fluid flow and heat transfer are affected due to the existence of magnetohydrodynamics. MATLAB's bvp4c method is used to solve the system

of ordinary differential equations (ODEs) that originate as a result of performing similarity transformations on the governing equations.

Chapter 4 analyses the hybrid nanofluid and the flow across linearly stretching sheet in a medium of porosity. Among the factors considered in this work are thermal radiation, mixed convection, Joule heating, non-uniform heat generation/heat absorption. The system is solved with the help of the bvp4c approach once the governing equations have been shifted to ordinary differential equations (ODEs).

Chapter 5 reveals outcomes from the study on the hybrid nanofluid flow problem. Some prospective future research endeavors are also included.

Chapter 2

Basic Concepts and Definitions

2.1 Fluid

A fluid [81], show some defiance to the applied force of shearing when subjected to an external force, but eventually continue to flow and deform. Stated differently, fluids cannot withstand shear loads.

2.2 Fluid Mechanics

An area of applied mechanics that examines the behaviors and properties of fluids [81]. There are two main subfields within fluid mechanics.

2.2.1 Fluid Static

Fluid statics [81] is a discipline of fluid mechanics focusing on the characteristics of fluids at rest.

2.2.2 Fluid Dynamics

A fluid that flows and exhibits variations in pressure, velocity, and other features while flowing is often referred to the field of fluid dynamics [81]. In other words, this branch of fluid mechanics deals with the flowing fluid along with the forces that the fluid experiences.

2.3 Stress

It is the mean force exerted by various elements on an object's surface. Typically, stress is defined according to of its intensity and trajectory.

$$\text{Stress} = \frac{Force(F)}{Area(A)}. \tag{2.1}$$

Its dimensions are $\left[\frac{M}{LT^2}\right]$and the SI units for stress are Nm^{-2} or kg/ms^{-2}.

It consists of two components.

2.3.1 Shear Stress

One kind of stress that originates when a force exerted throughout the sectional area of an element is shear stress [81].

2.3.2 Normal Stress

The particular kind of stress that results from an applied force acting orthogonal to the sectional area of a material is known as normal stress [81].

2.4 Viscosity

Shear deformation of fluids is referred to as viscosity [81], a physical property of fluids that may be defined in two ways.

2.4.1 Dynamic Viscosity

Dynamic viscosity [82], frequently referred to as absolute viscosity (μ), is a property that illustrates the relation between tangential stress and the fluid's internal velocity change rate. Mathematically,

$$\text{Viscosity } (\mu) = \frac{\text{Tangential stress}}{Velocity\ gradient}. \tag{2.2}$$

It has the dimensions $\left[\frac{M}{LT}\right]$ with the SI units of Ns/m^2 or kg/m.s .

2.4.2 Kinematic Viscosity

The dynamic viscosity quotient by its density of the fluid is known as kinematic viscosity [82].

$$\nu = \frac{dynamic\ viscosity}{density} = \frac{\mu}{\rho}, \tag{2.3}$$

where the fluid's density is indicated by ρ, the viscosity with μ , and the kinematic viscosity through ν. The SI unit of kinematic viscosity is m^2/s with dimensions $\left[\frac{L^2}{T}\right]$.

2.5 Newton's Law of Viscosity

Newton's law of viscosity [82] demonstrates that the tangential stress within contiguous layers of fluid is directly related to the rate of change in velocity (shear rate) with respect to those layers.

Mathematically, it can expressed as

$$\tau_{yx} \propto \frac{du}{dy'}, \tag{2.4}$$

$$\tau_{yx} = k\frac{du}{dy'}, \tag{2.5}$$

where (*du/dy*) signifies the rate at which the fluid aspect is subjected to shear stress, which is indicated by τ_{yx}.

2.6 Newtonian Fluids

Newton's viscosity law, which asserts that shear stress and shear rate have a linear relationship, is what distinguishes Newtonian fluids [82]. Glycerin, milk, honey, air are Newtonian fluids.

2.7 Non Newtonian Fluids

Non-Newtonian fluids are defined as those that contradict Newton's law of viscosity and having a correlation which is not linear among tangential stress and strain rate. [82]. The following is a mathematical representation of this relationship.

$$\tau_{yx} \propto \left(\frac{du}{dy}\right)^{n}, \qquad n \neq 1. \tag{2.6}$$

$$\tau_{yx} = \eta\left(\frac{du}{dy}\right)^{n}, \qquad \eta = k\left(\frac{du}{dy}\right)^{n-1}, \tag{2.7}$$

where η represents the viscosity, the flow behavior index referred by n and k denotes the consistency index. Whipped cream and toothpaste are the exemplers of non-Newtonian fluids.

2.8 Nanofluids

The nanoparticles are dispersed into a basefluid to form nanofluids [82].

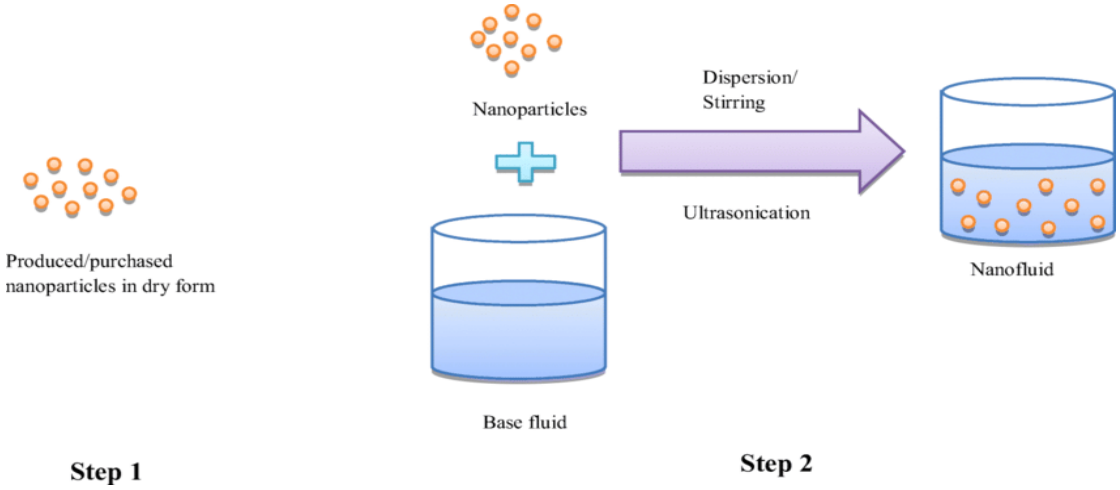

Fig.1: Manufacturing of Nanofluids.

2.9 Hybrid Nanofluids

Hybrids are the most developed kind of nanofluids; they are created by combining two distinct kinds of nanoparticles in a basefluid [82].

2.10 Flow

Flow is the movement of gases or liquids through a channel [82]. When fluid flow is subjected to imbalance forces, fluid motion continues as long as the forces that are out of balance are still being used. The following sections discuss the many forms of flow.

2.10.1 Compressible Flow

When the fluid's density varies while the flow is occurring, it is said to be compressible [82]. It is crucial in many fluid systems, particularly those at high speeds and temperature, such as those seen in supersonic aircraft or missile engines.

2.10.2 Incompressible Flow

When the fluid's density does not change during the course of flow, it is said to be incompressible flow [82]. For instance, while building a pump or turbine, incompressible flow could be taken into account when the fluid is moving slowly and with little density variations.

2.10.3 Laminar Flow

Laminar flow [82] is the motion of particles of fluid through consecutive layers or along predetermined routes without overlapping or mixing with one another. When the fluid velocity is not high and the viscosity is high, the flow is usually laminar.

2.10.4 Turbulent flow

When fluid particle motion is erratic and devoid of a predictable sequence or direction, it is known to as turbulent flow [82]. When the fluid velocity is high and the viscosity is low, the flow is often turbulent.

2.10.5 Steady Flow

Steady flow occurs when the fluid's density, speed, thickness, and pressure are stable over time [82]. In this type of movement, these features are independent of time. Consequently, the fluid's conduct remains consistent over time.

$$\frac{D\eta}{Dt} = 0, \tag{2.8}$$

where η signifies fluid characteristics.

2.10.6 Unsteady Flow

Unsteady flow [82] occurs when fluid attributes change over time at a particular location. In this flow, these traits changes over time, rather than remain constant. Consequently, the behavior of the fluid varies across time at that particular point in time.

$$\frac{D\eta}{Dt} \neq 0, \tag{2.9}$$

where η signifies fluid characteristics.

2.11 Density

A property of materials called density [82] measures how much mass an object has in a specific volume. It is mathematically defined as the quotient of mass (m) to volume (V), expressed as

$$\rho = \frac{m}{V} = \frac{mass}{voulme}. \tag{2.10}$$

kg/m^3 are the SI units of density and the dimensions are $\left[\frac{M}{L^3}\right]$.

2.12 Pressure

The force exerted on an object divided by its surface area is known as pressure [83]. It explains how physical pressure is applied to an object.

$$\mathrm{P} = \frac{F}{A} = \frac{force}{area}. \tag{2.11}$$

N/m^2 are the SI units of pressure with dimensions [$ML^{-1}T^{-2}$].

2.13 Thermal Conductivity

The tendency of a material to transmit heat when there is variation in temperature can be described as thermal conductivity [83]. In terms of Mathematics,

$$\text{Thermal Conductivity} = \frac{Heat \times Distnace}{Area \times Temperature\ Gradient},$$

$$k = \frac{Q \times L}{A \times \Delta T^2}, \tag{2.12}$$

where k represents the thermal conductivity and A refers to the area of an substance.

2.14 Thermal Diffusivity

Thermal diffusivity [83] is the link between thermal conduction and the density and specific heat capacity of the material. Mathematically, it is expressed as

$$\alpha = \frac{k}{\rho c_p} = \frac{material\ conductivity}{density \times specific\ heat\ capacity}, \tag{2.13}$$

where c_p represents the specific heat capacity, ρ denotes the density and k symbol is used to indicate the thermal conductivity. The SI units of thermal diffusivity are m^2/s and $\left[\frac{L^2}{T}\right]$ are its dimensions.

2.15 Methods of Heat transfer

Conduction, radiation and convection are the three mechanisms through which heat can travel from a one point to a different one [83].

2.15.1 Conduction

The transfer of heat from a warmer area to a colder area via particle collisions and interactions inside a material is known as conduction [83].

2.15.2 Convection

Convection [83] is the process by which heat migrates from a warm region to a cool region due to the swirling of fluid particles.

$$Q = h \times A \times \nabla T. \tag{2.14}$$

The surface area of the surface is represented by A, h refers to the transfer's heat convective coefficient and ∇T denotes the temperature difference.

2.15.2.1 Forced Convection

Forced convection [83] is the technique by which heat is generated when fluid motion is purposefully triggered by outside forces, such as mechanical devices.

2.15.2.2 Natural Convection

The buoyant forces brought on by changes in density create natural convection or free convection [83]. Sea breezes, land breezes, and the rising of warm air are a few instances of free convection.

2.15.2.3 Mixed Convection

A kind of convection known as mixed convection [83] occurs when forced and natural convection coexist, usually as a result of the interplay of buoyancy and outside influences.

2.15.3 Radiation

Radiation is a process by which heated energy travels through a substance as particles or waves [83]. Nuclear power plants, imaging, medical diagnostics, and food preservation all benefit greatly from radiation.

2.16 Dimensionless Number

2.16.1 Prandtl Number

The Prandtl number [84] is a non-dimensional variable demonstrating the association among thermal diffusivity along with kinematic viscosity.

$$\Pr = \frac{viscous\ diffusion\ rate}{thermal\ diffusion\ rate},$$

$$\Pr = \frac{v}{a^*} = \frac{{}^{\mu}/_{p}}{{}^{\boldsymbol{k}}/_{\boldsymbol{\rho c_p}}} = {}^{c_p\mu}/_{k}, \tag{2.16}$$

where kinematic viscosity is denoted by ν, specific heat capacity by c_p, thermal diffusivity by $\alpha*$, and thermal conductivity by k.

2.16.2 Reynolds Number

The quotient of inertial to viscous forces in a fluid flow is represented by the Reynolds number. It aids in predicting the flow patterns.
Mathematically,

$$\mathrm{Re} = \frac{inertial\ forces}{viscous\ forces},$$

$$\mathrm{Re} = \frac{{}^{\rho v^2}/_{L}}{\frac{\mu u}{L^2}} = \frac{vL}{u}, \tag{2.15}$$

where L denotes the characteristic length, v represents kinematic viscosity, ρ refers to density, velocity is represented by u and $\mu$is the dynamic viscosity.

2.16.3 Eckert Number

The association between kinetic and thermal energies in fluid flow is clarified by this non-dimensional variable.

$$Ec = \frac{kinetic\ energy}{thermal\ energy} = \frac{u^2}{c_p \Delta T}, \tag{2.17}$$

where the specific heat capacity, fluid's velocity and temperature differential is indicated by c_p, u, and ΔT.

2.16.4 Nusselt Number

The Nusselt number [84] is the value that describes the interplay among convective versus conductive heat flow across the barrier. In terms of mathematics,

$$\text{Nu}sselt\ number = \frac{convective\ heat\ transfer}{conductive\ heat\ transfer} = \frac{hL}{k}, \tag{2.18}$$

where h indicates transfer of heat by means of convection, L provides the distinctive length, and k denotes the thermal conductivity.

2.16.5 Skin Friction

A particular type of friction known as "skin friction" [84] occurs when something that flows, such as air or water, moves along a rigid surface. It is caused by the varied velocity of the fluid layers that encounter the solid's surface.

$$\text{Skin friction} = C_f = \frac{\tau_w}{\frac{1}{2}\rho u^2}, \tag{2.19}$$

where the fluid's density expressed as ρ,velocity denotes by u, the shear stresses at the wall is denoted by τ_w. Skin friction has less an influence on laminar flow versus turbulent flow because there isn't as large of a boundary layer.

2.16.6 Grashof Number

It is employed to form the fluid barrier in laminar systems and highlights how they react in terms of buoyant forces to viscous forces in a fluid that is changing [84].

$$\text{Gr} = \frac{L^3}{v^2} g\beta(T - T_\infty), \tag{2.20}$$

T_∞ is the outside temperature, where g is the acceleration caused by gravity, L indicates the specific length, T denotes the fluid and its environs temperature, β is the factor of cubic thermal expansion and v indicates the kinematic velocity.

Chapter 3

The Mixed Convection Flow of Hybrid Nanofluid over a Stretching Sheet with Magnetohydrodynamics

3.1 Introduction

The behavior of hybrid nanofluids has been the subject of extensive research due to their unique thermal characteristics. The conduct of thermal radiation, MHD and mixed convection on the hybrid nanofluid across an inclined plate is examined in this chapter. By using the proper similarity transformations, the fluid model which was initially characterized by a system of partial differential equations (PDEs) is altered into a system of ordinary differential equations. The temperature, friction drag, and Nusselt number and velocity are then calculated by using the MATLAB Bvp4c solver and displayed graphically. A comparative study gets underway in accordance with the earlier research to guarantee the validity of the results acquired.

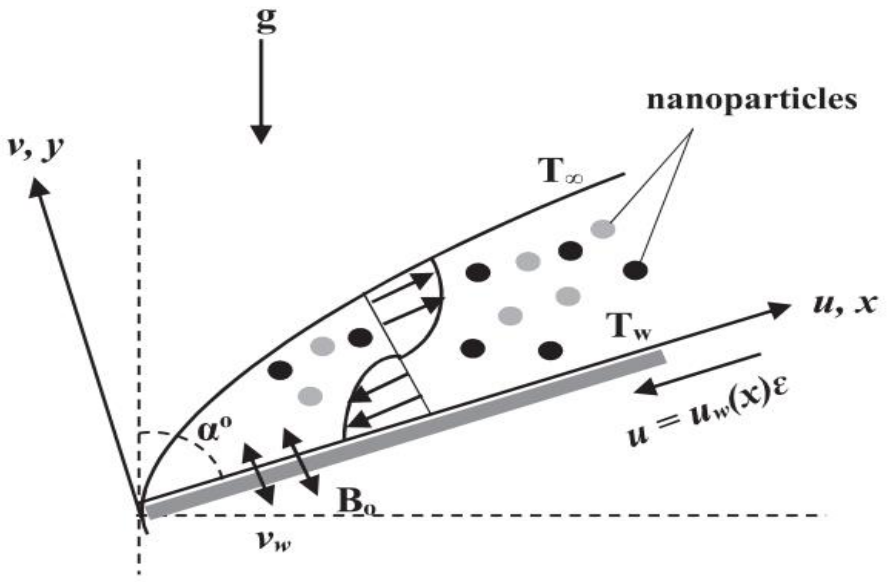

Fig. 3.1: An illustration of flow toward an inclined plate.

3.2 Mathematical Formulation of Fluid Model

The incompressible, viscous and two-dimensional hybrid nanofluid flowing over an inclined plate serves as the basis for the current model and Cu and Al_2O_3 are considered nanoparticles, water is the base fluid. The magnetohydrodynamics (MHD) effect is induced by using a magnetic field with strength B_o. $u_w(x) = ax$ serves as surface velocity . The wall, ambient, and reference temperatures of the sheet is denoted by the symbols T_w, T_∞, and T_o respectively. The effects of mixed convection, thermal radiation and convective boundary conditions further alter the model.

The velocity field implemented in this framework is

$$\mathbf{V} = [u(x, y), v(x, y), 0]. \tag{3.1}$$

The hybrid nanofluid model with considered assumptions is expressed in the form of fundamentals equations. The continuity, energy and momentum equations that regulate the flow problem are given as below:

$$\boldsymbol{\nabla}.\mathbf{V} = 0, \tag{3.2}$$

$$\rho_{hnf}[(\mathbf{V}.\boldsymbol{\nabla})\mathbf{V}] = \boldsymbol{\nabla}.\boldsymbol{\tau} + \rho_{hnf}\boldsymbol{b}, \tag{3.3}$$

$$\left(\rho c_p\right)_{hnf}[(\boldsymbol{V}.\boldsymbol{\nabla})T] = -\boldsymbol{\nabla}.\boldsymbol{q}, \tag{3.4}$$

In the above expressions, ρ_{hnf} denotes the density of hybrid nanofluids, **V** denotes the velocity field, T is for fluid's temperature, **q**$= -kgradT$ denotes the heat flux, c_p denotes specific heat at constant pressure, $\boldsymbol{\tau} = -p\boldsymbol{I} + \mu\boldsymbol{A_1}$ is Cauchy stress tensor I is for the unit tensor, τ stands for stress tensor, **b** is for body force and A_1 is the first Rivilin Erickson tensor. When boundary layer assumptions are applied, the following subsequent equations are generated.

$$\frac{\partial u}{\partial x} + \frac{\partial v}{\partial y} = 0, \tag{3.5}$$

$$u\frac{\partial T}{\partial x} + v\frac{\partial T}{\partial y} = \frac{k_{hnf}}{(\rho C_P)_{hnf}}\frac{\partial^2 T}{\partial y^2} - \frac{1}{(\rho C_P)_{hnf}}\frac{\partial q_r}{\partial y}, \tag{3.6}$$

$$u\frac{\partial u}{\partial x} + v\frac{\partial u}{\partial y} = \frac{\mu_{hnf}}{\rho_{hnf}}\frac{\partial^2 u}{\partial y^2} + \beta_{hnf}(T - T_\infty)\mathrm{g}\cos\alpha - \frac{\sigma_{hnf}}{\rho_{hnf}}B_O^2 u, \tag{3.7}$$

where q_r is expressed as

$$qr = -\frac{4\sigma^*}{3k_1}\frac{\partial T^4}{\partial y} \quad \text{and } T^4 \approx 4T_\infty^3 T - 3T_\infty^4, \tag{3.8}$$

so Eq. (3.8) becomes

$$u\frac{\partial T}{\partial x} + v\frac{\partial T}{\partial y} = \frac{1}{(\rho C_P)_{hnf}}\left(k_{hnf} + \frac{16\sigma^* T_\infty^3}{3k_1}\right)\frac{\partial^2 T}{\partial y^2}\ . \tag{3.9}$$

Where k^*symbolizes the cofficient of mean of mean absorbption, σ^* denotes the constant of Stefan-Boltzmann.

The current framework relates to the following boundary conditions.

$$v = v_w\ , -k_{hnf}\frac{\partial T}{\partial y} = h_f(T_w(x) - T) \text{ and } u = u_w(x)\epsilon\ , \text{ at y = 0,} \tag{3.10}$$

$$\text{As } y \to \infty \text{ then } u \to 0 \text{ and } T \to T_\infty. \tag{3.11}$$

The local Nusselt number (Nu_x) and the viscous drag coefficient (C_f) are two significant factors which are given as

$$C_f = \frac{\mu_{hnf}}{\rho_f(ax)^2}\left(\frac{\partial u}{\partial y}\right)_{y=0} \text{ and } Nu_x = \frac{xk_{hnf}}{k_f(T_w(x) - T_\infty)}\left(-\frac{\partial T}{\partial y}\right)_{y=0} + \frac{x}{k_f(T_w(x) - T_\infty)}(q_r)_{y=0}. \tag{3.12}$$

The similarity dimensionless variables considered for the flow problem are:

$u = axf'(\eta), \theta(\eta) = \frac{T-T_\infty}{T_w(x)-T_\infty}, \eta = y\sqrt{\frac{a}{v_f}}$ and $v = -\sqrt{av_f}f(\eta)$

and $v_w = -\sqrt{av_f}$ S. (3.13)

Using Eq. (3.13) in Eq. (3.6) and Eq. (3.9) the following ODEs are acquired,

$$\frac{\mu_{hnf}/\mu_f}{\rho_{hnf}/\rho_f}f''' + ff'' - f'^2 + \frac{\beta_{hnf}}{\beta_f}\theta\lambda\cos\alpha - \frac{\sigma_{hnf}/\sigma_f}{\rho_{hnf}/\rho_f}Mf' = 0, \quad (3.14)$$

$$\frac{1}{Pr}\frac{1}{(\rho C_P)_{hnf}/(\rho C_P)_f}\left(\frac{k_{hnf}}{k_f} + \frac{4}{3}Rd\right)\theta'' + f\theta' - f'\theta = 0. \quad (3.15)$$

Subject to the boundary conditions:

$$f(0) = S, -\frac{k_{hnf}}{k_f}\theta'(0) = Bi\big(1-\theta(0)\big), f'(0) = \varepsilon\,, \quad (3.16)$$

$$\text{As } \eta \to \infty \text{ then } f'(\eta) \to 0 \text{ and } \theta(\eta) \to 0. \quad (3.17)$$

where Pr indicates the Prandtl numer, *M* refers to magentic parameter, *Rd* represents the radiation parameter, Biot number is referred by Bi and constant mixed convection variation is denoted by λ

Table 3.1: Dimensionless Parameters involved in the hybrid nanofluid flow.

Non -dimensional Parameters	**Mathematical Parameter**
Mixed Convection Parameter	$\lambda = \frac{Gr_x}{Re_x^2} = \frac{g\beta_f(T_w - T_\infty)x^3/v_f^2)}{(ax)x/v_f}$
Radiation Parameter	$\mathrm{Rd} = \frac{4\sigma^* T_\infty^3}{k_f k_1}$
Magnetic Paramter	$M = \frac{\sigma_f B_o^2}{a\rho_f}$
Biotic Number	$Bi = \frac{h_f}{k_f}\sqrt{\frac{v_f}{a}}$
Prandtl Number	$\mathrm{Pr} = \frac{(v\rho C_p)_f}{k_f}$

Additionally, the dimensionless parameters of Nu_x and C_f in Eq. (3.12) are reduced to the following form

$$(Re_x)^{\frac{-1}{2}} Nu_x = -\left(\frac{k_{hnf}}{k_f} + \frac{4}{3}Rd\right)\theta'(0) \; and \; (Re_x)^{\frac{1}{2}} C_f = \frac{\mu_{hnf}}{\mu_f} f''(0). \tag{3.18}$$

3.3 Numerical Strategy

The regulating flow ODEs are solved by using MATLAB's bvp4c module. The following equations represent the alteration of the higher order ODEs into first order form, they are further executed using the MATLAB bvp4c technique.

$$f = y(1)\,, \tag{3.19}$$

$$f' = y(2), \tag{3.20}$$

$$f'' = y(3), \tag{3.21}$$

$$\theta = y(5), \tag{3.22}$$

$$\theta' = y(6), \tag{3.23}$$

$$f''' = \frac{1}{\frac{\mu_{hnf}/\mu_f}{\rho_{hnf}/\rho_f}}\left(y(2)y(2) - \frac{\beta_{hnf}}{\beta_f}y(5)\lambda\cos\alpha + \frac{\sigma_{hnf}/\sigma_f}{\rho_{hnf}/\rho_f}My(2) - y(1)y(3)\right), \quad (3.24)$$

$$\theta'' = \frac{1}{\frac{1}{Pr}\frac{1}{(\rho C_P)_{hnf}/(\rho C_P)_f}\left(\frac{k_{hnf}}{k_f} + \frac{4}{3}Rd\right)}\big(y(2)y(5) - y(1)y(6)\big). \quad (3.25)$$

with boundary conditions,

$$ya(1) - S, \quad -\frac{k_{hnf}}{k_f}ya(6) - Bi(1 - ya(5)), ya(2) - \varepsilon, yb(5), yb(2). \quad (3.26)$$

3.4 Graphical Analysis and Discussion

The analysis is done on the hybrid nanofluid flow's on an inclined plate. The substantial impact that several dimensionless factors have on coefficient of skin friction (C_f), velocity and temperature of the fluid and Nusselt number (Nu_x), is thoroughly highlighted in this section. Therefore, using a numerical approach (bvp4c technique) in MATLAB induce the important outputs of dimensionless quantities on the significant entities. Figure 3.2 shows the significant impact of volume of the solid nanoparticle ϕ_2 on temperature of the fluid $\theta(\eta)$. The figure illustrates how a continuous favorable influence on the temperature profile ensues from an elevation in φ_2.The influence of the volume fraction coefficient ϕ_2 on $f'(\eta)$ can be seen in Figure 3.3. A spike in ϕ_2 causes $f'(\eta)$ to enhance due to greater energy transfer. It is perceivable in Figure 3.4 that the temperature profile $\theta(\eta)$ drops as the mixed convection parameter λ improves. The variation in the consequence of mixed convection with respect to λ. on the velocity profile can be observed in Figure 3.5. The figure makes it clear that an improvement in the velocity profile is associated with an improvement in λ. Figure 3.6 shows the magnetic parameter *M* impact in relation to the temperature profile $\theta(\eta)$. The temperature declines as a result of the modification in *M*. Figure 3.7 shows the magnetic parameter influence in relation to the velocity profile $f'(\eta)$. The velocity $f'(\eta)$ elevates as a result of the enhancement of *M* values. The change in temperature of the fluid $\theta(\eta)$ with the modification in the inclination angle α is shown in Figure 3.8, where a decline in temperature is observed. The change in velocity against the increasing values of the inclination angle α can be seen in Figure 3.9. The rise of $f'(\eta)$ is observed through this figure. Figure 3.10 highlights the influence of suction parameter *S* establishing on the temperature profile $\theta(\eta)$. As the suction

goes up, it becomes apparent that the temperature falls. Figure 3.11 emphasizes how the suction modifies the velocity profile $f'(\eta)$. It is visible in the graphic that an elevation in suction is associated with a rise in the velocity profile. The consequence of the radiation parameter *Rd* on the temperature of the fluid $\theta(\eta)$ can be observed in Figure 3.12. The graphical analysis make it clear that a diminution in the temperature profile is correlated with an improvement in *Rd.* The Nusselt number behavior is shown in Figure 3.13 for the increasing range of the thermal radiation quantity *Rd* and the shrinking quantity ϵ. The boost in *Rd* leads to increased heat transfer rate . Figure 3.14 illustrates how Biot number *Bi* influences Nusselt number in an increasing manner and there is comparable incline behavior for ϵ. Figure 3.15 assesses the behavior of Nusselt number with variation in ϵ and ϕ_2. The figure points out that while mounting shrinking parameter ϵ, the Nusselt number declines. The conduct of magnetic parameter *M* and shrinking quantity ϵ on the viscous drag force is demonstrated in Figure 3.16. According to the illustration, the skin friction coefficient will grow with a modification in *M* and is strongly influenced with the values of ϵ. The effect of the shrinking quantity ϵ and volume fraction of solid nanoparticle ϕ_2 on the friction drag is illustrated in Figure 3.17. The viscous drag force coefficient rises as the quantities of ϕ_2 are increased. Figure 3.18 indicates the relationship amongst the suction parameter S, shrinking parameter ϵ and the skin friction coefficient. As the values of S and ϵ grow, the skin friction coefficient shows opposite behavior.

Table 3.1 exhibits the dimensionless parameters mentioned in the ODEs. The thermo-physical characteristics needed for the study are mentioned in Tables 3.2 and 3.3. Tables 3.4 and 3.5 are based on the comparative analysis for the drag force (C_f) and Nusselt number (Nu_x). The tables exhibit an excellent accordance of the obtained and already calculate d values. Table 3.6 provides the range of values of dimensionless parameters used in the analysis.

Table 3.2: Hybrid nanofluid thermophysical aspects [89].

Properties	**Hybrid nanofluid**
Density (ρ)	$\rho_{hnf} = \varphi_{cu}\rho_{cu} + (1-\varphi_{hnf})\rho_{f+}\varphi_{Al_2O_3}\rho_{Al_2O_3}$
Heat capacity	$(\rho C_p)_{hnf} = \varphi_{Al_2O_3}(\rho C_p)_{Al_2O_3} + \varphi_{cu}(\rho C_p)_{cu} + (1-\varphi_{hnf})(\rho C_P)_f$
Dynamic viscosity	$\mu_{hnf} = \mu_f(1-\varphi_{hnf})^{-2.5}$
Thermal conductivity	$\frac{k_{hnf}}{k_f} = \left[\frac{2k_f + 2(\varphi_{Al_2O_3}k_{Al_2O_3} + \varphi_{cu}k_{cu}) - 2\varphi_{hnf}k_f + \left(\frac{\varphi_{Al_2O_3}k_{Al_2O_3}+\varphi_{cu}k_{cu}}{\varphi_{hnf}}\right)}{\left(\frac{\varphi_{Al_2O_3}k_{Al_2O_3}+\varphi_{cu}k_{cu}}{\varphi_{hnf}}\right) - (\varphi_{Al_2O_3}k_{Al_2O_3} + \varphi_{cu}k_{cu}) + 2k_f + +\varphi_{hnf}k_f}\right]$
Thermal expansion	$(\rho\beta)_{hnf} = +\varphi_{cu}\rho_{cu}\beta_{cu} + (1-\varphi_{hnf})(\rho\beta)_f + \varphi_{Al_2O_3}\rho_{Al_2O_3}\beta_{Al_2O_3}$
Electrical Conductivity	$\frac{\sigma_{hnf}}{\sigma_f} = \left[\frac{2(\varphi_{Al_2O_3}\sigma_{Al_2O_3} + \varphi_{cu}\sigma_{cu}) - 2\varphi_{hnf}\sigma_f + \left(\frac{\varphi_{Al_2O_3}\sigma_{Al_2O_3}+\varphi_{cu}\sigma_{cu}}{\varphi_{hnf}}\right) + 2k_f}{\varphi_{hnf}\sigma_f + \left(\frac{\varphi_{Al_2O_3}\sigma_{Al_2O_3}+\varphi_{cu}\sigma_{cu}}{\varphi_{hnf}}\right) + 2k_f - (\varphi_{Al_2O_3}\sigma_{Al_2O_3} + \varphi_{cu}\sigma_{cu})}\right]$

Table 3.3: Thermo-physical components of hybrid nanofluid [90].

Properties	**Water (*f*)**	**Alumina**	**Copper**
$\boldsymbol{\sigma(S/m)}$	5.5×10^{-6}	35×10^{6}	59.6×10^{6}
$\boldsymbol{C_p(J/kgK)}$	4197	765	385
$\boldsymbol{k(W/mK)}$	0.613	40	400
Pr	6.2		
$\boldsymbol{\beta(1/K)}$	21×10^{-5}	0.85×10^{-5}	1.67×10^{-5}
$\boldsymbol{\rho(kg/m^3)}$	997.1	3970	8933

Table 3.4: Comparative estimates of attributes ϵ and S on $f''(0)$ if $\phi_1 = \phi_2 = \lambda = M = 0$.

ε	S	Wahid *et al.* [85]	Alabdulhadi *et al.*[86]	Anuar *et al.* [87]	Present (bvp4c) values
		$f''(0)$	$f''(0)$	$f''(0)$	$f''(0)$
1	2	-2.414214	-2.414214	-2.414214	-2.414214
	2.5	-2.850781	-2.850781	-2.850781	-2.850781
	3	-3.302776	-3.302776	-3.302776	-3.302776
	3.5	-3.765564	-3.765564	-	-3.765564
-1	2.5	2.0000000	2.000000	2.00000	2.000000
	3	2.618034	2.618034	2.61803	2.618034
	3.5	3.186141	3.186141	-	3.186141

Table 3.5: Comparative estimation of attribute λ on $-\theta'(0)$ if $\varepsilon = 1, Bi \to \infty$, $\phi_1 = \phi_2 = Rd = M = S = 0$, $\alpha = 0°$and Pr =1.

λ	Wahid *et al*. [85]	Alabdulhadi *et al.* [86]	Anuar *et al.* [87]	Rosca and pop [88]	Present (bvp4c)
	$-\theta'(0)$	$\theta'(0)$	$\theta'(0)$	$\theta'(0)$	$\theta'(0)$
0	1.000000	1.000008	1.000008	1.0000	1.0000
1	1.087278	1.087275	1.087275	1.0872	1.0873
5	1.252700	1.252700	-	-	1.2525
10	1.371564	1.371564	1.371564	1.3715	1.3715

Table 3.6: Parametric values were used in the present analysis.

Parameters	Symbol	Values
Prandtl number	Pr	6.2
Radiation Parameter	Rd	0.1, 0.2, 0.3
Suction	S	2, 3
Mixed convection parameter	λ	-1, 1
Shrinking parameter	ϵ	-1
Volume fraction coefficient	φ_1	0.1
Volume fraction coefficient	φ_2	0.01, 0.1
Magnetic parameter	M	0.1, 2.5
Biotic Number	Bi	1, 3

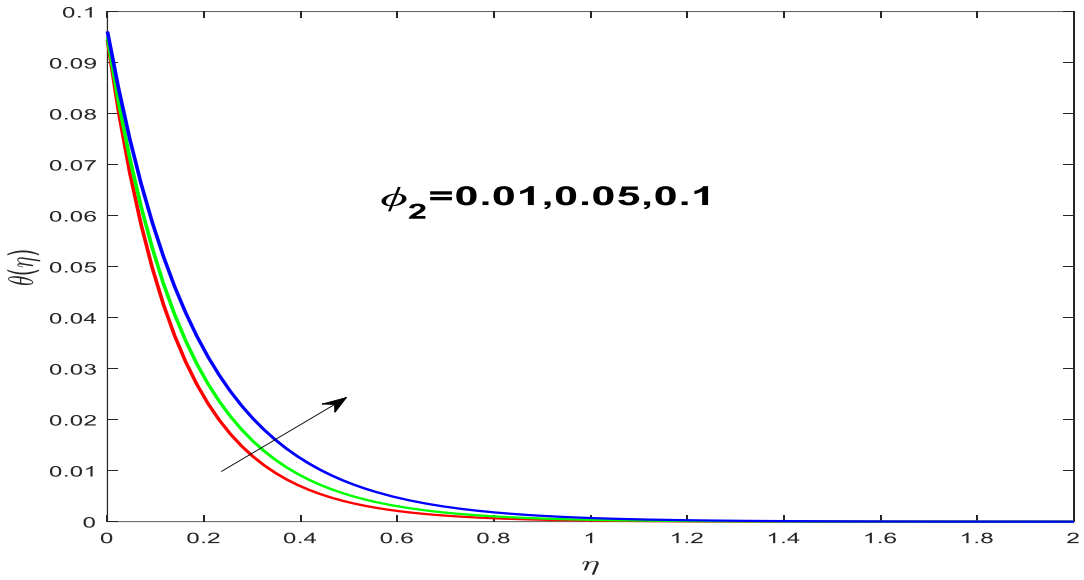

Fig 3.2: $\theta(\eta)$ with altering quantities of ϕ_2.

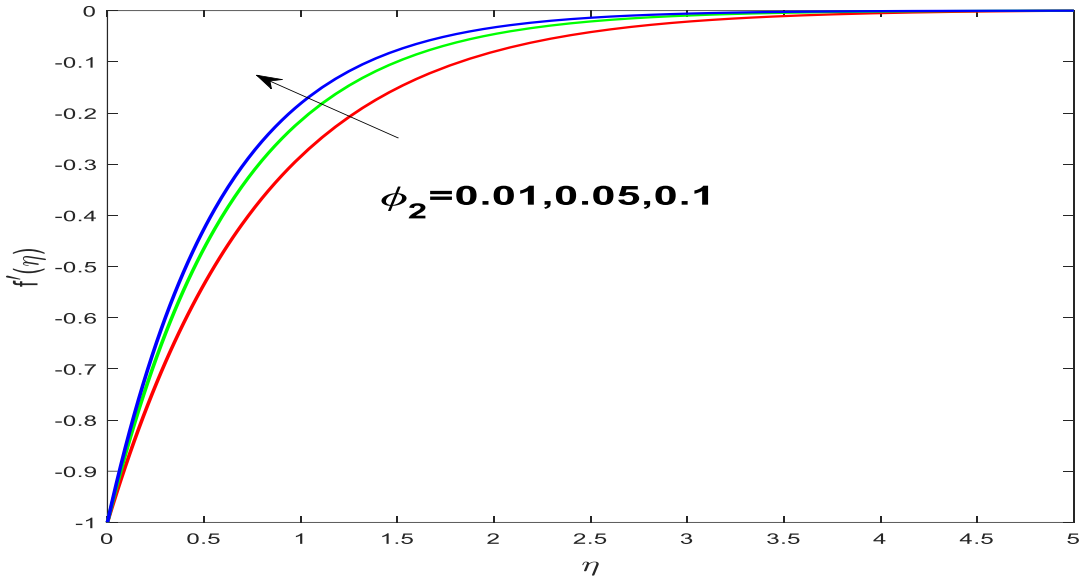

Fig. 3.3: $f'(\eta)$ with altering quantities of φ_2.

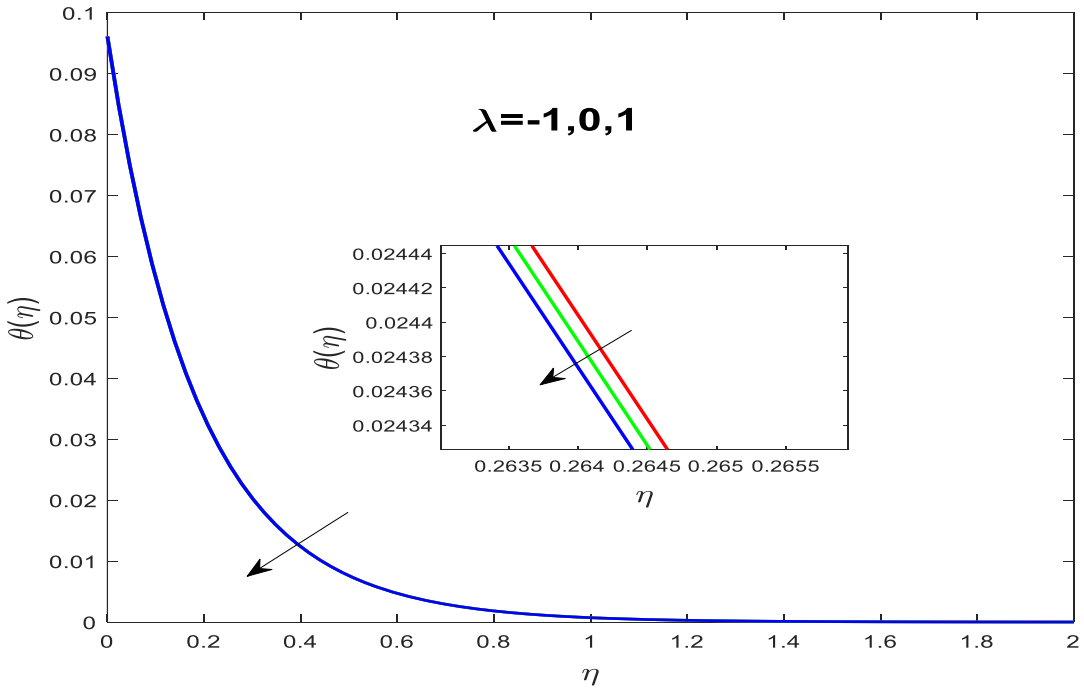

Fig. 3.4: $\theta(\eta)$ with altering quantities of λ.

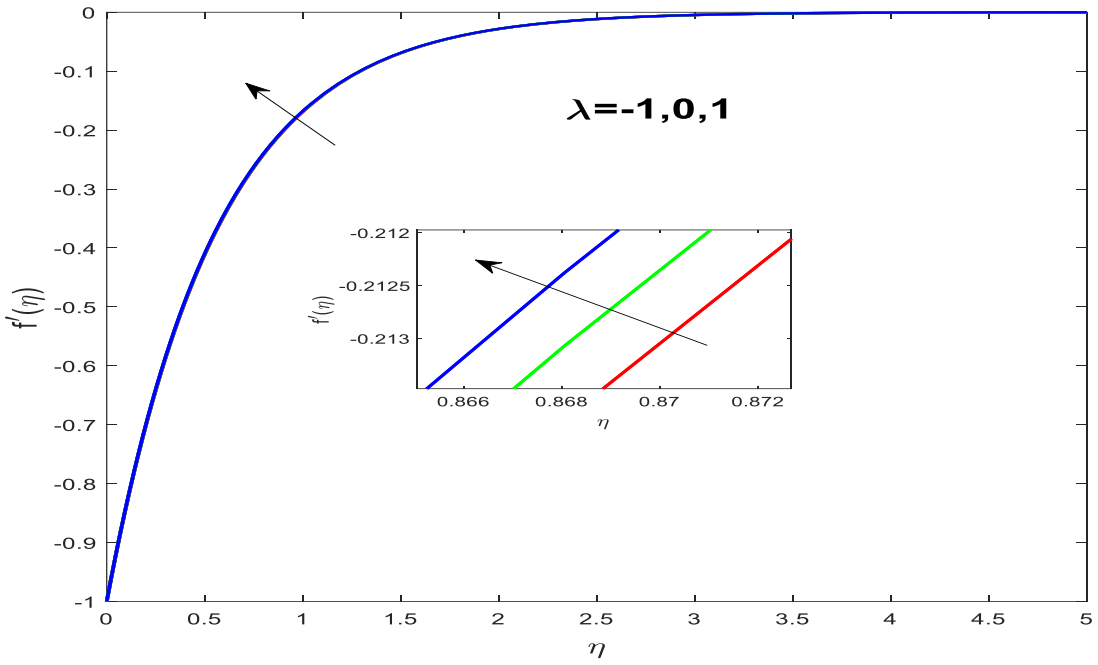

Fig. 3.5: $f'(\eta)$ with altering quantities of λ.

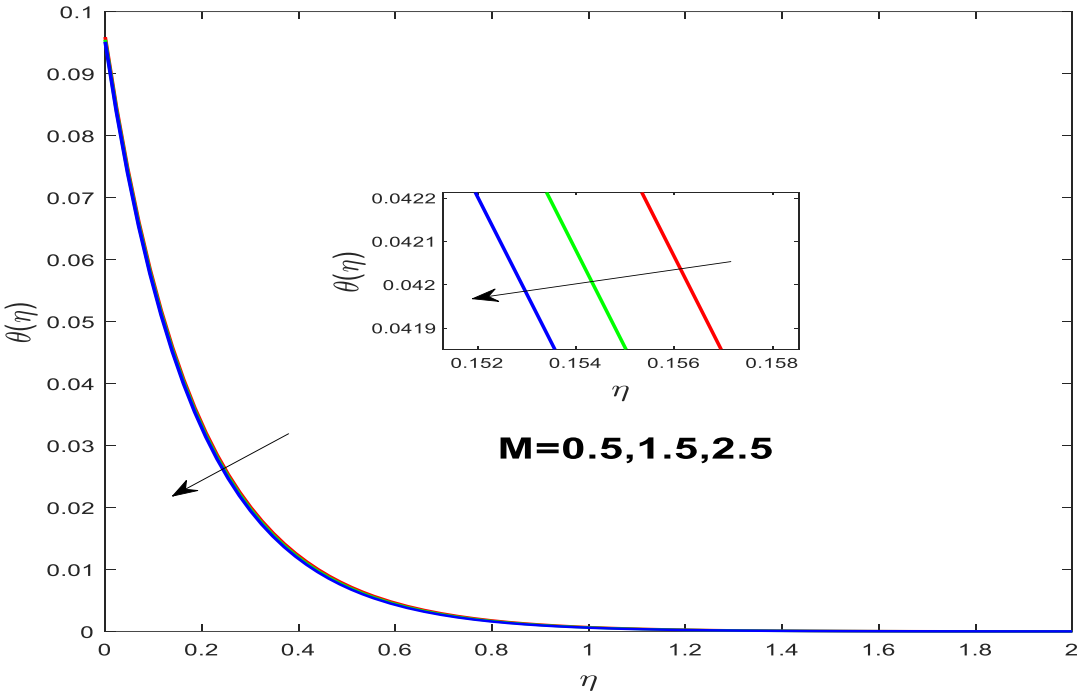

Fig. 3.6: $\theta(\eta)$ with altering quantities of M.

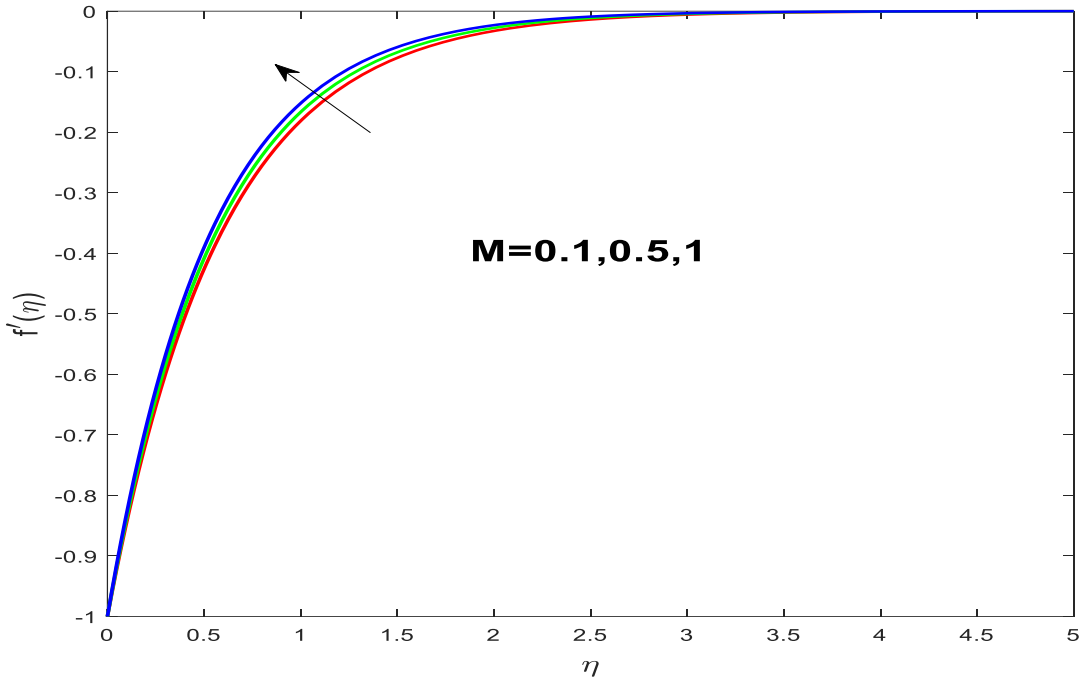

Fig. 3.7: $f'(\eta)$ with altering quantities of *M*.

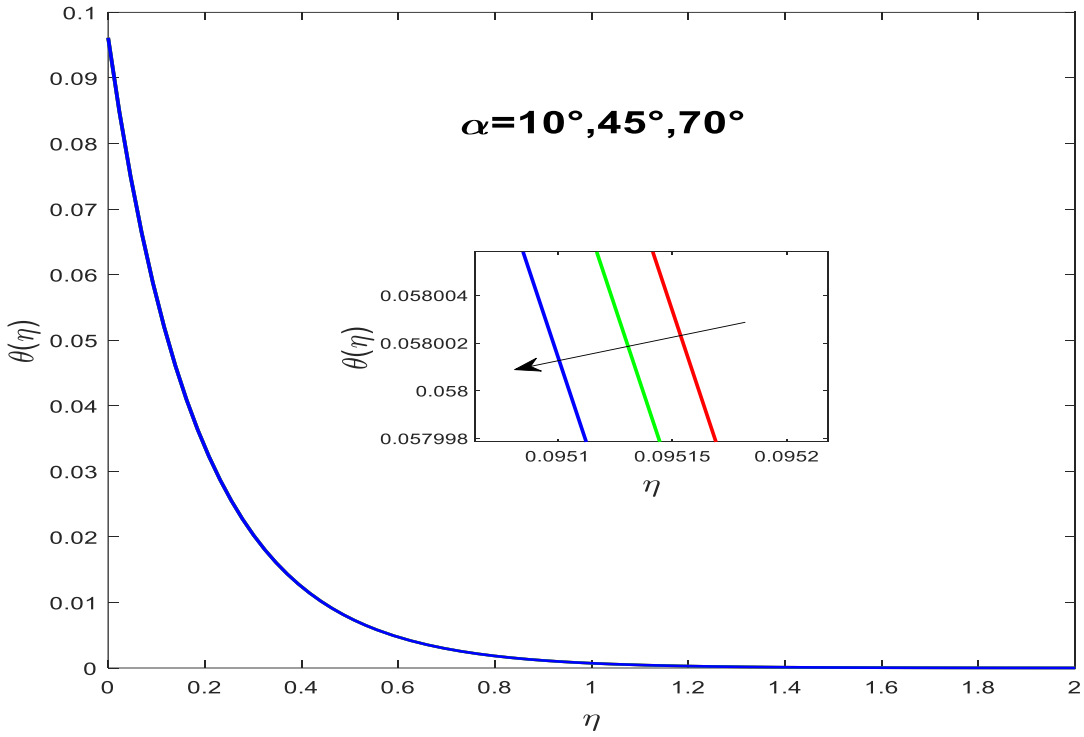

Fig. 3.8: $\theta(\eta)$ with altering quantities of α.

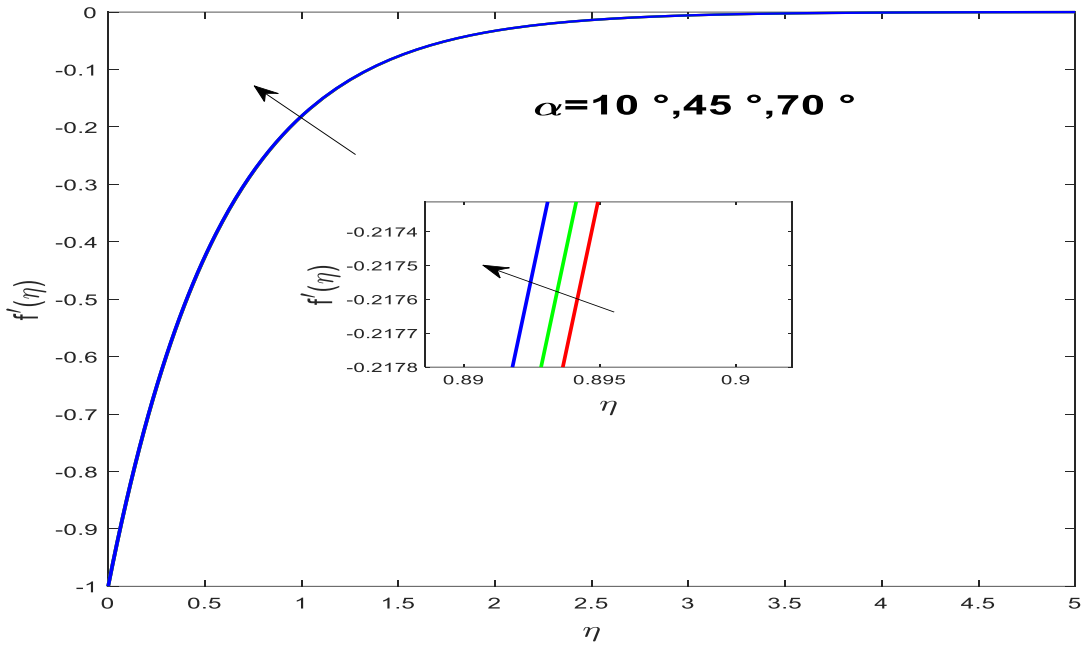

Fig. 3.9: $f'(\eta)$ with altering quantities of α .

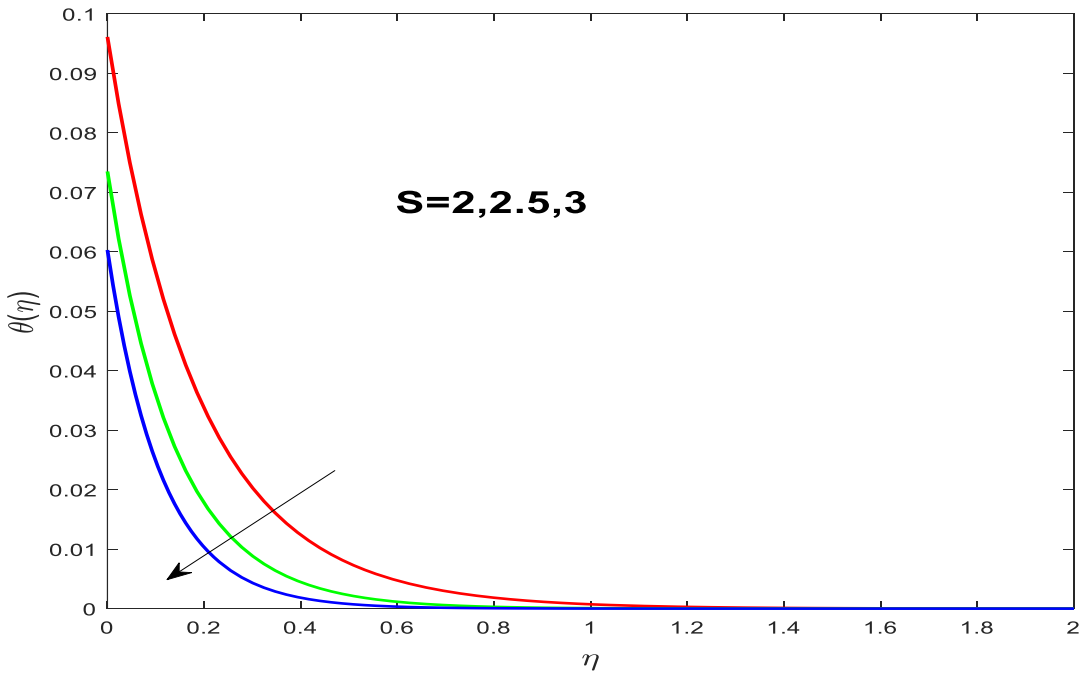

Fig. 3.10: $\theta(\eta)$ with altering quantities of *S*.

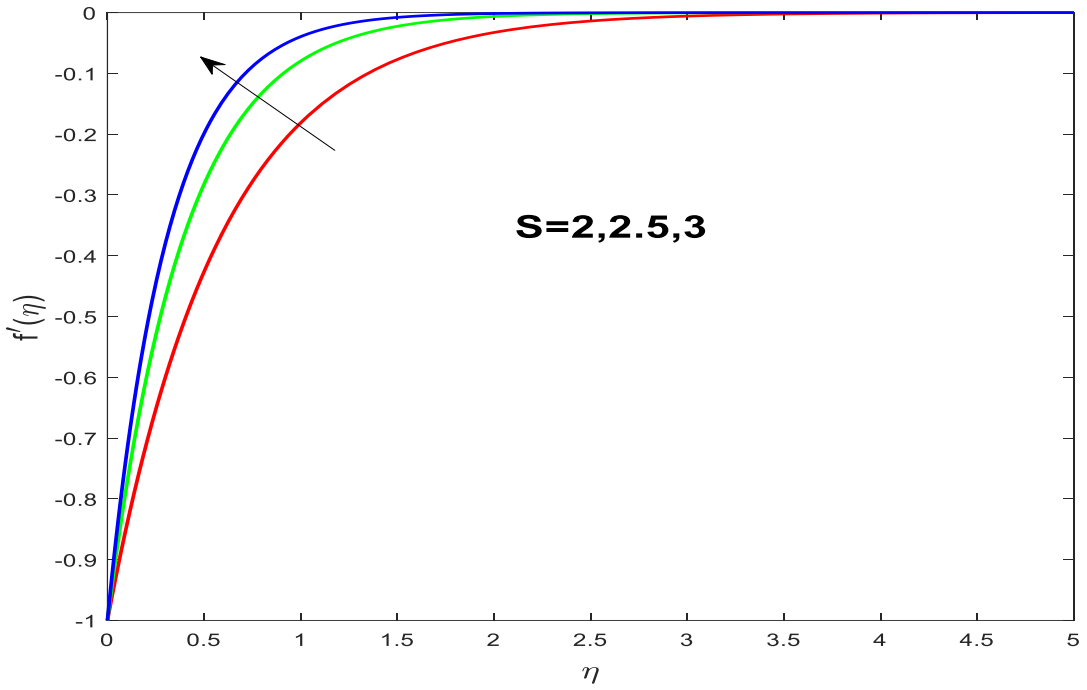

Fig. 3.11: $f'(\eta)$ with altering quantities of *S*.

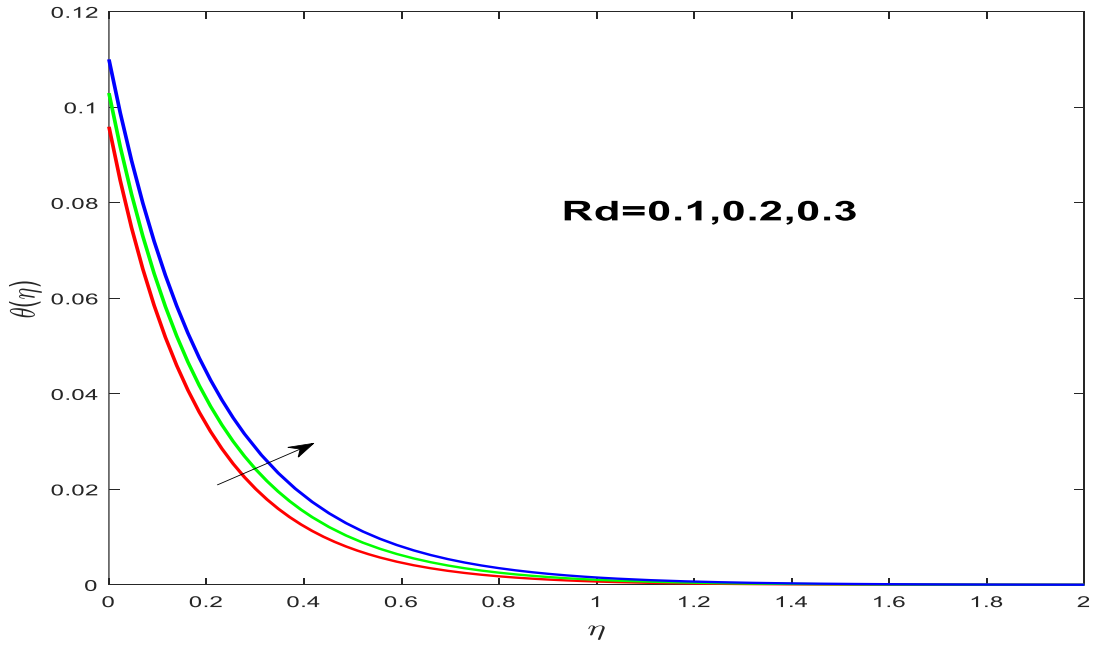

Fig. 3.12: $\theta(\eta)$ with altering quantities of *Rd* .

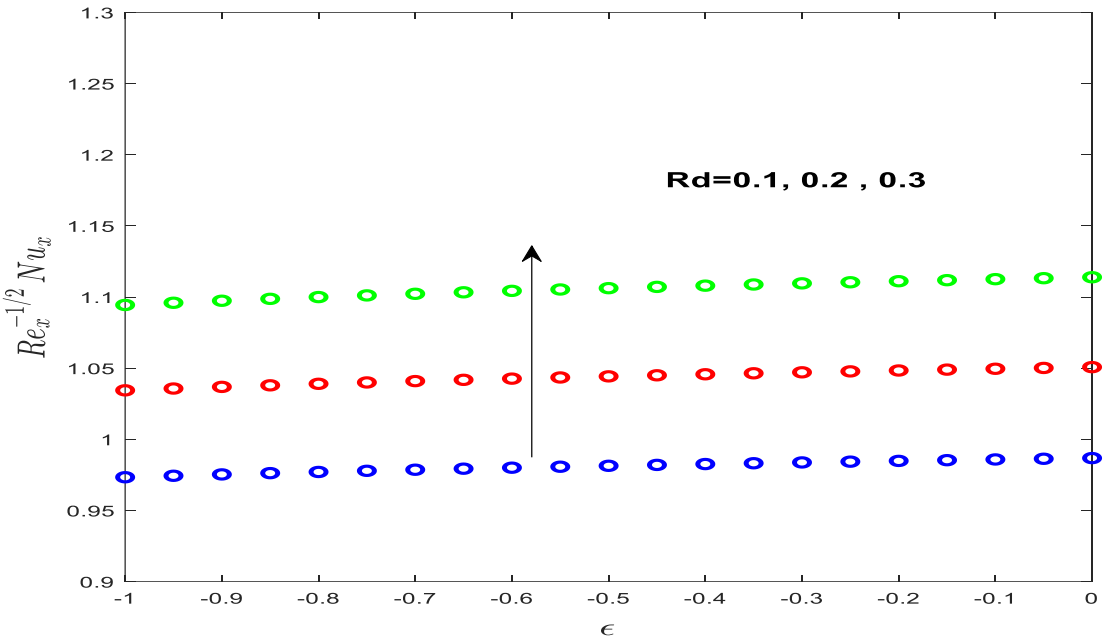

Fig. 3.13: Nusselt number towards ϵ with altering values of Rd.

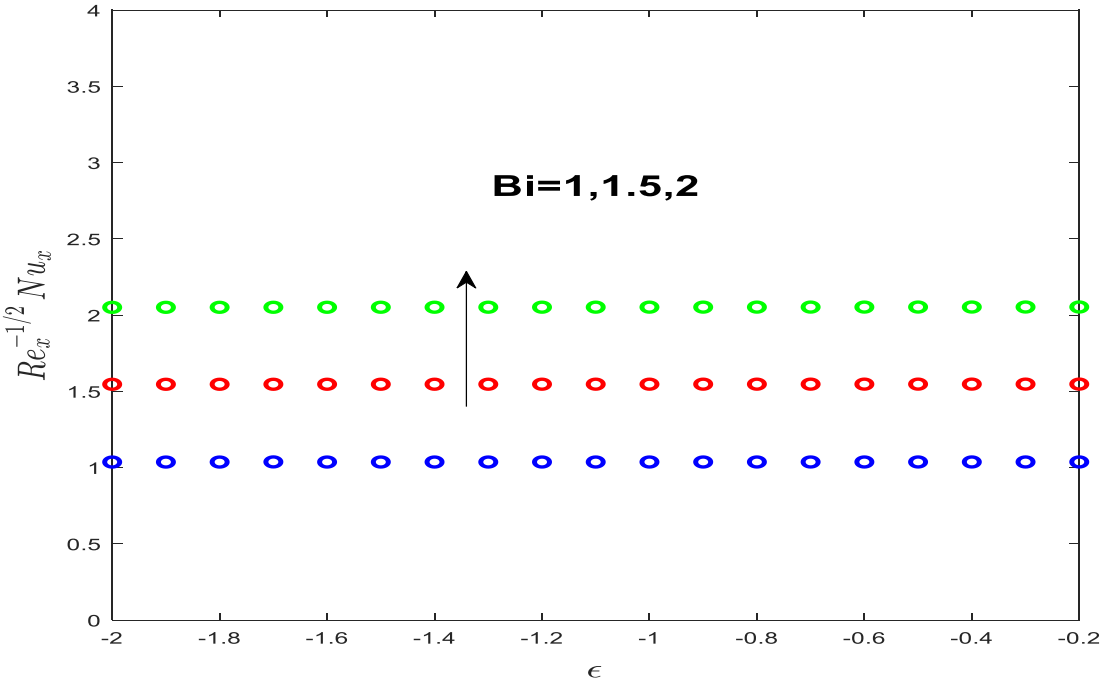

Fig. 3.14: Nusselt number towards ϵ with altering values of Bi.

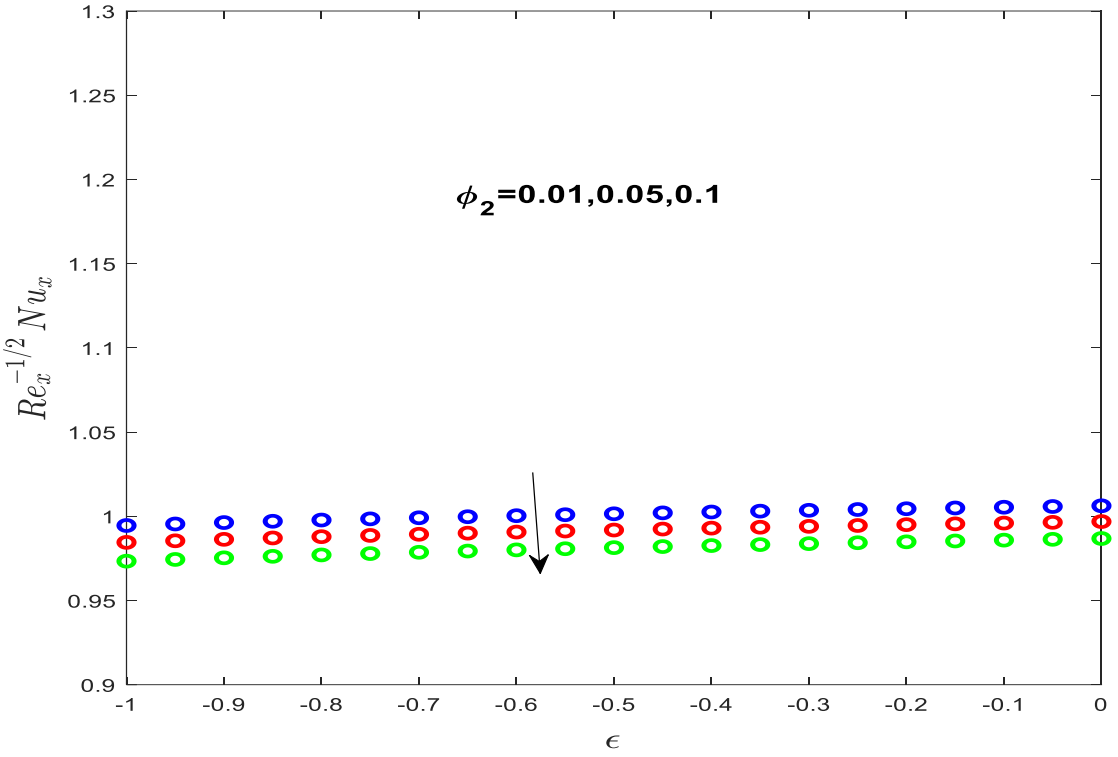

Fig. 3.15 : Nusselt number towards ϵ with altering values of ϕ_2.

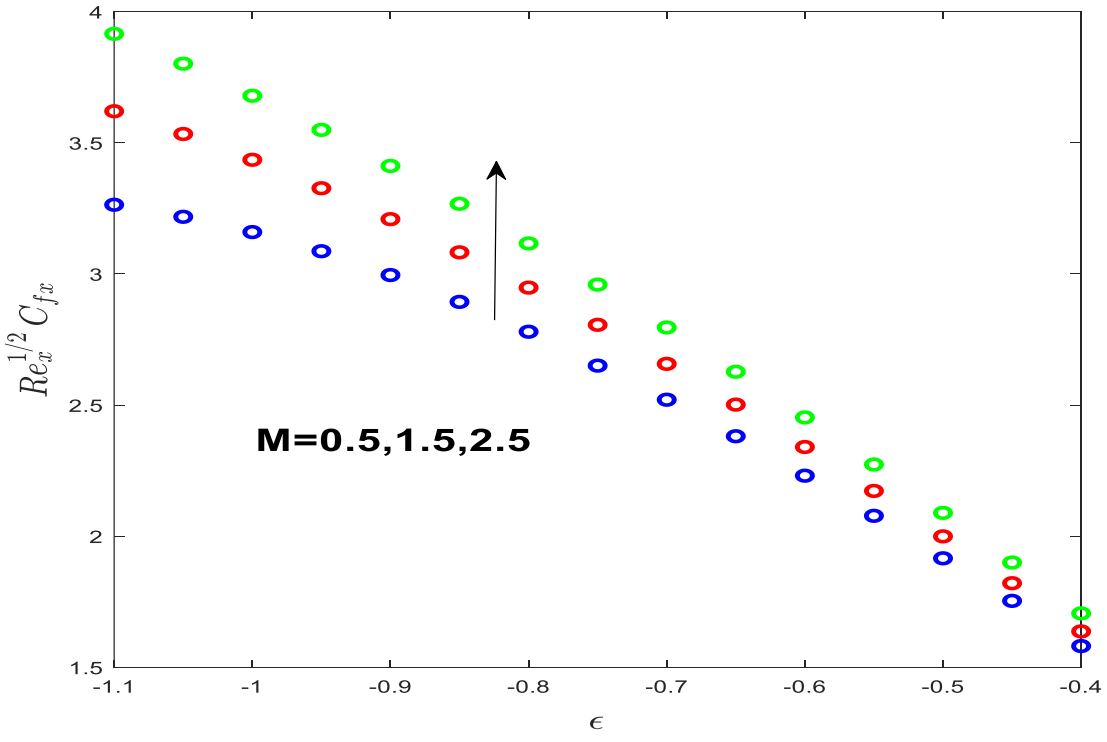

Fig. 3.16: Skin friction towards ϵ with altering values of *M*.

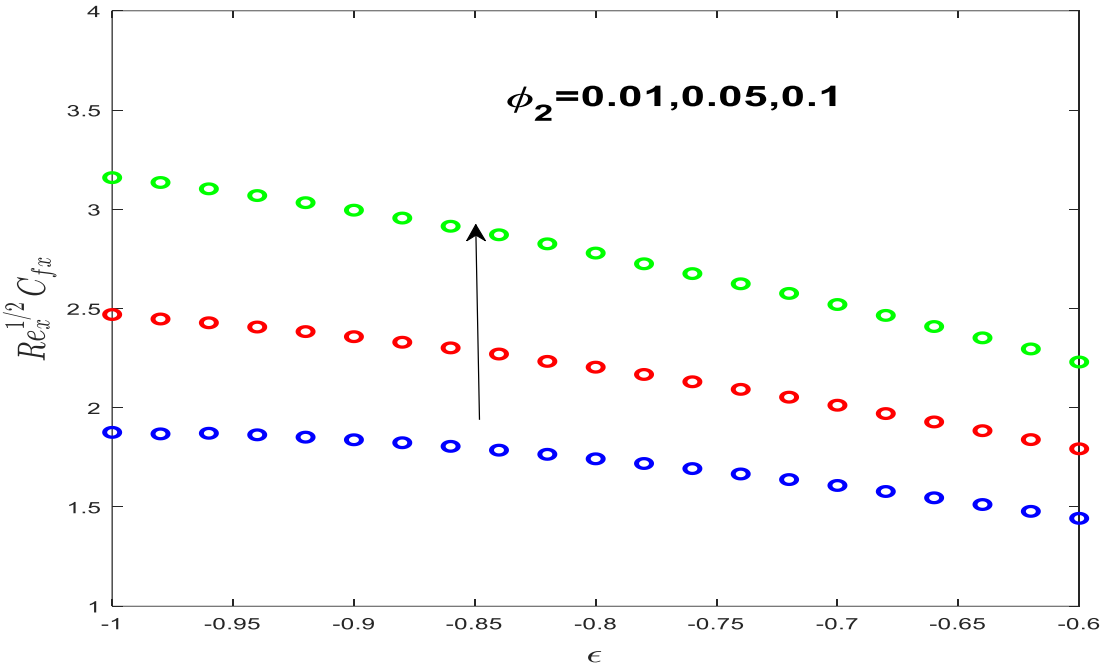

Fig. 3.17: Skin friction towards ϵ with altering values of ϕ_2.

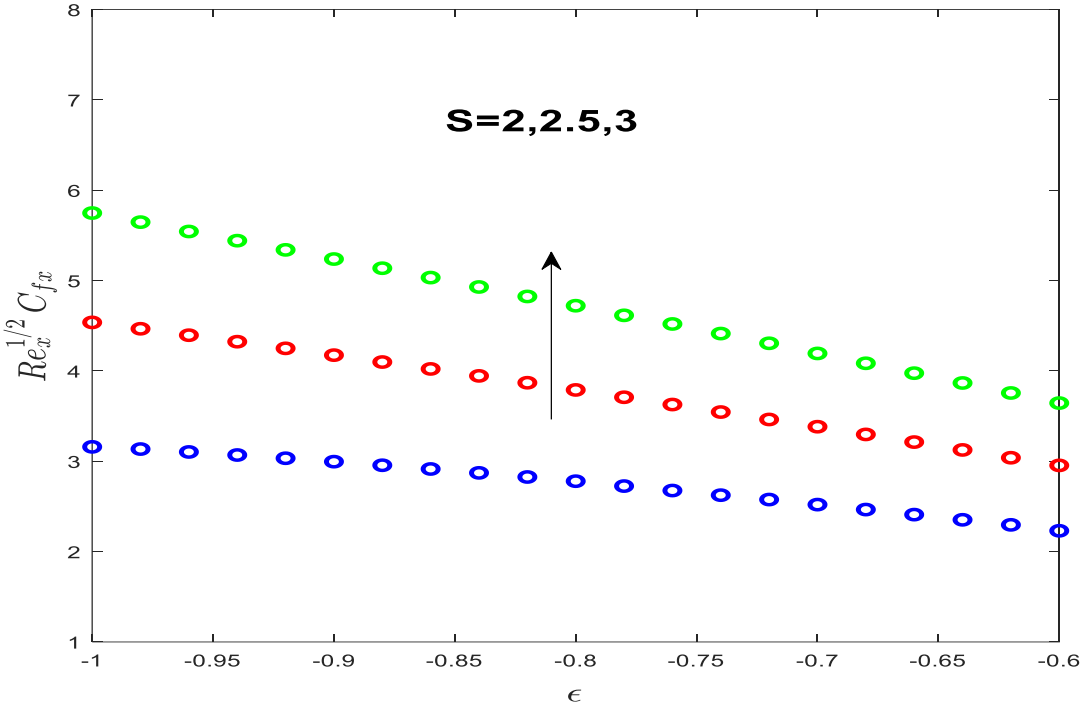

Fig. 3.18: Skin friction towards ϵ with altering values of *S*.

Chapter 4

Investigation of Hybrid Nanofluid Flow over an Inclined Surface in a Porous Medium in the presence of Non-Uniform Heat Source/Sink.

4.1 Introduction

This chapter deals with the flow dynamics of a hybrid nanofluid ($Cu - Al_2O_3/H_2O$) flowing by an inclined plate in the porosity medium. The combined impact of non-uniform heat source/sink and magnetohydrodynamics on the flow is one of the objectives of this study. While examining the heat transfer, the effects of mixed convection, Joule heating and thermal radiation are also taken into account. After adopting the similarity transformation processes, the basic complicated coupled PDEs in the model are transformed into ODEs. The bvp4c function in MATLAB software is then utilized to provide the quantitative results of the obtained ODEs. The velocity and temperature distributions are observed for a number of significant parameters. The graphical effects resulting from various kinds of factors are investigated for Nusselt number and skin friction coefficient. The results gained through the numerical technique are validated and a good accuracy is observed.

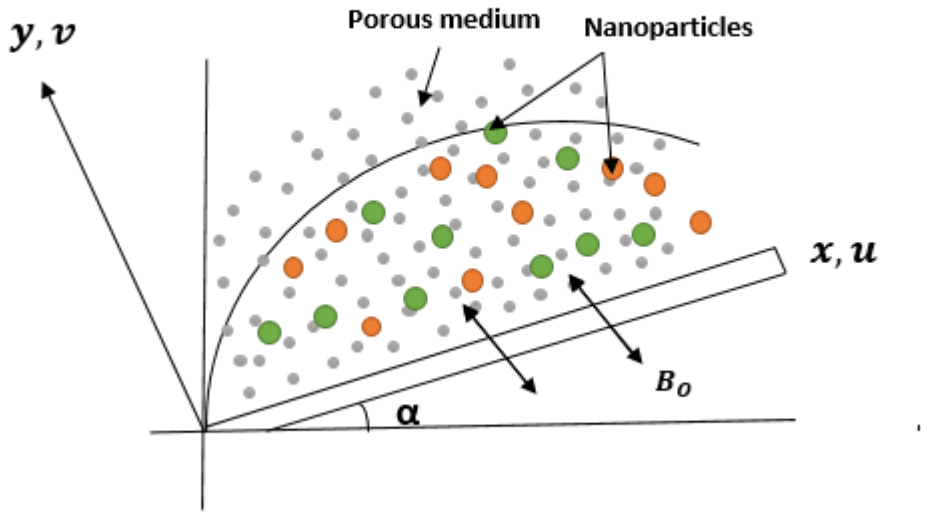

Fig. 4.1: An illustration of flow toward inclined plate in a porous medium.

4.2 Mathematical Formulation

A two dimensional, time independent, incompressible, and laminar flow of hybrid nanofluid (a mixture of H_2O as base fluid with nanoparticles Cu and Al_2O_3) past an inclined stretching plate that is permeable, is taken under consideration. The Cartesian coordinates are indicated by the letters x and y. The sheet's velocity in the x-axis direction is given by $u_w(x) = ax$. The magnetohydrodynamics (MHD) effect occurs when a magnetic field of strength B of the same magnitude is applied perpendicular to the sheet. $T_W(x) = T_\infty + T_O\left(x/l\right)$ provides the temperature of the sheet. The ambient, and reference temperatures of the sheet are indicated by T_∞ and T_0 respectively. The effects of heat source/sink, thermal radiation and Joule heating further modify the flow problem.

The considered velocity field is represented as

$$\mathbf{V} = [u(x,y), v(x,y), 0] \tag{4.1}$$

The fluid model under study is constructed in the form of governing equations. The continuity, momentum, and energy equations are the basic equations needed for the execution of the analysis.

$$\boldsymbol{\nabla}.\mathbf{V} = 0, \tag{3.2}$$

$$\rho_{hnf}[(\mathbf{V}.\boldsymbol{\nabla})\mathbf{V}] = \boldsymbol{\nabla}.\boldsymbol{\tau} + \rho_{hnf}\boldsymbol{b}, \tag{3.3}$$

$$\left(\rho c_p\right)_{hnf}[(\boldsymbol{V}.\boldsymbol{\nabla})T] = -\boldsymbol{\nabla}.\boldsymbol{q}, \tag{3.4}$$

In the above expressions, ρ_{hnf} denotes the density of hybrid nanofluids, **V** denotes the velocity field, *T* is for fluid's temperature, $\mathbf{q}= -kgradT$ denotes the heat flux, c_p denotes specific heat at constant pressure, $\boldsymbol{\tau} = -p\boldsymbol{I} + \mu\boldsymbol{A_1}$ is Cauchy stress tensor *I* is for the unit tensor, τ stands for stress tensor, **b** is for body force and A_1 is the first Rivilin Erickson tensor. The boundary layer theory plays an important role to obtain the following partial differential equations.

$$\frac{\partial u}{\partial x} + \frac{\partial v}{\partial y} = 0, \tag{4.5}$$

$$u\frac{\partial u}{\partial x} + v\frac{\partial u}{\partial y} = \frac{\mu_{hnf}}{\rho_{hnf}}\frac{\partial^2 u}{\partial y^2} + \beta_{hnf}(T - T_\infty)g\cos\alpha - \frac{\sigma_{hnf}}{\rho_{hnf}}B_0^2 u \; - \; \mu_{hnf}/\rho_{hnf} \; \frac{u}{k^*}, \tag{4.6}$$

$$u\frac{\partial T}{\partial x} + v\frac{\partial T}{\partial y} = \frac{k_{hnf}}{(\rho C_P)_{hnf}}\frac{\partial^2 T}{\partial y^2} - \frac{1}{(\rho C_P)_{hnf}}\frac{\partial q_r}{\partial y} + \frac{\sigma_{hnf}}{(\rho C_P)_{hnf}}\; B_0^2\, u^2 + \frac{q'''}{(\rho C_P)_{hnf}}, \tag{4.7}$$

where q_r and q''' are expressed as

$$q_r = -\frac{4\sigma^*}{3k_1}\frac{\partial T^4}{\partial y} \quad \text{and } T^4 \approx 4T_\infty^3 T - 3T_\infty^4\,, \tag{4.8}$$

$$q''' = \frac{k_{hnf}u_w(x)}{x\nu_{hnf}}[\zeta_1(T_w - T_\infty)f' + \zeta_2(T - T_\infty)], \tag{4.9}$$

where k^*denotes the cofficient of mean absorbption, σ^* symbolizes the constant of Stefan-Boltzmann.

After using Eqs. (4.8) and (4.9) into Eq. (4.7) the following equation is acquired,

$$\begin{aligned} u\frac{\partial T}{\partial x} + v\frac{\partial T}{\partial y} = {} & \frac{\sigma_{hnf}}{(\rho C_P)_{hnf}}\; B_0^2 u^2 + \quad \frac{k_{hnf}u_w(x)}{(\rho C_P)_{hnf}x\nu_{hnf}}[\zeta_1 + \zeta_2(T - T_\infty)] \\ & + \frac{1}{(\rho C_P)_{hnf}}\left(k_{hnf} \; + \frac{16\sigma^* T_\infty^3}{3k^*} \;\right)\frac{\partial^2 T}{\partial y^2}. \end{aligned} \tag{4.10}$$

The present model provides the following boundary conditions

$$u = u_w(x)\epsilon\ , -k_{hnf}\frac{\partial T}{\partial y} = h_f(T_w(x) - T) \text{ and } v = v_w \text{ at y = 0,} \tag{4.11}$$

$$u \to 0, T \to T_\infty \text{ as } y \to \infty. \tag{4.12}$$

The C_f (viscous drag force) and Nusselt number (Nu_x) are expressed as

$$C_f = \frac{\mu_{hnf}}{\rho_f (ax)^2}\left(\frac{\partial u}{\partial y}\right)_{y=0}, \quad Nu_x = \frac{x}{k_f(T_w(x)-T_\infty)}\,(q_r)_{y=0.} + \frac{xk_{hnf}}{k_f(T_w(x)-T_\infty)}\left(-\frac{\partial T}{\partial y}\right)_{y=0}, \tag{4.13}$$

The similarity dimensionless variables used for the current problem are

$$u = axf'(\eta)\ , \eta = y\sqrt{\frac{a}{v_f}}, v = -\sqrt{av_f}f(\eta)\ , \theta\ (\eta) = \frac{T-T_\infty}{T_w(x)-T_\infty}\ , \tag{4.14}$$

so that,

$$v_w = -\sqrt{av_f}\ \text{S}. \tag{4.15}$$

After putting Eq. (4.15) into Eqs. (4.6) and (4.10) the following equations are acquired

$$\frac{\mu_{hnf}/\mu_f}{\rho_{hnf}/\rho_f}f''' + ff'' - f'^2 + \frac{\beta_{hnf}}{\beta_f}\theta\lambda\cos\alpha - \frac{\sigma_{hnf}/\sigma_f}{\rho_{hnf}/\rho_f}Mf' - \frac{\mu_{hnf}/\mu_f}{\rho_{hnf}/\rho_f}Kf' = 0, \tag{4.16}$$

$$\frac{1}{Pr}\frac{1}{(\rho C_P)_{hnf}/(\rho C_P)_f}\left(\frac{k_{hnf}}{k_f} + \frac{4}{3}Rd\right)\theta'' + f\theta' - f'\theta + \frac{\sigma_{hnf}/\sigma_f}{(\rho C_P)_{hnf}/(\rho C_P)_f}MEcf'^2 + \frac{\frac{k_{hnf}}{k_f}}{\Pr(\rho C_P)_{hnf}/(\rho C_P)_f}(\zeta_1 f' + \zeta_2\theta) = 0. \tag{4.17}$$

The boundary condition are following

$$f(0) = S, \quad -\frac{k_{hnf}}{k_f}\theta'(0) = Bi\big(1 - \theta(0)\big), f'(0) = \varepsilon\ , \tag{4.18}$$

$$\text{as } \eta \to \infty \text{ then } f'(\eta) \to 0 \quad \theta(\eta) \to 0. \tag{4.19}$$

where Pr specifies the Prandtl number, the radiation parameter signifies by *Rd*, Biot number is referred by *Bi*, mixed convection parameter is represented by λ, the Eckert Number is mentioned by *Ec*, porosity parameter is represented by *K* and *M* denotes magnetic parameter.

Table 4.2: Dimensionless parameters involved in the hybrid nanofluid flow.

Non -dimensional Parameters	**Mathematical Parameter**
Mixed Convection Parameter	$\lambda = \frac{Gr_x}{Re_x^2} = \frac{g\beta_f(T_w - T_\infty)x^3/v_f^2)}{(ax)x/v_f}$
Radiation Parameter	Rd= $\frac{4\sigma^* T_\infty^3}{k_f k_1}$
Magnetic Paramter	$M = \frac{\sigma_f B_o^2}{a\rho_f}$
Biotic Number	$Bi = \frac{h_f}{k_f}\sqrt{\frac{v_f}{a}}$
Prandtl Number	$\Pr = \frac{(v\rho c_p)_f}{k_f}$
Eckert Number	Ec = $\frac{u_w^2}{(Cp)_{f(T_W - T\infty)}}$
Porous Medium Parameter	K= $\frac{v_f}{ak^*}$

The dimensionless form of Nu_x and C_f of Eq. 4.13 are attainable as

$$(Re_x)^{\frac{-1}{2}} Nu_x = -\left(\frac{k_{hnf}}{k_f} + \frac{4}{3}Rd\right)\theta'(0) \; and \; (Re_x)^{\frac{1}{2}} C_f = \frac{\mu_{hnf}}{\mu_f} f''(0). \tag{4.20}$$

4.3 Numerical Strategy

The flow model is represented through higher order ordinary differential equations. These higher order differential equations undergo conversion to first order differential equations for their solution using MATLAB's bvp4c method, after which the bvp4c technique is further utilized.

$$f = y(1)\,, \tag{4.21}$$

$$f' = y(2), \tag{4.22}$$

$$f'' = y(3), \tag{4.23}$$

$$\theta = y(5), \tag{4.24}$$

$$\theta' = y(6), \tag{4.25}$$

$$f''' = \frac{1}{\frac{\mu_{hnf}/\mu_f}{\rho_{hnf}/\rho_f}}\left(-y(1)y(3) + \frac{\sigma_{hnf}/\sigma_f}{\sigma_{hnf}/\sigma_f}My(2) - \frac{\beta_{hnf}}{\beta_f}y(5)\lambda\cos\alpha + Ky(2) + y(2)y(2)\right), \tag{4.26}$$

$$\theta'' = \frac{1}{\frac{1}{Pr}\frac{1}{(\rho C_P)_{hnf}/(\rho C_P)_f}\left(\frac{k_{hnf}}{k_f} + \frac{4}{3}Rd\right)}\left(-\frac{\sigma_{hnf}/\sigma_f}{(\rho C_P)_{hnf}/(\rho C_P)_f}MEc(y(2)y(2) + \big(y(2)y(5)\big) - \frac{\frac{k_{hnf}}{k_f}}{\Pr\,(\rho C_P)_{hnf}/(\rho C_P)_f}(\zeta_1 y(2) + \zeta_2 y(6)) - y(1)y(6)\right). \tag{4.27}$$

with boundary conditions

$$ya(1) - S, \quad -\frac{k_{hnf}}{k_f}ya(6) - Bi(1 - ya(5)), ya(2) - \varepsilon, yb(2), yb(5). \tag{4.28}$$

4.4 Graphical Analysis and Discussion

The hybrid nanofluid on an inclined plate placed in a medium of poristy is considered for examination in the presence of various significant impacts. The extensive impacts of dimensionless parameters on temperature profile, friction drag, velocity profile and Nusselt number are the center of focus for the analysis. Using a Bvp4c technique (MATLAB), the fluid's response to dimensionless factors is noted. As perceived in Figure 4.2, the fluid's temperature profile augments as the magnetic parameter *M* values enhance. This result is caused by the Lorentz force which improves as the *M* increases. Figure 4.3 illustrates how the velocity of the fluid is influenced by the higher values of *M*(magnetic parameter). The $f'(\eta)$ declines as the *M* (magnetic parameter) values increase. Fluid motion is decelerated as the Lorentz force improves with the magnetic field's strength. The decrease of the temperature distribution for

increased values of suction parameter *S* is evident through Figure 4.4. Figure 4.5 is plotted to observe the change in the velocity profile by rising the suction parameter *S*. This figure illustrates that the $f'(\eta)$ declines with high suction parameter values. The rise in the values of stretching parameter ε can lead to the increase in temperature profile which is shown in Figure 4.6. Figure 4.7 illustrates how the velocity profile $f'(\eta)$ is modified by the stretching parameter ϵ and a boost in ϵ causes a rise in the $f'(\eta)$. Figures 4.8 and 4.9 illustrate how the temperature and velocity distributions are influenced by the nanoparticle's volume fraction ϕ_2 respectively. The $\theta(\eta)$ improves by rising of nanoparticle volume fraction ϕ_2, whereas the $f'(\eta)$ declines. Figures 4.10 and 4.11 illustrate how the temperature distribution and velocity distribution are influenced by the inclination angle α. Both the $\theta(\eta)$and $f'(\eta)$ the enhance upon increase in value of the angle. Figure 4.12 illustrates the way the porosity element influences the velocity profile $f'(\eta)$. A spike in the permeability parameter is frequently noticed to reduce the velocity. It is observed that Figure 4.13 represents the temperature distribution influenced by the Eckert number *Ec*. The fluid's temperature is demonstrated to be elevated through higher *Ec* values. It can be seen that frictional warming retains the fluid's energy from heat. The alteration in the values of the non-uniform heat source/sink parameter ς_1 and its influence on temperature profile are illustrated in Figure 4.14. The $\theta(\eta)$ climbs as a result of a rise in parameter ς_1. Figure 4.15 demonstrates how the temperature is influenced by rising the non-uniform heat source/sink parameter ς_2. The $\theta(\eta)$ increases with the increased values of ς_2. As indicated by Figure 4.16, an upward trend in fluid's temperature is noticed for higher values of Biot number *Bi* due to the raised thermal conduction. Figure 4.17 presents the results for Nusselt number with modification of *Rd* (radiation parameter) and stretching parameter ε. The Nusselt number rises with *Rd*, but the opposite is seen for ε. This is due to the fact that radiation parameter values contribute to a faster rate of heat transfer, which improves the Nusselt number.In order to comprehend the impact of non-uniform parameter ς_1 and stretching parameter ε on the Nusselt number, Figure 4.18 is sketched. It illustrates that ς_1 influences Nusselt number in a decreasing manner. There is comparable declining behavior for ε . Figure 4.19 shows the impact of non-uniform parameter ς_2 and stretching parameter ε on the Nusselt number. It displays a decline relation for Nusselt number when ς_2 is increased. Fig. 4.20 illustrates how the Eckert number affects together with stretching parameter ε on the Nusselt number. The thermal conduction rate lessen as the Eckert number *Ec* rises, and the same pattern is observed for ε. The influence of the stretching parameter ε and porosity parameter *K* on the skin friction coefficient is illustrated in Figure 4.21. The skin friction coefficient declines as ε and *K* are increased. Figure

4.22 highlights how the skin friction is influenced by the elevating stretching parameter ε and solid volume fraction ϕ_2. As the values of ε and ϕ_2 enhance, the skin friction coefficient decline. When additional particles in the fluid cause more flow resistance, skin friction decline as the volume fraction declines. Both the suction parameter *S* and the stretching parameter ε decline the skin friction coefficient which is displayed in Figure 4.23. Figure 4.24 demonstrates how the friction drag can be modified by the altered values of stretching ϵ and the magnetic parameter *M*. According to the illustration, the coefficient of skin friction diminishes with a boosts in M and ε. The magnetic field resists the fluid's motion, dragging it down and diminishing the velocity gradients.

Tables 4.2 and 4.3 present the thermo-physical aspects of the considered nanofluid. Tables 4.4 and 4.5 present an analysis of the viscous drag force C_f and Nusselt number, respectively. The comparison clearly validates the gained results. Table 4.6 presents the parameters' values used in finding the results.

Table 4.2: Thermophysical characteristics of the considered hybrid nanofluid.[89]

Properties	**Hybrid nanofluid**
Heat capacity	$(\rho C_p)_{hnf} = \varphi_{cu}(\rho C_p)_{cu} + (1-\varphi_{hnf})(\rho C_P)_f + \varphi_{Al_2O_3}(\rho C_p)_{Al_2O_3}$
Dynamic viscosity	$\mu_{hnf} = \mu_f(1-\varphi_{hnf})^{-2.5}$
Electrical Conductivity	$\frac{\sigma_{hnf}}{\sigma_f} = \left[\frac{\left(\frac{\varphi_{Al_2O_3}\sigma_{Al_2O_3}+\varphi_{cu}\sigma_{cu}}{\varphi_{hnf}}\right)+2k_f-2\varphi_{hnf}\sigma_f+2\left(\varphi_{Al_2O_3}\sigma_{Al_2O_3}+\varphi_{cu}\sigma_{cu}\right)}{\varphi_{hnf}\sigma_f+\left(\frac{\varphi_{Al_2O_3}\sigma_{Al_2O_3}+\varphi_{cu}\sigma_{cu}}{\varphi_{hnf}}\right)+2k_f-\left(\varphi_{Al_2O_3}\sigma_{Al_2O_3}+\varphi_{cu}\sigma_{cu}\right)}\right]$
Thermal expansion	$(\rho\beta)_{hnf} = \varphi_{Al_2O_3}\rho_{Al_2O_3}\beta_{Al_2O_3} + \varphi_{cu}\rho_{cu}\beta_{cu} + (1-\varphi_{hnf})(\rho\beta)_f$
Thermal conductivity	$\frac{k_{hnf}}{k_f} = \left[\frac{\left(\frac{\varphi_{Al_2O_3}k_{Al_2O_3}+\varphi_{cu}k_{cu}}{\varphi_{hnf}}\right)+2k_f+2\left(\varphi_{Al_2O_3}k_{Al_2O_3}+\varphi_{cu}k_{cu}\right)-2\varphi_{hnf}k_f}{\left(\frac{\varphi_{Al_2O_3}k_{Al_2O_3}+\varphi_{cu}k_{cu}}{\varphi_{hnf}}\right)+2k_f-\left(\varphi_{Al_2O_3}k_{Al_2O_3}+\varphi_{cu}k_{cu}\right)+\varphi_{hnf}k_f}\right]$
Density (ρ)	$\rho_{hnf} = \varphi_{Al_2O_3}\rho_{Al_2O_3} + \varphi_{cu}\rho_{cu} + (1-\varphi_{hnf})\rho_f$

Table 4.3: Thermophysical attributes for the considered hybrid nanofluid.[90]

Properties	**Water (f)**	**Alumina** (Al_2O_3)	**Copper (Cu)**
$C_p(J/kgK)$	4197	765	385
$\beta(1/K)$	21×10^{-5}	0.85×10^{-5}	1.67×10^{-5}
Pr	6.2		
$k(W/mK)$	0.613	40	400
$\sigma(S/m)$	5.5×10^{-6}	35×10^{6}	59.6×10^{6}
$\rho(kg/m^3)$	997.1	3970	8933

Table 4.4: Comparative values of stretching parameter ε suction parameter S for $f''(0)$ if $\phi_1 = \phi_2 = \lambda = Ec = K = M = 0$.

ε	S	Wahid *et al*. [85]	Alabdulhadi *et al*. [86]	Anuar *et al*. [87]	Present (bvp4c)
		$f''(0)$	$f''(0)$	$f''(0)$	$f''(0)$
1	2	-2.414214	-2.414214	-2.414214	-2.414224
	2.5	-2.850781	-2.850781	-2.850781	-2.850783
	3	-3.302776	-3.302776	-3.302776	-3.302776
	3.5	-3.765564	-3.765564	-	-3.765564
-1	2.5	2.0000000	2.000000	2.00000	2.000155
	3	2.618034	2.618034	2.61803	2.618041
	3.5	3.186141	3.186141	-	3.186141

Table 4.5: Comparative estimation of mixed convection parameter λ for $-\theta'(0)$ if $\varepsilon = 1$,$\phi_1 = \phi_2 = Rd = M = Ec = \zeta_1 = \zeta_2 = S = 0$, $Bi \to \infty$,$\alpha = 0°$and Pr =1.

λ	Wahid *et al.* [85]	Alabdulhadi *et al.* [86]	Anuar *et al.* [87]	Rosca and pop [88]	Present (bvp4c)
	$-\theta'(0)$	$\theta'(0)$	$\theta'(0)$	$\theta'(0)$	$\theta'(0)$
0	1.000000	1.000008	1.000008	1.0000	1.0001
1	1.087278	1.087275	1.087275	1.0872	1.0870
5	1.252700	1.252700	-	-	1.2525
10	1.371564	1.371564	1.371564	1.3715	1.3715

Table 4.6: Parametric values were used in the present analysis.

Parameters	Symbol	Values
Eckert number	Ec	0.1, 0.2, 0.3
Prandtl number	Pr	6.2
Radiation Parameter	Rd	0.1,0.2, 0.3
Suction	S	2, 3
Mixed convection parameter	λ	-1, 1
Stretching parameter	ϵ	1
Space dependent parameter	ζ_1	0.1
Temperature dependent parameter	ζ_2	0.1
Volume fraction coefficient	ϕ_1	0.1
Volume fraction coefficient	ϕ_2	0.01, 0.1
Magnetic parameter	M	0.1, 0.5

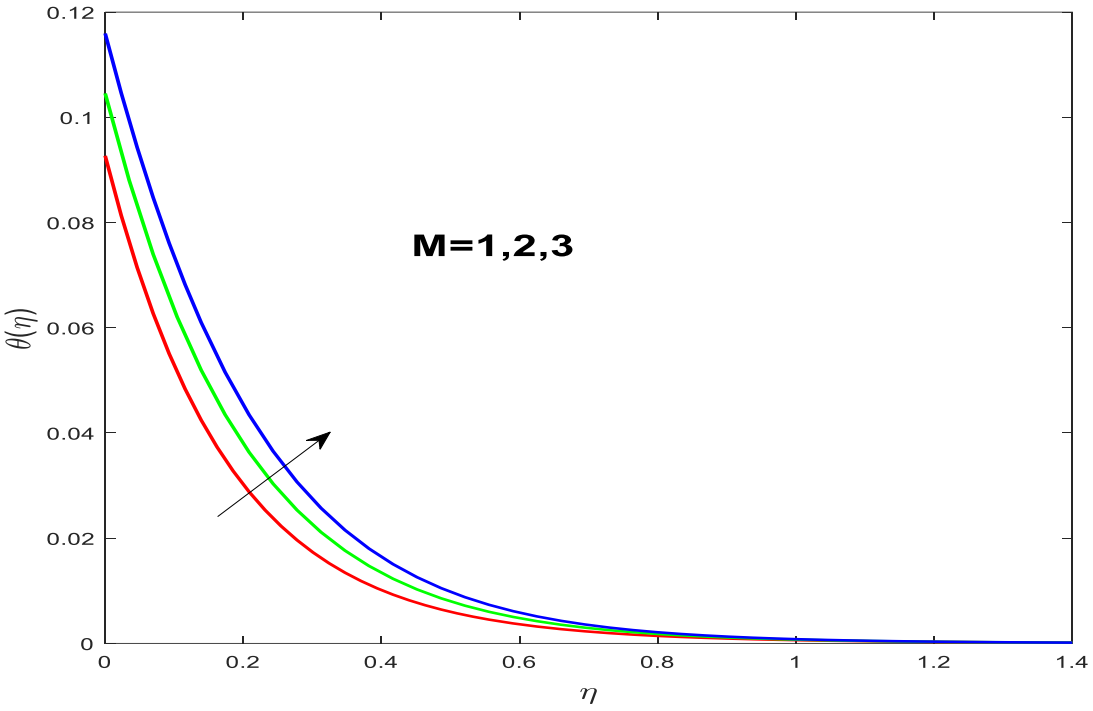

Fig. 4.2: $\theta(\eta)$ with altering quantities of *M*.

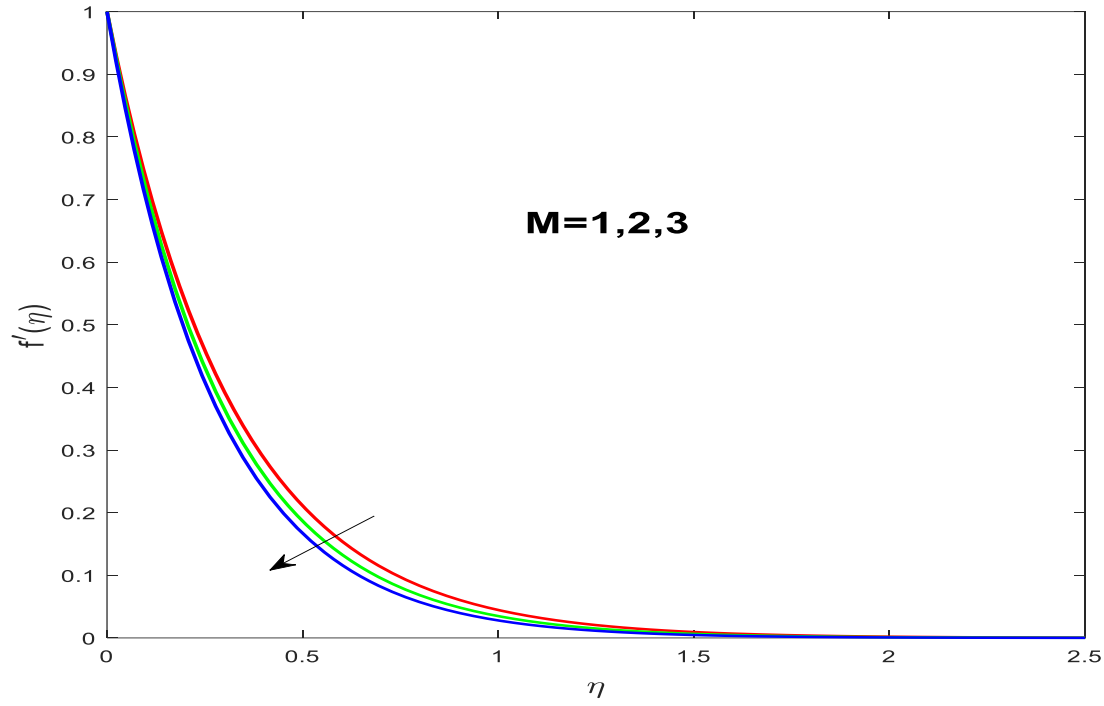

Fig. 4.3: $f'(\eta)$ with altering quantities of M.

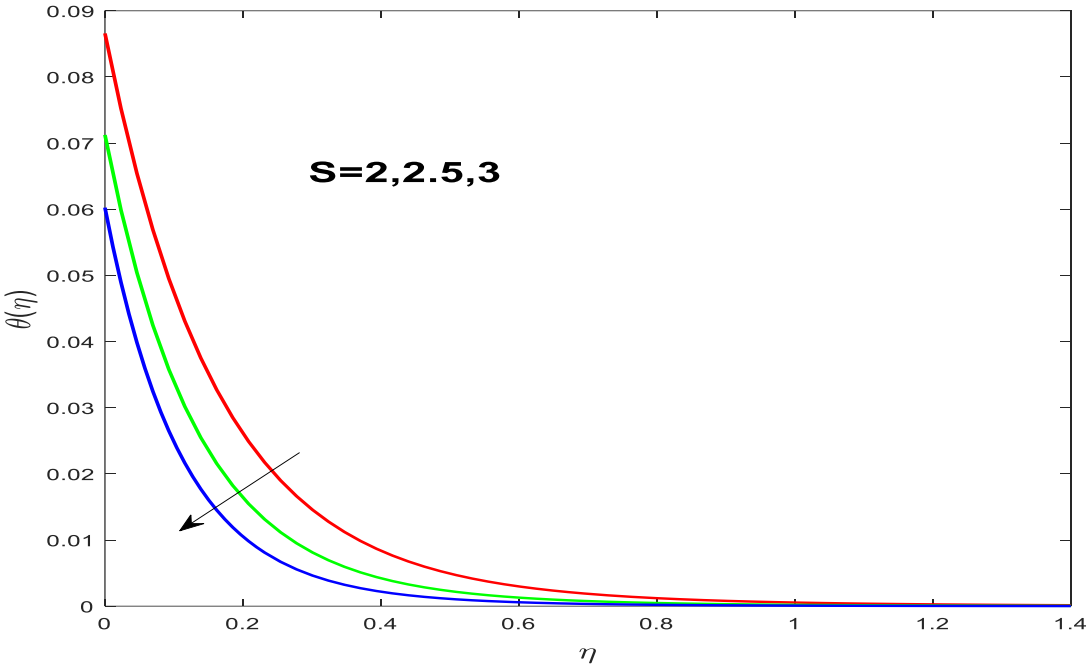

Fig. 4.4: $\theta(\eta)$ with altering quantities of S.

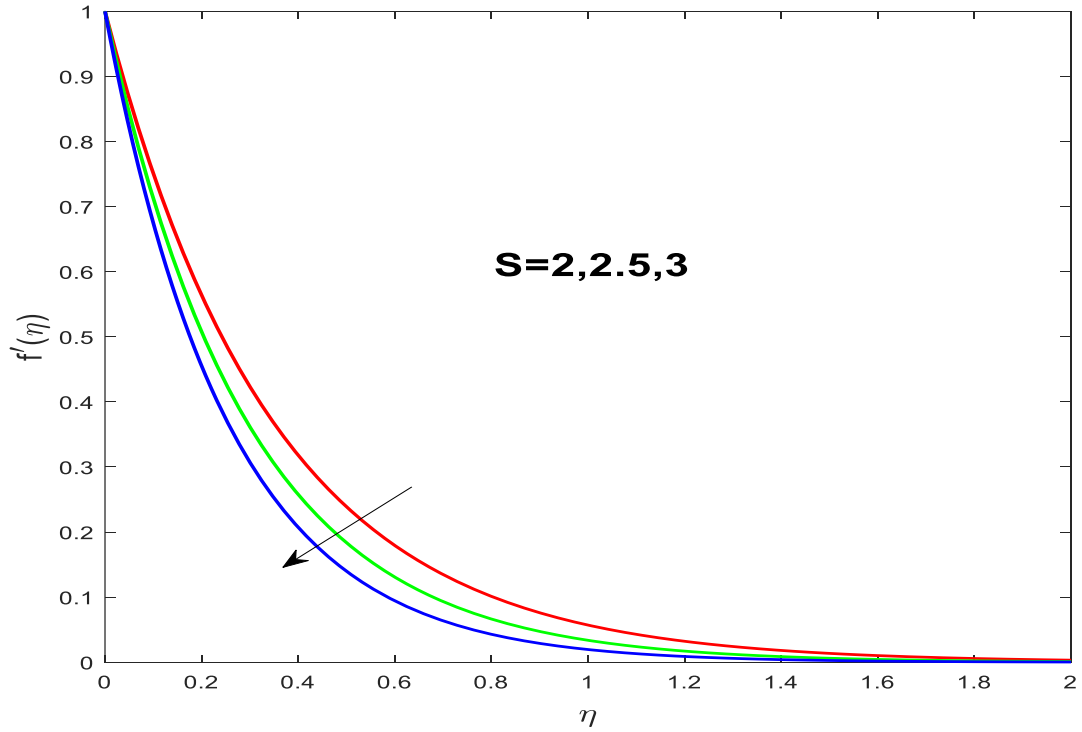

Fig. 4.5: $f'(\eta)$ with altering quantities of S.

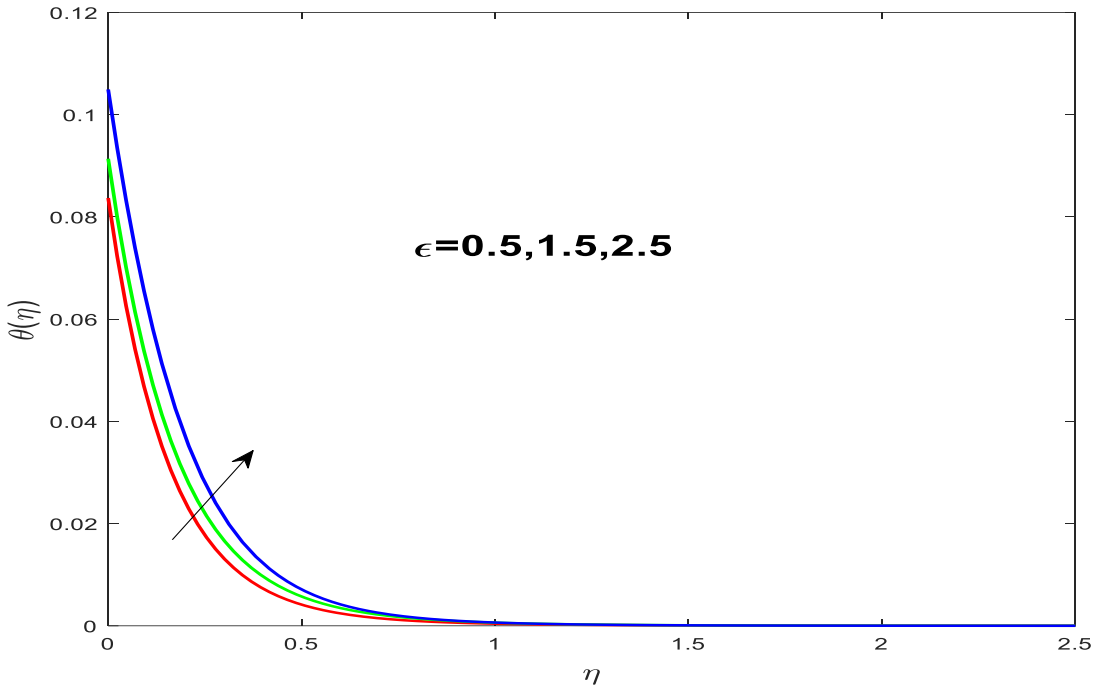

Fig. 4.6: $\theta(\eta)$ with altering quantities of ϵ.

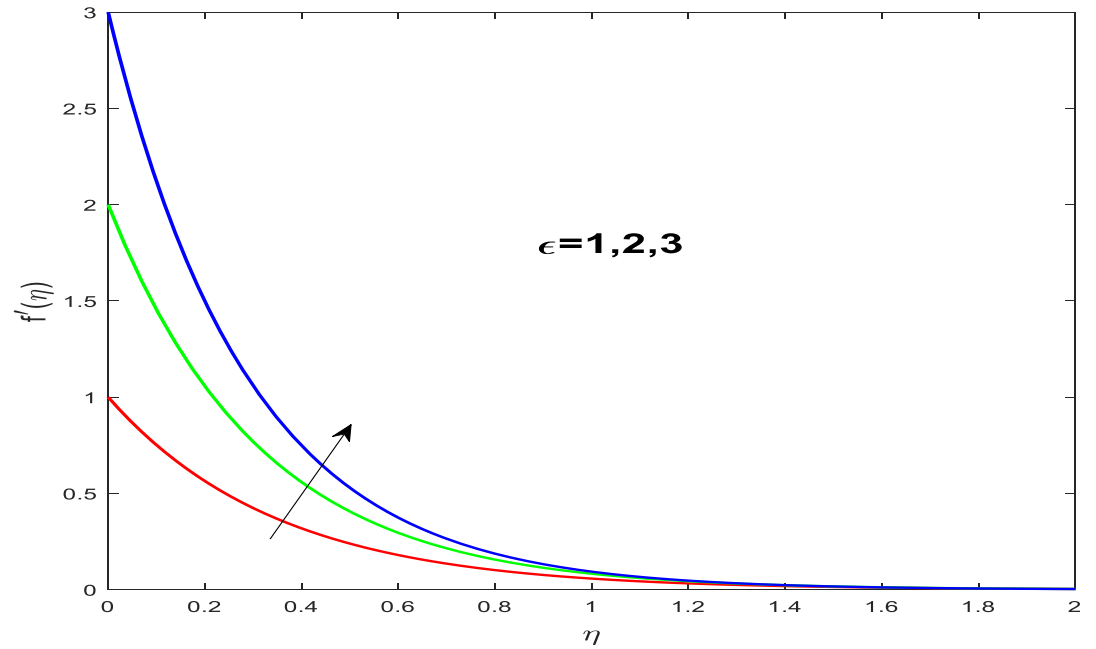

Fig. 4.7: $f'(\eta)$ with altering quantities of ϵ.

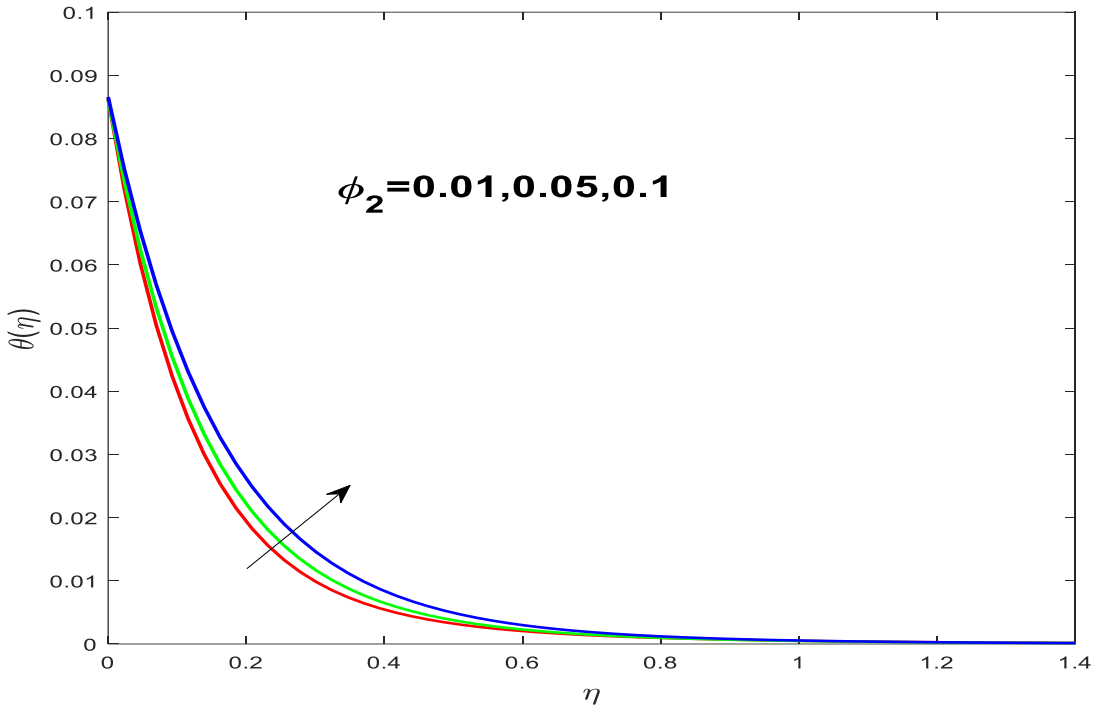

Fig.4.8: $\theta(\eta)$ with altering quantities of ϕ_2.

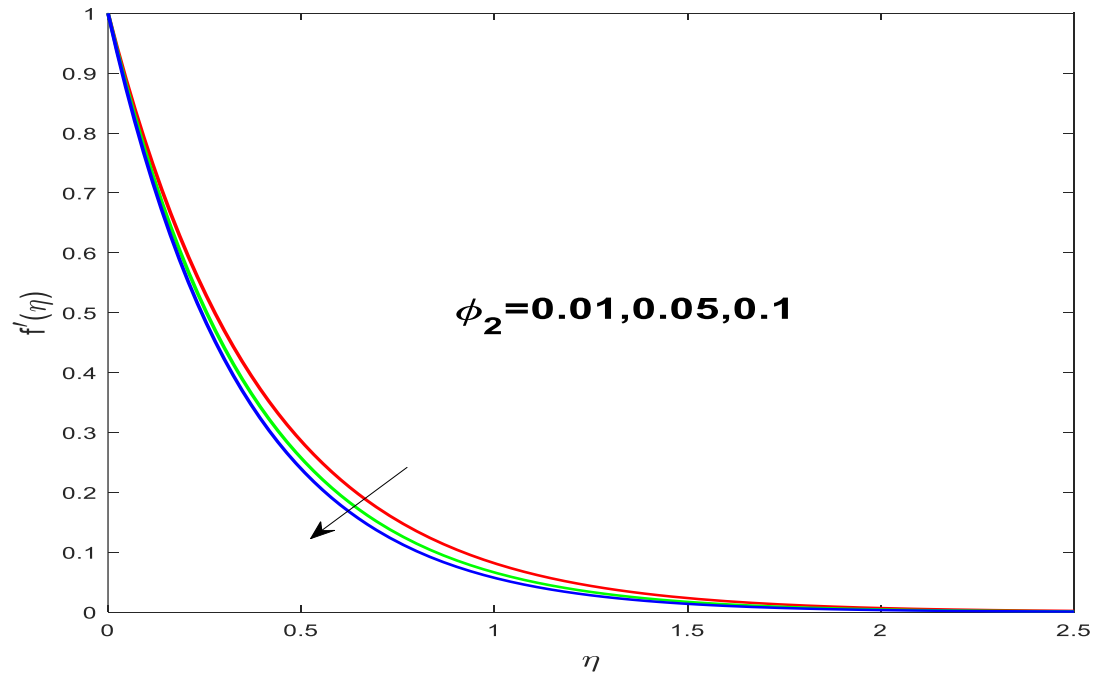

Fig. 4.9: $f'(\eta)$ with altering quantities of ϕ_2.

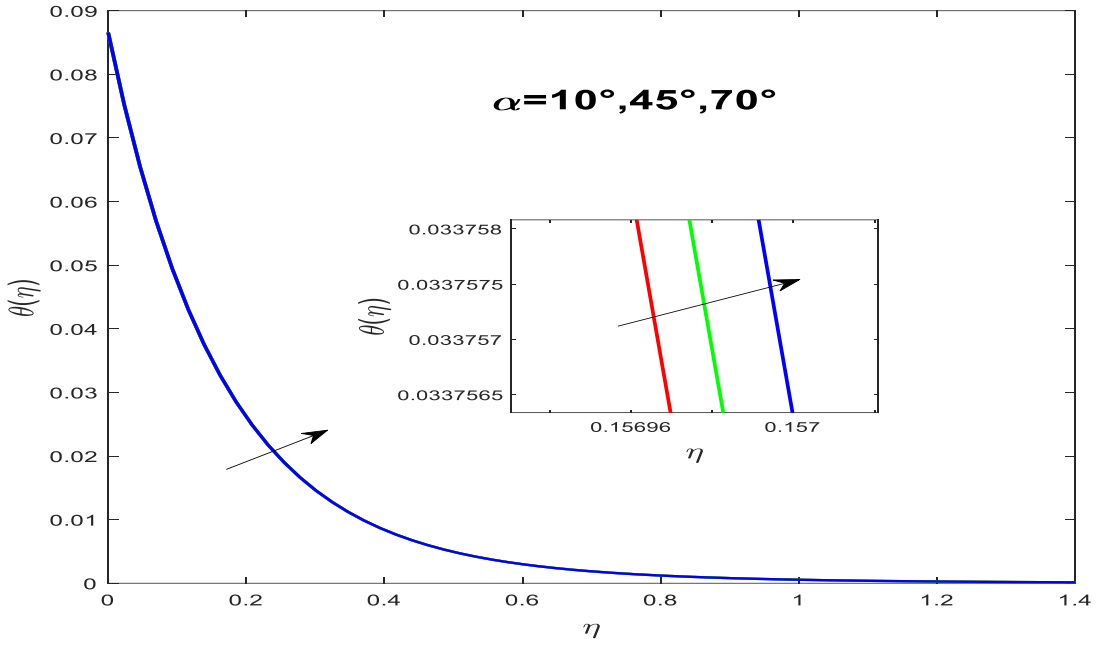

Fig. 4.10: $\theta(\eta)$ with altering quantities of α.

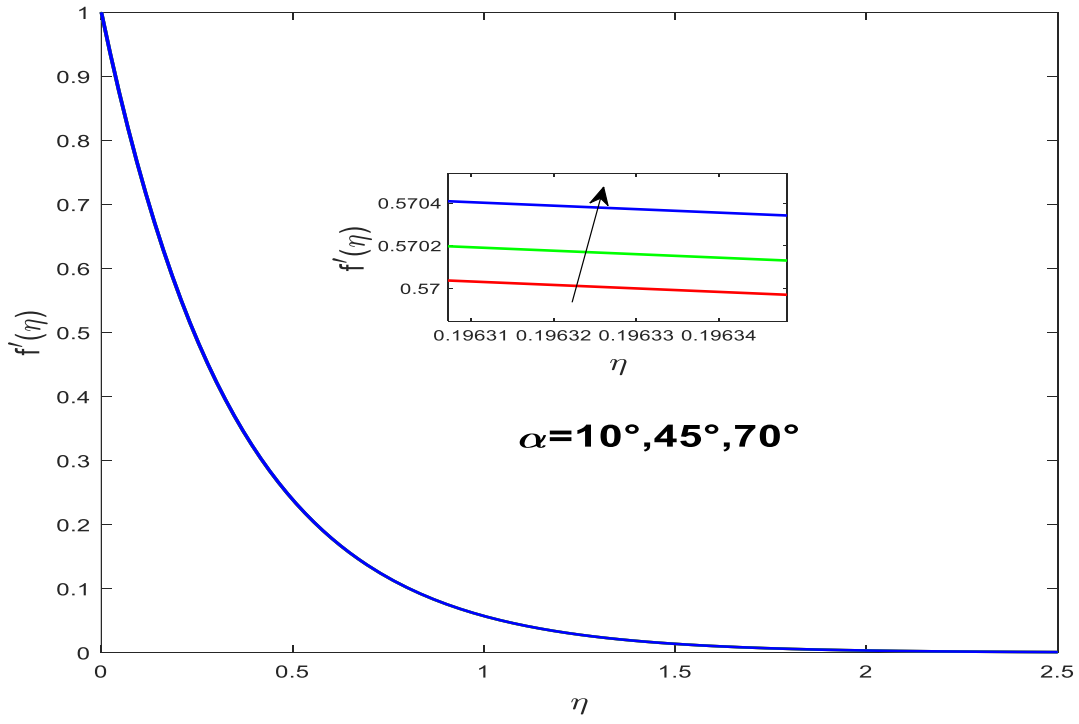

Fig. 4.11: $f'(\eta)$ with altering quantities of α.

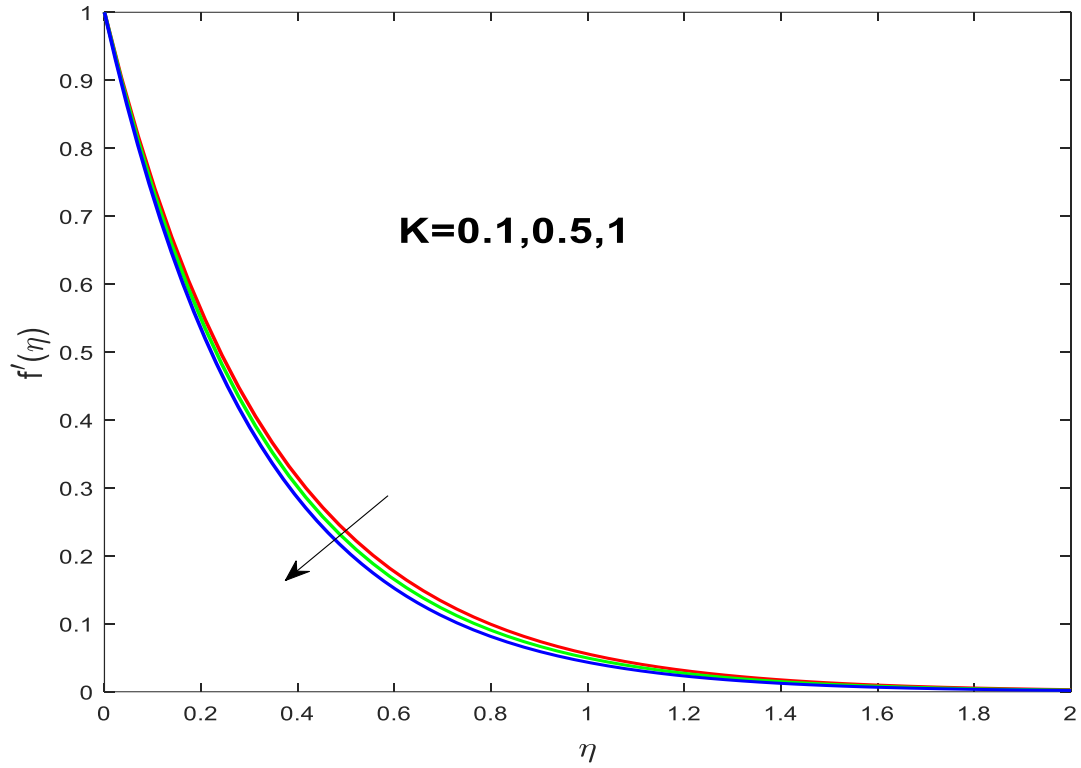

Fig. 4.12: $f'(\eta)$ with altering quantities of K.

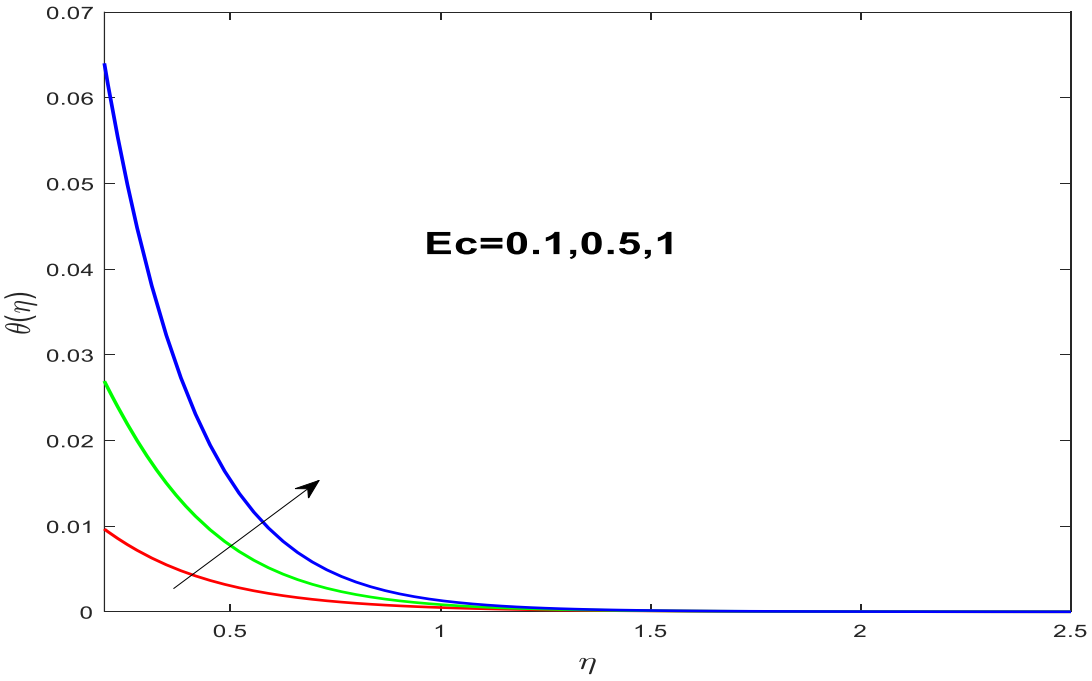

Fig. 4.13: $\theta(\eta)$ with altering quantities of Ec.

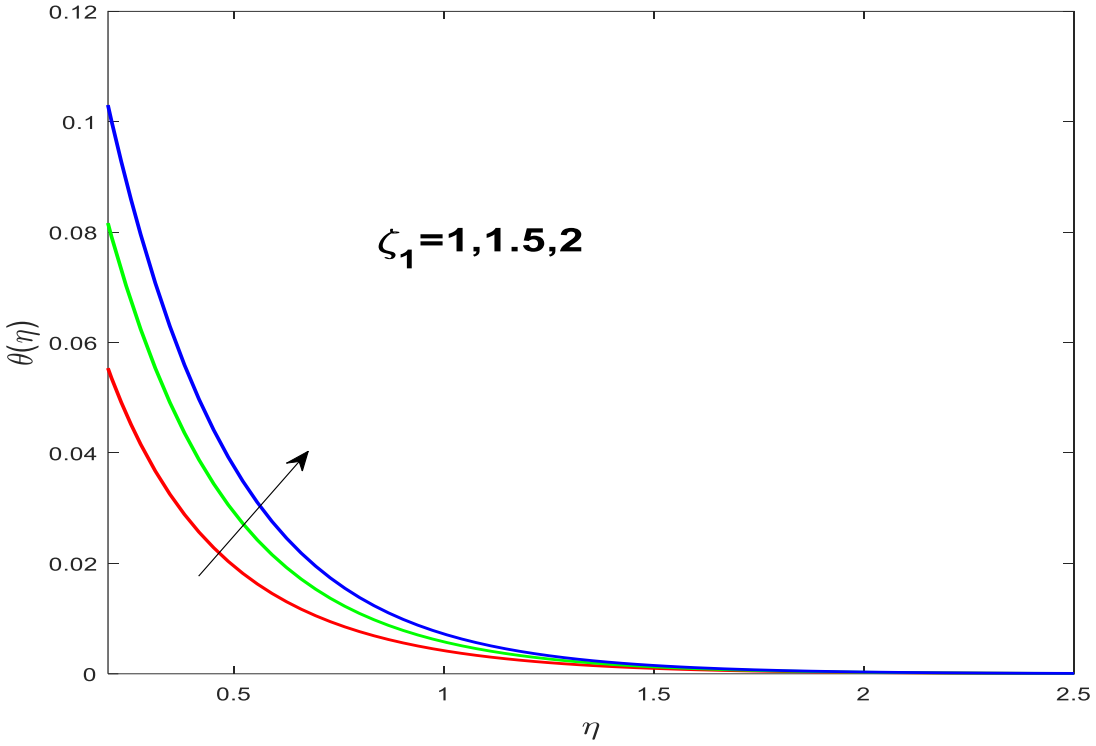

Fig. 4.14: $\theta(\eta)$ with altering quantities of ζ_1.

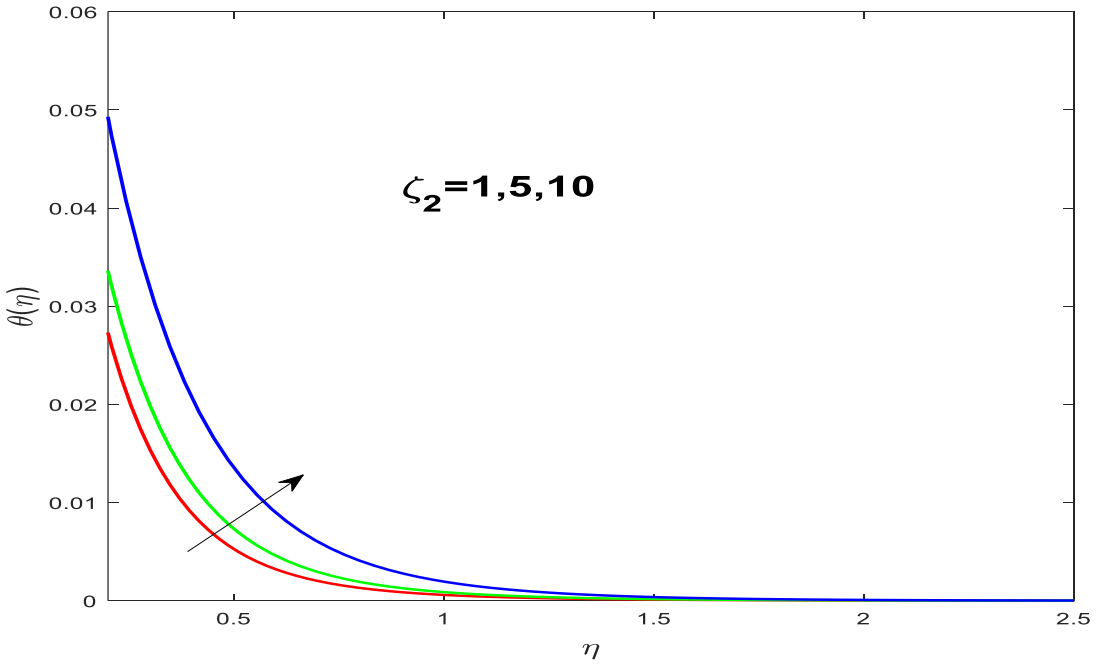

Fig. 4.15: $\theta(\eta)$ with altering quantities of ζ_2

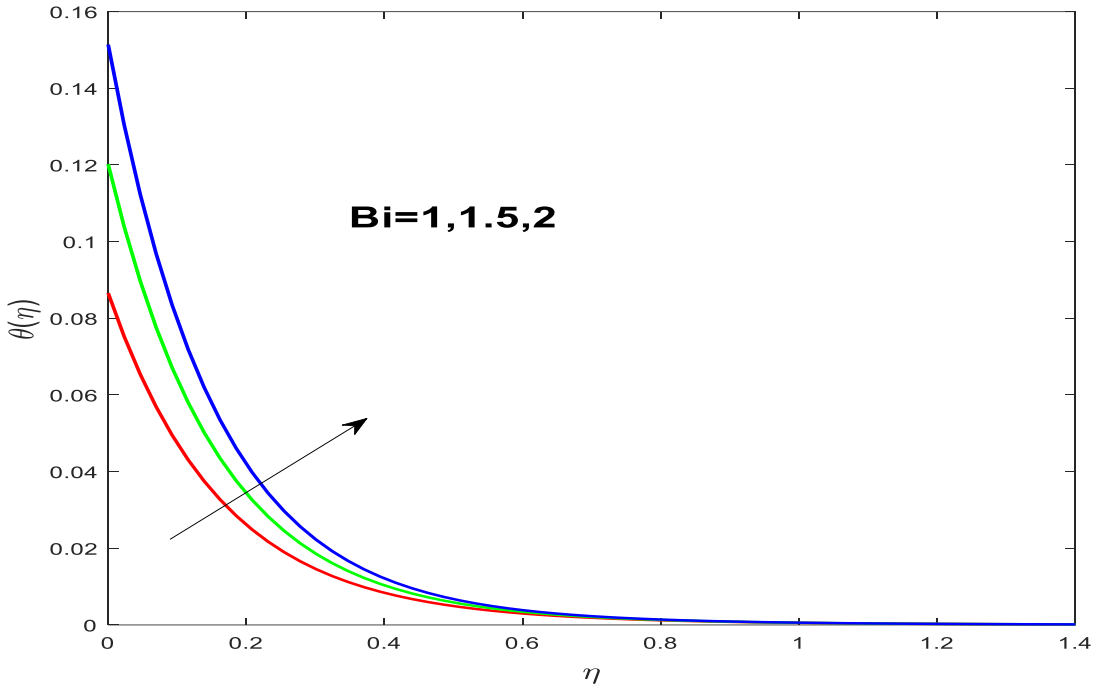

Fig. 4.16: $\theta(\eta)$ with altering quantities of Bi.

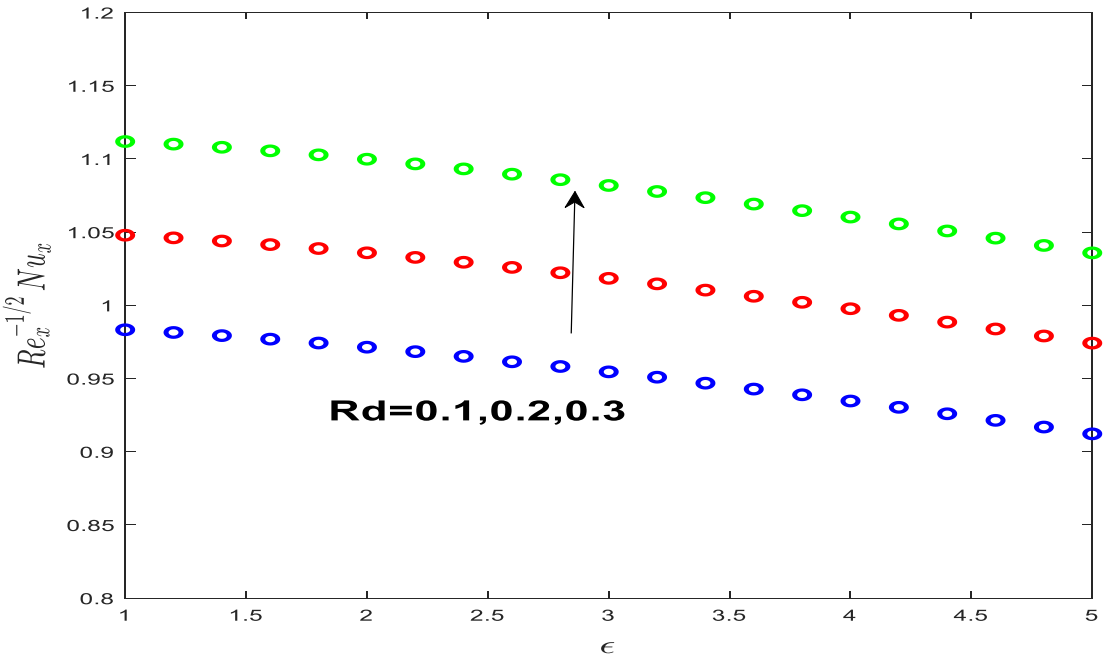

Fig. 4.17: Nusselt number towards ϵ with altering *Rd* quantities.

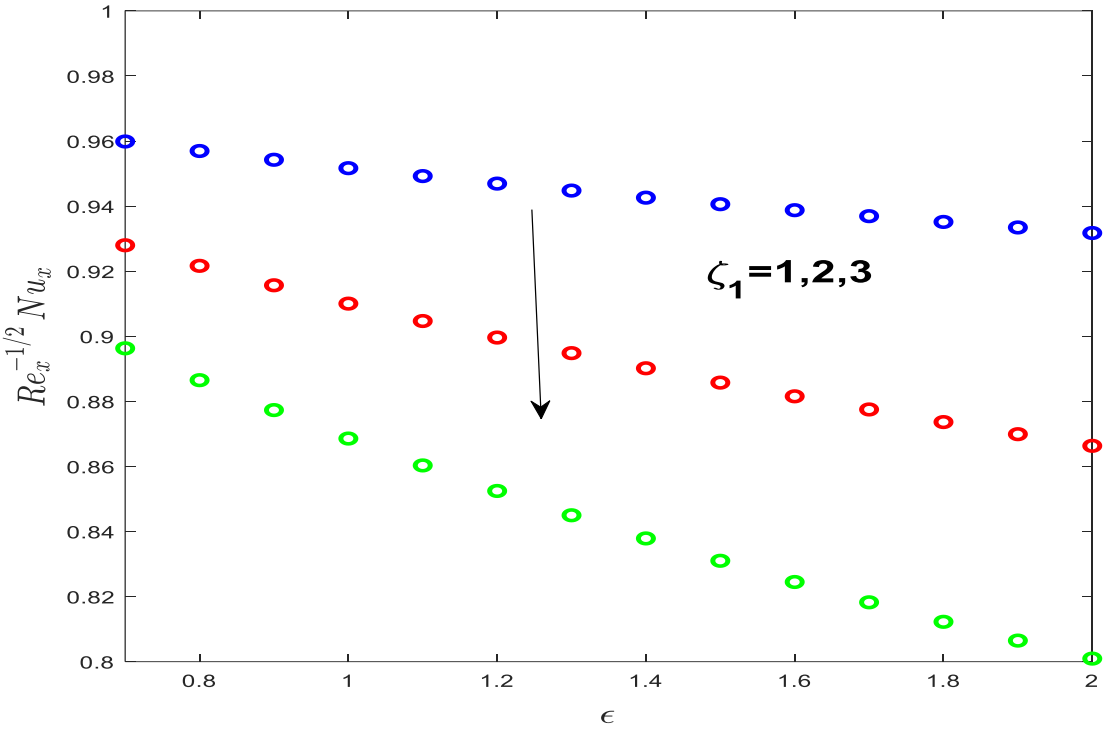

Fig. 4.18: Nusselt number towards ϵ with altering $\zeta_1$values.

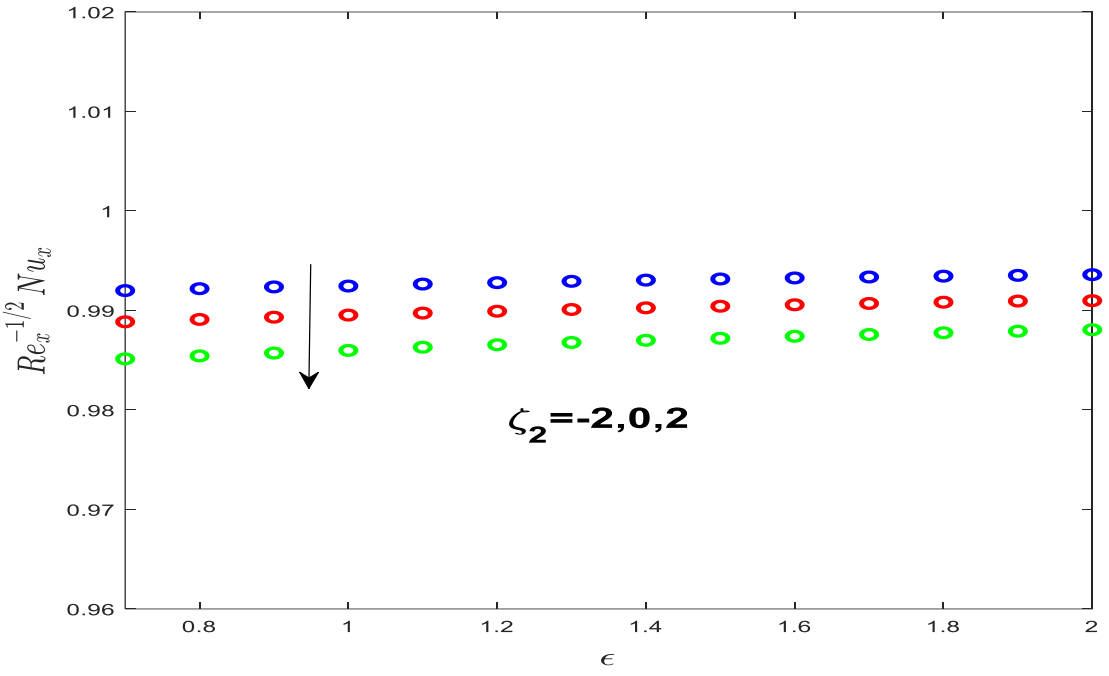

Fig. 4.19: Nusselt number towards ϵ with altering values of ζ_2.

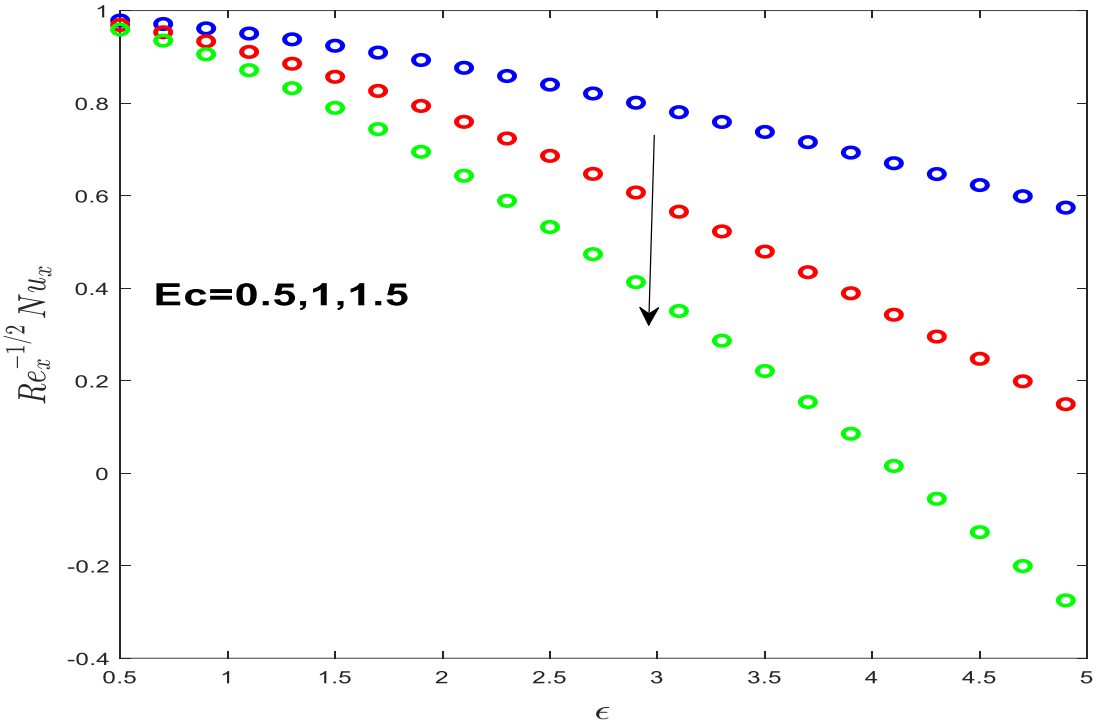

Fig. 4.20: Nusselt number towards ϵ with altering values of Ec.

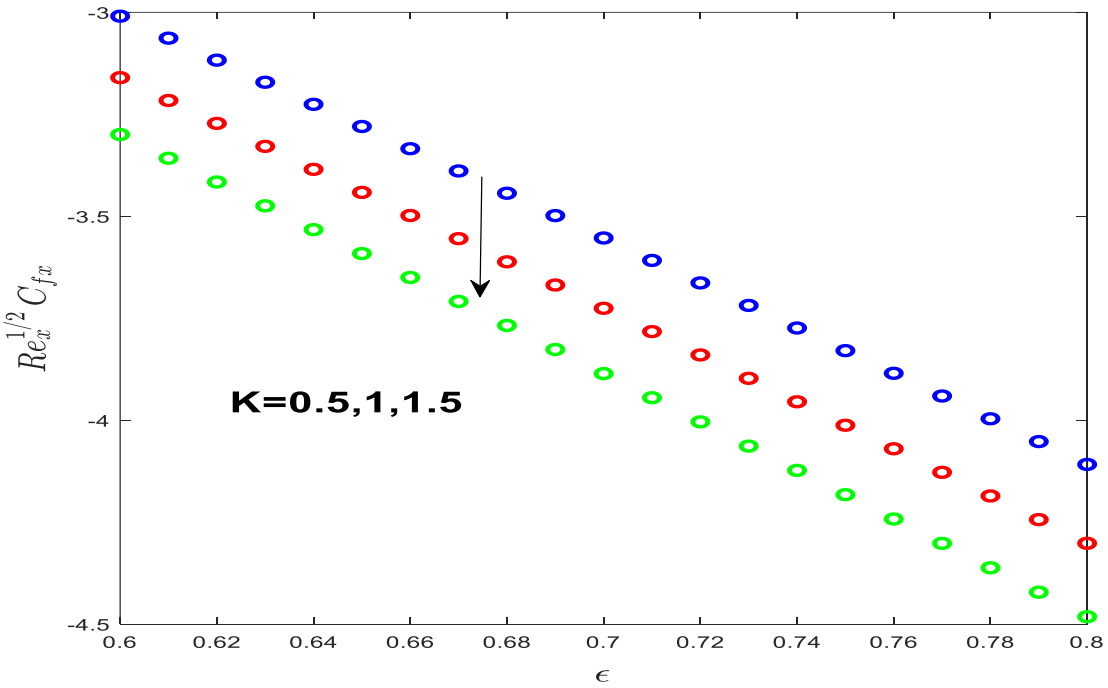

Fig. 4.21: Skin friction towards ϵ with altering K values.

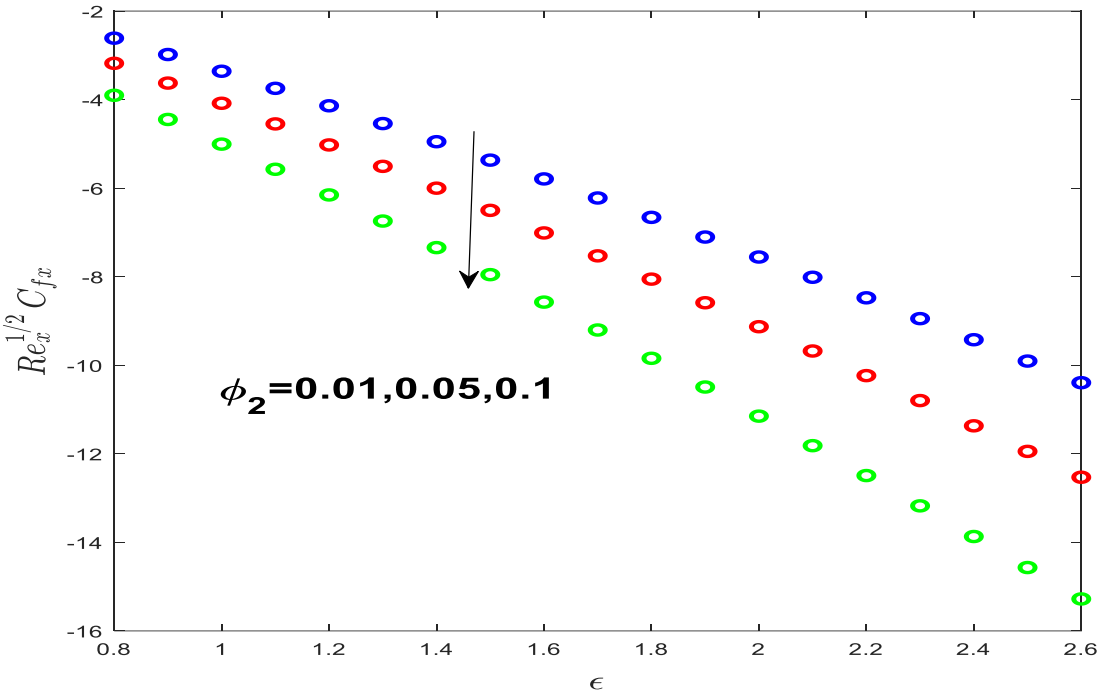

Fig. 4.22: Skin friction towards ϵ with altering ϕ_2 quantities.

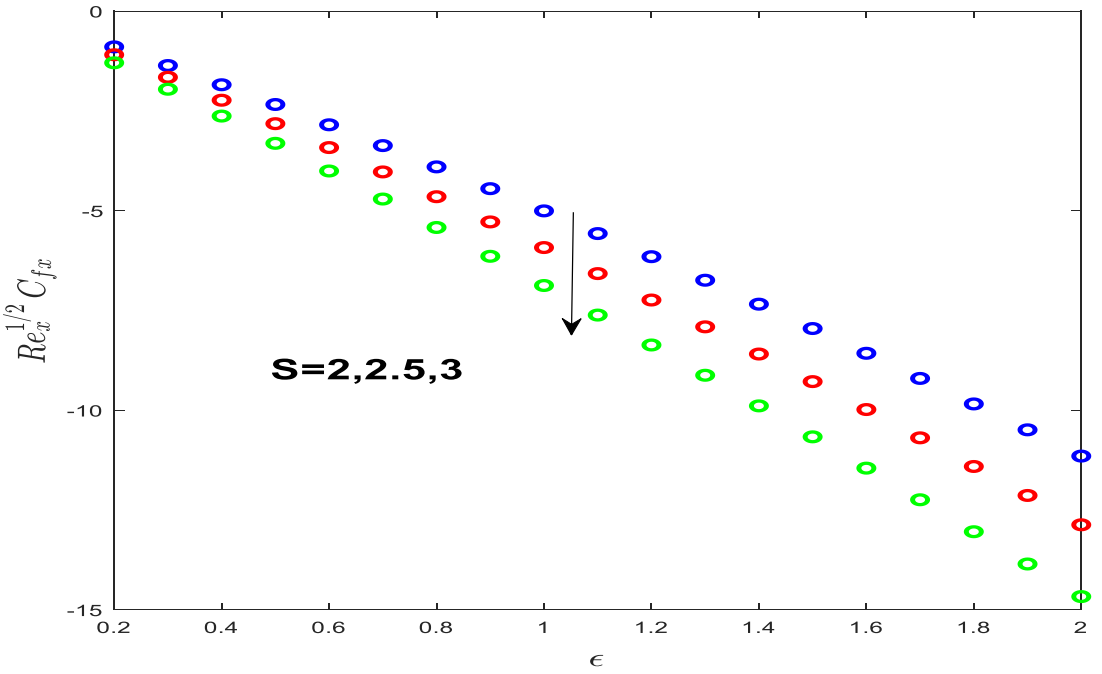

Fig. 4.23: Skin friction towards ϵ with altering S quantities.

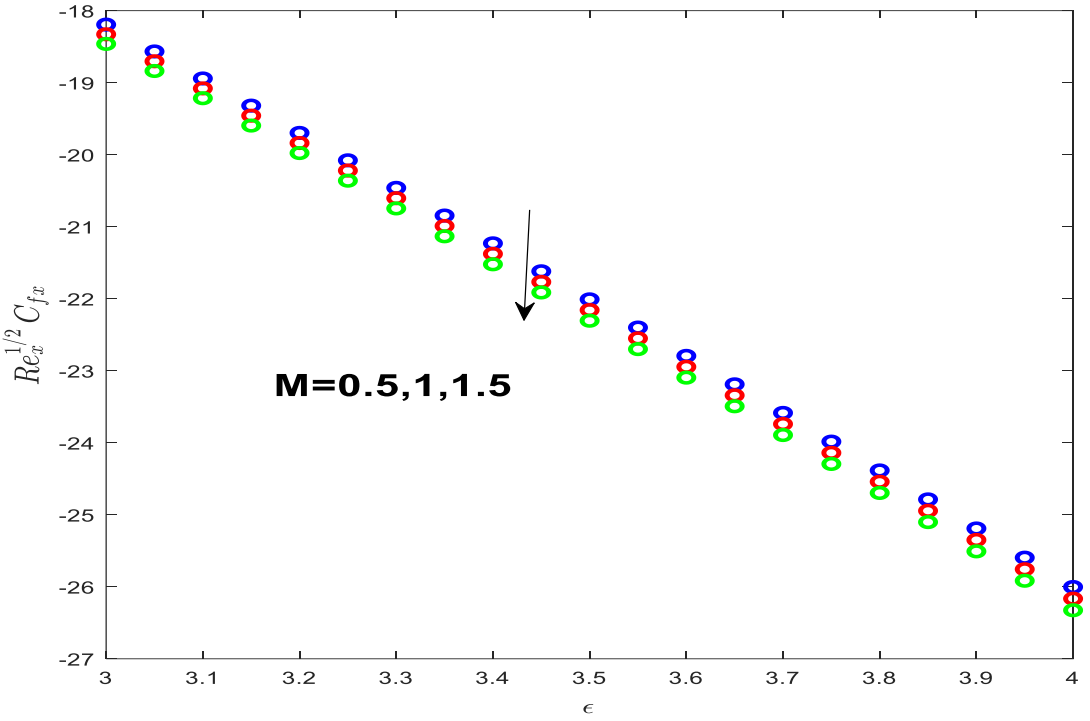

Fig. 4.24: Skin friction towards ϵ with altering M values.

Chapter 5

Conclusion and Future Work

5.1 Conclusion Remarks

There are multiple scientific and industrial applications for hybrid nanofluids, which enhance the effectiveness and functionality of different systems. The hybrid nanofluids have a various applications like in cooling systems, cancer treatment, vehicle power generation, chemical reactions and many more are among the technical and industrial uses for hybrid nanofluids. Numerous experimental investigations have revealed that, when compared to regular fluids and nanoliquids, hybrid nanoliquids show a higher heat transfer rate. By assisting more effective heat dissipation and thermal management, they aid in reducing the energy usage and operational costs. The usage of hybrid nanofluids offer higher thermal properties, stability, and versatility, thus providing novel possibilities for more effective and justifiable thermal controlling solutions in numerous technological fields. Keeping in view the applications of hybrid nanofluids, this study emphasizes on the flow of hybrid nanofluid through an inclined surface in a medium because of its numerous potential uses. A hybrid nanofluid built from Cu and Al_2O_3 nanoparticles with its basefluid as water, is examined for non-uniform absorption and generation of heat in relation to mixed convection, thermal radiation and Joule heating. The PDEs representing the fluid flow are reduced via the proper similarity transformation. Each of the partial differential equations that make up the fluid model's system of equations are reduced to a collection of ODEs. The mathematical examination of the problem using the Bvp4c function in MATLAB program has yielded some important findings. The research shows useful results from a detailed analysis of the flow under discussion. The velocity distribution declines as the solid volume fraction of copper oxide nanoparticles ϕ_2 rises. The similar behavior of

velocity profile is observed for suction parameter *S*, porosity parameter *K*, and the magnetic parameter *M*. The velocity profile experiences an upsurge for the rise in stretching parameter ε and inclination angle α. The temperature of the fluid is improved by the solid volume fraction of the nanoparticle copper oxide ϕ_2, stretching parameter ε, Biot number *Bi*, heat source/sink parameters ζ, Eckert number *Ec* and the inclination angle α, while increase in the magnetic parameter M and the suction parameter *S* show a decline in temperature distribution. A noticeable trend is seen for the Nusselt number, which rises for the higher values of the radiation parameter and reduces for Eckert number Ec, non-uniform heat source/sink parameters ζ and the stretching quantities ε, thus reducing the rate of heat transfer. The skin friction coefficient declines with the higher quantities of the magnetic parameter *M*, volume fraction of solid nanoparticles of copper oxide ϕ_2, porosity parameter and suction parameter.

6.2 Future Work

With assumptions taken into consideration, the influence of a hybrid nanofluid flowing by a linearly stretched inclined plate with the combined influence of nonuniform heat source and heat sink has been investigated in the current study. Nonetheless, this study paves the path for further intriguing initiatives. These intriguing researches could turn out to be significant in the future.

- Examination of a ternary hybrid nanofluid with inclined MHD over a cylinder in the precence of Ohmic heating.
- Investigation of the inclined MHD of the hybrid nanofluids over a stretched inclined cylinder with combined influence of ohmic heating.
- The inspection of ternary hybrid nanofluid's mixed convection flow with chemical reaction and activation energy.

References

[1] S. U. S. Choi and J. A. Eastman, *Enhancing Thermal Conductivity of Fluids with Nanoparticles*, Argonne National Lab., Argonne, IL, USA, Rep. ANL/MSD/CP-84938; CONF-951135-29, 1995.

[2] J. Sarkar, P. Ghosh, and A. Adil, "A review on hybrid nanofluids: recent research, development and applications," *Renew. Sustain. Energy Rev.*, vol. 43, pp. 164–177, Mar. 2015, doi: 10.1016/j.rser.2014.11.023.

[3] L. Yang, W. Ji, M. Mao, and J. Huang, "An updated review on the properties, fabrication and application of hybrid-nanofluids along with their environmental effects," *J. Cleaner Prod.*, vol. 257, p. 120408, Jun. 2020, doi: 10.1016/j.jclepro.2020.120408.

[4] M. Muneeshwaran, G. Srinivasan, P. Muthukumar, and C.-C. Wang, "Role of hybrid-nanofluid in heat transfer enhancement–A review," *Int. Commun. Heat Mass Transfer*, vol. 125, p. 105341, Jun. 2021, doi: 10.1016/j.icheatmasstransfer.2021.105341.

[5] Y. Yang, Z. G. Zhang, E. A. Grulke, W. B. Anderson, and G. Wu, "Heat transfer properties of nanoparticle-in-fluid dispersions (nanofluids) in laminar flow," *Int. J. Heat Mass Transfer*, vol. 48, no. 6, pp. 1107–1116, Mar. 2005, doi: 10.1016/j.ijheatmasstransfer.2004.09.038.

[6] S. Suresh, K. P. Venkitaraj, P. Selvakumar, and M. Chandrasekar, "Effect of Al_2O_3–Cu/water hybrid nanofluid in heat transfer," *Exp. Therm. Fluid Sci.*, vol. 38, pp. 54–60, Apr. 2012, doi: 10.1016/j.expthermflusci.2011.11.007.

[7] J. Sarkar, P. Ghosh, and A. Adil, "A review on hybrid nanofluids: recent research, development and applications," *Renew. Sustain. Energy Rev.*, vol. 43, pp. 164–177, Mar. 2015, doi: 10.1016/j.rser.2014.11.023.

[8] M. Shoaib et al., "Numerical investigation for rotating flow of MHD hybrid nanofluid with thermal radiation over a stretching sheet," *Sci. Rep.*, vol. 10, no. 1, p. 18533, Oct. 2020, doi: 10.1038/s41598-020-75254-8.

[9] A.Hussain et al., "Heat transport investigation of magneto-hydrodynamics (SWCNT-MWCNT) hybrid nanofluid under the thermal radiation regime," *Case Stud. Therm. Eng.*, vol. 27, p. 101244, Oct. 2021, doi: 10.1016/j.csite.2021.101244.

[10] M. Basavarajappa and D. Bhatta, "Unsteady nonlinear convective flow of a nanofluid over a vertical plate due to impulsive motion: Optimization and sensitivity analysis," *Int. Commun. Heat Mass Transfer*, vol. 134, p. 106036, May 2022, doi: 10.1016/j.icheatmasstransfer.2022.106036.

[11] K. N. Sneha, U. S. Mahabaleshwar, and S. Bhattacharyya, "An effect of thermal radiation on inclined MHD flow in hybrid nanofluids over a stretching/shrinking sheet," *J. Therm. Anal. Calorim.*, vol. 148, no. 7, pp. 2961–2975, Sep. 2023, doi: 10.1007/s10973-022-11552-9.

[12] R. Mahesh, U. S. Mahabaleshwar, P. V. Kumar, H. F. Öztop, and N. Abu-Hamdeh, "Impact of radiation on the MHD couple stress hybrid nanofluid flow over a porous sheet with viscous dissipation," *Results Eng.*, vol. 17, p. 100905, Mar. 2023, doi: 10.1016/j.rineng.2023.100905.

[13] A.K. Hussein et al., "A review of the application of hybrid nanofluids in solar still energy systems and guidelines for future prospects," *Sol. Energy*, vol. 272, p. 112485, Apr. 2024, doi: 10.1016/j.solener.2024.112485.

[14] Z. Mahmood, K. Rafique, U. Khan, M. Abd El-Rahman, and R. Alharbi, "Analysis of mixed convective stagnation point flow of hybrid nanofluid over sheet with variable thermal conductivity and slip conditions: A model-based study," *Int. J. Heat Fluid Flow*, vol. 106, p. 109296, Apr. 2024, doi: 10.1016/j.ijheatfluidflow.2024.109296.

[15] Z. Mahmood, F. Z. Duraihem, A. Adnan, U. Khan, and A. M. Hassan, "Model-based comparative analysis of MHD stagnation point flow of hybrid nanofluid over a stretching sheet with suction and viscous dissipation," *Numer. Heat Transfer B*, pp. 1–22, Feb. 2024, doi: 10.1080/10407782.2024.2321519.

[16] Z. Mahmood et al., "Heat transfer in radiative hybrid nanofluids over moving sheet with porous media and slip conditions: Numerical analysis of variable viscosity and thermal conductivity," *Mater. Today Commun.*, vol. 40, p. 109664, Aug. 2024, doi: 10.1016/j.mtcomm.2024.109664.

[17] A.Ali, S. Hussain, and M. Ashraf, "Theoretical investigation of unsteady MHD flow of Casson hybrid nanofluid in porous medium: Applications of thermal radiations and nanoparticle," *J. Radiat. Res. Appl. Sci.*, vol. 17, no. 3, p. 101029, Sep. 2024, doi: 10.1016/j.jrras.2024.101029.

[18] S. Khalil, H. Yasmin, T. Abbas, and T. Muhammad, "Analysis of thermal conductivity variation in magneto-hybrid nanofluids flow through porous medium with variable viscosity and slip boundary," *Case Stud. Therm. Eng.*, vol. 57, p. 104314, May. 2024, doi: 10.1016/j.csite.2024.104314.

[19] L. A. Lund, U. Yashkun, and N. A. Shah, "Multiple solutions of unsteady Darcy–Forchheimer porous medium flow of Cu–Al_2O_3/water based hybrid nanofluid with joule heating and viscous dissipation effect," *J. Therm. Anal. Calorim.*, vol. 149, no. 5, pp. 2303–2315, Jan. 2024, doi: 10.1007/s10973-023-12819-5.

[20] A.Abd-Elmonem et al., "Thermal characteristics of hybrid nanofluid (Cu-Al_2O_3) flow through Darcy porous medium with chemical effects via numerical successive over relaxation technique," *Case Stud. Therm. Eng.*, vol. 65, p. 105538, Jan. 2025, doi: 10.1016/j.csite.2024.105538.

[21] M. M. Molla, M. F. Hasan, and M. M. Islam, "Elucidating thermal phenomena of non-Newtonian experimental data based copper-alumina-ethylene glycol hybrid nanofluid in a cubic enclosure with central heated plate by machine learning validations of D3Q27 MRT-LBM," *Int. J. Thermofluids*, vol. 26, p. 101033, Mar. 2025, doi: 10.1016/j.ijft.2024.101033.

[22] A.Raza, U. Khan, A. Zaib, A. Ishak, and S. M. Hussain, "Insights into the thermodynamic efficiency of mixed convective hybrid nanofluid flow over a vertical channel through a fractal fractional computation," *Multidiscip. Model. Mater. Struct.*, Jan. 2025, doi: 10.1108/MMMS-04-2024-0104.

[23] H. Alfvén, "Existence of electromagnetic-hydrodynamic waves," *Nature*, vol. 150, no. 3805, pp. 405–406, Oct. 1942, doi: 10.1038/150405d0.

[24] M. Ramzan et al., "Computational assessment of Carreau ternary hybrid nanofluid influenced by MHD flow for entropy generation," *J. Magn. Magn. Mater.*, vol. 567, p. 170353, Feb. 2023, doi: 10.1016/j.jmmm.2023.170353.

[25] J. Jang and S. S. Lee, "Theoretical and experimental study of MHD (magnetohydrodynamic) micropump," *Sens. Actuators A Phys.*, vol. 80, no. 1, pp. 84–89, Mar. 2000, doi: doi.org/10.1016/S0924-4247(99)00302-7.

[26] J. Wu, "Generalized MHD equations," *J. Differ. Equ.*, vol. 195, no. 2, pp. 284–312, Dec. 2003, doi: 10.1016/j.jde.2003.07.007.

[27] A.Raptis and C. Perdikis, "Viscous flow over a non-linearly stretching sheet in the presence of a chemical reaction and magnetic field," *Int. J. Non-Linear Mech.*, vol. 41, no. 4, pp. 527–529, May 2006, doi: 10.1016/j.ijnonlinmec.2005.12.003.

[28] A.K. V. Prasad, K. Vajravelu, and P. S. Datti, "The effects of variable fluid properties on the hydro-magnetic flow and heat transfer over a non-linearly stretching sheet," *Int. J. Therm. Sci.*, vol. 49, no. 3, pp. 603–610, Mar. 2010, doi: 10.1016/j.ijthermalsci.2009.08.005.

[29] M. A. A. Hamad, "Analytical solution of natural convection flow of a nanofluid over a linearly stretching sheet in the presence of magnetic field," *Int. Commun. Heat Mass Transfer*, vol. 38, no. 4, pp. 487–492, Apr. 2011, doi: 10.1016/j.icheatmasstransfer.2010.12.042.

[30] B. Jalilpour, S. Jafarmadar, D. D. Ganji, A. B. Shotorban, and H. Taghavifar, "Heat generation/absorption on MHD stagnation flow of nanofluid towards a porous stretching sheet with prescribed surface heat flux," *J. Mol. Liq.*, vol. 195, pp. 194–204, Jul. 2014, doi: 10.1016/j.molliq.2014.02.021.

[31] T. Hayat, S. Bibi, M. Rafiq, A. Alsaedi, and F. M. Abbasi, "Effect of an inclined magnetic field on peristaltic flow of Williamson fluid in an inclined channel with convective conditions," *J. Magn. Magn. Mater.*, vol. 401, pp. 733–745, Mar. 2016, doi: 10.1016/j.jmmm.2015.10.107.

[32] N. Abbas, S. Nadeem, A. Saleem, M. Y. Malik, A. Issakhov, and F. M. Alharbi, "Models base study of inclined MHD of hybrid nanofluid flow over nonlinear stretching cylinder," *Chin. J. Phys.*, vol. 69, pp. 109–117, Feb. 2021, doi: 10.1016/j.cjph.2020.11.019.

[33] P. K. Dadheech et al., "Entropy analysis for radiative inclined MHD slip flow with heat source in porous medium for two different fluids," *Case Stud. Therm. Eng.*, vol. 28, p. 101491, Dec. 2021, doi: 10.1016/j.csite.2021.101491.

[34] F. A. Soomro, M. Usman, S. El-Sapa, M. Hamid, and R. U. Haq, "Numerical study of heat transfer performance of MHD Al_2O_3–Cu/water hybrid nanofluid flow over inclined surface," *Arch. Appl. Mech.*, vol. 92, no. 9, pp. 2757–2765, Jul. 2022, doi: 10.1007/s00419-022-02214-1.

[35] M. Khazayinejad and S. S. Nourazar, "Space-fractional heat transfer analysis of hybrid nanofluid along a permeable plate considering inclined magnetic field," *Sci. Rep.*, vol. 12, no. 1, p. 5220, Mar. 2022, doi: 10.1038/s41598-022-09179-9.

[36] K. N. Sneha, U. S. Mahabaleshwar, and S. Bhattacharyya, "An effect of thermal radiation on inclined MHD flow in hybrid nanofluids over a stretching/shrinking sheet," *J. Therm. Anal. Calorim.*, vol. 148, no. 7, pp. 2961–2975, Sep. 2023, doi: 10.1007/s10973-022-11552-9.

[37] E. A. Algehyne, A. Al-Bossly, F. S. Alduais, M. Y. Almusawa, and A. Saeed, "Significance of the inclined magnetic field on the water-based hybrid nanofluid flow over a nonlinear stretching sheet," *Nanotechnology*, vol. 34, no. 21, p. 215401, Mar. 2023, doi: 10.1088/1361-6528/acbda1.

[38] M. Yasin, S. Hina, and R. Naz, "Influence of inclined magnetic field on peristaltic flow of Ag–Cu/blood hybrid nanofluid in the presence of homogeneous–heterogeneous reactions with slip condition," *Arab. J. Sci. Eng.*, vol. 48, no. 1, pp. 31–46, Jun. 2023, doi: 10.1007/s13369-022-06942-y.

[39] A.M. Galal et al., "Numerical investigation of heat and mass transfer in three-dimensional MHD nanoliquid flow with inclined magnetization," *Sci. Rep.*, vol. 14, no. 1, p. 1207, Jan. 2024, doi: 10.1038/s41598-024-51195-4.

[40] S. Kirusakthika, S. Priya, A. A. Hakeem, and B. Ganga, "MHD slip effects on (50:50) hybrid nanofluid flow over a moving thin inclined needle with consequences of non-linear thermal radiation, viscous dissipation, and inclined Lorentz force," *Math. Comput. Simul.*, vol. 222, pp. 50–66, Aug. 2024, doi: 10.1016/j.matcom.2023.07.015.

[41] M. B. Jeelani, A. Abbas, and N. A. Alqahtani, "Thermal Transportation in Heat Generating and Chemically Reacting MHD Maxwell Hybrid Nanofluid Flow Past Inclined Stretching Porous Sheet in Porous Medium with Solar Radiation Effects," *Processes*, vol. 12, no. 6, p. 1196, Jun. 2024, doi: 10.3390/pr12061196.

[42] U. S. Mahabaleshwar, S. M. Sachhin, L. M. Pérez, and H. F. Oztop, "An impact of inclined MHD on biviscosity Bingham hybrid nanofluid flow over porous stretching/shrinking sheet with heat transfer," *J. Mol. Liq.*, vol. 398, p. 124244, Mar. 2024, doi: 10.1016/j.molliq.2024.124244.

[43] S. Yadav, S. Yadav, and P. K. Yadav, "The mixed convection thermally radiated hybrid nanofluid flow through an inclined permeable shrinking plate with slip condition and inclined magnetic effect," *Chin. J. Phys.*, vol. 89, pp. 1041–1050, Jun. 2024, doi: 10.1016/j.cjph.2023.12.039.

[44] H. Risken, *The Fokker-Planck Equation*, 2nd ed. Berlin, Germany: Springer, 1996, doi: 10.1007/978-3-642-61544-3_4.

[45] A. Mohammadein and M. F. El-Amin, "Thermal radiation effects on power-law fluids over a horizontal plate embedded in a porous medium," *Int. Commun. Heat Mass Transf.*, vol. 27, no. 7, pp. 1025–1035, Oct. 2000, doi: 10.1016/S0735-1933(00)00182-2.

[46] S. Basu, Z. M. Zhang, and C. J. Fu, “Review of near-field thermal radiation and its application to energy conversion,” *Int. J. Energy Res.*, vol. 33, no. 13, pp. 1203–1232, Sep. 2009, doi: **10.1002/er.1607**.

[47] E. Haile and B. Shankar, “Boundary-layer flow of nanofluids over a moving surface in the presence of thermal radiation, viscous dissipation and chemical reaction,” *Appl. Appl. Math.*, vol. 10, no. 2, p. 21, 2015.

[48] A. Hakeem, N. V. Ganesh, and B. Ganga, “Magnetic field effect on second order slip flow of nanofluid over a stretching/shrinking sheet with thermal radiation effect,” *J. Magn. Magn. Mater.*, vol. 381, pp. 243–257, May 2015, doi: 10.1016/j.jmmm.2014.12.010.

[49] A.S. Dogonchi and D. D. Ganji, “Investigation of MHD nanofluid flow and heat transfer in a stretching/shrinking convergent/divergent channel considering thermal radiation,” *J. Mol. Liq.*, vol. 220, pp. 592–603, Aug. 2016, doi: 10.1016/j.molliq.2016.05.022.

[50] T. Hayat and S. Nadeem, “Heat transfer enhancement with Ag–CuO/water hybrid nanofluid,” *Results Phys.*, vol. 7, pp. 2317–2324, 2017, doi: 10.1016/j.rinp.2017.06.034.

[51] Y. S. Daniel, Z. A. Aziz, Z. Ismail, and F. Salah, "Entropy analysis in electrical magnetohydrodynamic (MHD) flow of nanofluid with effects of thermal radiation, viscous dissipation, and chemical reaction," *Theoretical and Applied Mechanics Letters*, vol. 7, no. 4, pp. 235-242, 2017, doi: 10.1016/j.taml.2017.06.003.

[52] Z. Iqbal, N. S. Akbar, E. Azhar, and E. N. Maraj, "Performance of hybrid nanofluid (Cu-CuO/water) on MHD rotating transport in oscillating vertical channel inspired by Hall current and thermal radiation," *Alexandria Engineering Journal*, vol. 57, no. 3, pp. 1943-1954, Sep. 2018, doi: 10.1016/j.aej.2017.03.047.

[53] M. Shoaib, M. A. Z. Raja, M. T. Sabir, S. Islam, Z. Shah, P. Kumam, and H. Alrabaiah, "Numerical investigation for rotating flow of MHD hybrid nanofluid with thermal radiation over a stretching sheet," *Scientific Reports*, vol. 10, no. 1, p. 18533, Oct. 2020, doi: 10.1038/s41598-020-75254-8.

[54] U. Yashkun, K. Zaimi, N. A. Abu Bakar, A. Ishak, and I. Pop, "MHD hybrid nanofluid flow over a permeable stretching/shrinking sheet with thermal radiation effect," *International Journal of Numerical Methods for Heat & Fluid Flow*, vol. 31, no. 3, pp. 1014-1031, Jul. 2021, doi: 10.1108/HFF-02-2020-0083.

[55] M. F. Md Basir, J. Mackolil, B. Mahanthesh, K. S. Nisar, T. Muhammad, N. S. Anuar, and N. Bachok, "Stability and statistical analysis on melting heat transfer in a hybrid nanofluid with thermal radiation effect," *Proceedings of the Institution of Mechanical*

Engineers, Part E: Journal of Process Mechanical Engineering, vol. 235, no. 6, pp. 2129-2140, Aug. 2021, doi: 10.1177/09544089211033161.

[56] I. Waini, A. Jamaludin, R. Nazar, and I. Pop, "MHD flow and heat transfer of a hybrid nanofluid past a nonlinear surface stretching/shrinking with effects of thermal radiation and suction," *Chinese Journal of Physics*, vol. 79, pp. 13-27, Oct. 2022, doi: 10.1016/j.cjph.2022.06.026.

[57] H. Waqas, U. Farooq, D. Liu, M. Abid, M. Imran, and T. Muhammad, "Heat transfer analysis of hybrid nanofluid flow with thermal radiation through a stretching sheet: A comparative study," *International Communications in Heat and Mass Transfer*, vol. 138, p. 106303, Nov. 2022, doi: 10.1016/j.icheatmasstransfer.2022.106303.

[58] A. Asghar, L. A. Lund, Z. Shah, N. Vrinceanu, W. Deebani, and M. Shutaywi, "Effect of thermal radiation on three-dimensional magnetized rotating flow of a hybrid nanofluid," *Nanomaterials*, vol. 12, no. 9, p. 1566, May 2022, doi: 10.3390/nano12091566.

[59] Z. H. Khan, W. A. Khan, S. M. Ibrahim, K. Swain, and Z. Huang, "Impact of multiple slips and thermal radiation on heat and mass transfer in MHD Maxwell hybrid nanofluid flow over porous stretching sheet," *Case Studies in Thermal Engineering*, vol. 61, p. 104906, Sep. 2024, doi: 10.1016/j.csite.2024.104906.

[60] S. M. Muhammad Raza Shah Naqvi, U. Manzoor, H. Waqas, D. Liu, H. Naeem, S. M. Eldin, and T. Muhammad, "Numerical investigation of thermal radiation with entropy generation effects in hybrid nanofluid flow over a shrinking/stretching sheet," *Nanotechnology Reviews*, vol. 13, no. 1, p. 20230171, Feb. 2024, doi: 10.1002/fld.2294.

[61] A. Asghar, L. A. Lund, Z. Shah, N. Vrinceanu, W. Deebani, and M. Shutaywi, "Effect of thermal radiation on three-dimensional magnetized rotating flow of a hybrid nanofluid," *Nanomaterials*, vol. 12, no. 9, p. 1566, Feb. 2022, doi: **10.3390/nano12091566**

[62] M. G. Reddy and K. V. Reddy, "Influence of Joule heating on MHD peristaltic flow of a nanofluid with compliant walls," *Procedia Engineering*, vol. 127, pp. 1002-1009, 2015, doi: 10.1016/j.proeng.2015.11.449.

[63] X. Xuan, D. Sinton, and D. Li, "Thermal end effects on electroosmotic flow in a capillary," *International Journal of Heat and Mass Transfer*, vol. 47, no. 14-16, pp. 3145-3157, Jul. 2004, doi: 10.1016/j.ijheatmasstransfer.2004.02.023.

[64] G. Y. Tang, C. Yang, J. C. Chai, and H. Q. Gong, "Joule heating effect on electroosmotic flow and mass species transport in a microcapillary," *International Journal of Heat and*

Mass Transfer, vol. 47, no. 2, pp. 215-227, Jan. 2004, doi: 10.1016/j.ijheatmasstransfer.2003.07.006.

[65] B. Kates and C. L. Ren, "Study of Joule heating effects on temperature gradient in diverging microchannels for isoelectric focusing applications," *Electrophoresis*, vol. 27, no. 10, pp. 1967-1976, May 2006, doi: 10.1002/elps.200500784.

[66] M. Sajid, S. A. Iqbal, M. Naveed, and Z. Abbas, "Joule heating and magnetohydrodynamic effects on ferrofluid (Fe_3O_4) flow in a semi-porous curved channel," *Journal of Molecular Liquids*, vol. 222, pp. 1115-1120, Oct. 2016, doi: 10.1016/j.molliq.2016.08.001.

[67] S. S. Ghadikolaei, M. Yassari, H. Sadeghi, K. Hosseinzadeh, and D. D. Ganji, "Investigation on thermophysical properties of TiO_2–Cu/H_2O hybrid nanofluid transport dependent on shape factor in MHD stagnation point flow," *Powder Technology*, vol. 322, pp. 428-438, Oct. 2017, doi: 10.1016/j.powtec.2017.09.006.

[68] W. F. Xia, M. U. Hafeez, M. I. Khan, N. A. Shah, and J. D. Chung, "Entropy optimized dissipative flow of hybrid nanofluid in the presence of non-linear thermal radiation and Joule heating," *Scientific Reports*, vol. 11, no. 1, p. 16067, Aug. 2021, doi: 10.1038/s41598-021-95604-4.

[69] B. Mahanthesh, S. A. Shehzad, T. Ambreen, and S. U. Khan, "Significance of Joule heating and viscous heating on heat transport of MoS2–Ag hybrid nanofluid past an isothermal wedge," *Journal of Thermal Analysis and Calorimetry*, vol. 143, pp. 1221-1229, Mar. 2021, doi: 10.1007/s10973-020-09578-y.

[70] N. S. Khashi'ie, N. M. Arifin, R. Nazar, E. H. Hafidzuddin, N. Wahi, and I. Pop, "Magnetohydrodynamics (MHD) axisymmetric flow and heat transfer of a hybrid nanofluid past a radially permeable stretching/shrinking sheet with Joule heating," *Chinese Journal of Physics*, vol. 64, pp. 251-263, Apr. 2020, doi: 10.1016/j.cjph.2019.11.008

[71] N. S. Khashi'ie, N. M. Arifin, I. Pop, and N. S. Wahid, "Flow and heat transfer of hybrid nanofluid over a permeable shrinking cylinder with Joule heating: A comparative analysis," *Alexandria Engineering Journal*, vol. 59, no. 3, pp. 1787-1798, 2020.

[72] U. Yashkun, K. Zaimi, A. Ishak, I. Pop, and R. Sidaoui, "Hybrid nanofluid flow through an exponentially stretching/shrinking sheet with mixed convection and Joule heating," *International Journal of Numerical Methods for Heat & Fluid Flow*, vol. 31, no. 6, pp. 1930-1950, 2021.

[73] Y. Y. Teh and A. Ashgar, "Three dimensional MHD hybrid nanofluid Flow with rotating stretching/shrinking sheet and Joule heating," *CFD Letters*, vol. 13, no. 8, pp. 1-19, Aug. 2021, doi: 10.37934/cfdl.13.8.119.

[74] N. S. Khashi'ie, N. M. Arifin, and I. Pop, "Magnetohydrodynamics (MHD) boundary layer flow of hybrid nanofluid over a moving plate with Joule heating," *Alexandria Engineering Journal*, vol. 61, no. 3, pp. 1938-1945, Mar. 2022, doi: 10.1016/j.aej.2021.07.032.

[75] K. Ramesh, A. S. Warke, K. Kotecha, and K. Vajravelu, "Numerical and artificial neural network modelling of magnetorheological radiative hybrid nanofluid flow with Joule heating effects," *Journal of Magnetism and Magnetic Materials*, vol. 570, p. 170552, Mar. 2023, doi: 10.1016/j.jmmm.2023.170552.

[76] L. A. Lund, A. Asghar, G. Rasool, and U. Yashkun, "Magnetized Casson SA-hybrid nanofluid flow over a permeable moving surface with thermal radiation and Joule heating effect," *Case Studies in Thermal Engineering*, vol. 50, p. 103510, Oct. 2023, doi: 10.1016/j.csite.2023.103510.

[77] R. Razzaq, M. N. Abrar, S. Sagheer, and U. Farooq, "Non-similar investigation of magnetohydrodynamics hybrid nanofluid flow over a porous medium with Joule heating and radiative effects," *Chaos, Solitons & Fractals*, vol. 189, p. 115700, Dec. 2024, doi: 10.1016/j.chaos.2024.115700.

[78] S. Mishra, K. Swain, and R. Dalai, "Joule heating and viscous dissipation effects on heat transfer of hybrid nanofluids with thermal slip," *Iranian Journal of Science and Technology, Transactions of Mechanical Engineering*, vol. 48, no. 2, pp. 531-539, Jun. 2024, doi: 10.1007/s40997-023-00681-7.

[79] H. Gul, M. Ayaz, A. Rashid, A. Ullah, T. K. Ibrahim, E. A. Ismail, and F. A. Awwad, "Chemically reactive and mixed convective hybrid nanofluid flow between two parallel rotating disks with Joule heating: A thermal computational study," *Proceedings of the Institution of Mechanical Engineers, Part N: Journal of Nanomaterials, Nanoengineering and Nanosystems*, vol. 23977914241259338, Jul. 2024, doi: 10.1177/23977914241259338.

[80] H. A. Nabwey, A. M. A. EL-Hakiem, W. A. Khan, Z. M. Abdelrahman, A. M. Rashad, and M. A. Hawsah, "Magnetic Williamson hybrid nanofluid flow around an inclined stretching cylinder with Joule heating in a porous medium," *Chemical Engineering Journal Advances*, vol. 18, p. 100604, May 2024, doi: 10.1016/j.ceja.2024.100604.

[81] D. R. Dowling, P. K. Kundu, and I. M. Cohen, *Fluid Mechanics*, 6th ed., Germany: Elsevier Science, 2012.

[82] P. J. Pritchard, R. W. Fox, and A. T. McDonald, *Introduction to Fluid Mechanics*, John Wiley & Sons, 2010.

[83] P. J. Pritchard, R. W. Fox, and A. T. McDonald, *Introduction to Fluid Mechanics*, John Wiley & Sons, 2010.

[84] F. Durst and I. Arnold, *Fluid mechanics: an introduction to the theory of fluid flows*, vol. 675. Berlin: Springer, 2008.

[85] N. S. Wahid, N. M. Arifin, N. S. Khashi'ie, and I. Pop, "Mixed convection MHD hybrid nanofluid over a shrinking permeable inclined plate with thermal radiation effect," *Alexandria Engineering Journal*, vol. 66, pp. 769-783, Mar. 2023, doi: 10.1016/j.aej.2022.10.075.

[86] S. Alabdulhadi, I. Waini, S. E. Ahmed, and A. Ishak, "Hybrid nanofluid flow and heat transfer past an inclined surface," *Mathematics*, vol. 9, no. 24, p. 3176, Dec. 2021, doi: 10.3390/math9243176.

[87] N. S. Anuar, N. Bachok, and I. Pop, "Influence of buoyancy force on Ag-MgO/water hybrid nanofluid flow in an inclined permeable stretching/shrinking sheet," *International Communications in Heat and Mass Transfer*, vol. 123, p. 105236, Apr. 2021, doi: 10.1016/j.icheatmasstransfer.2021.105236.

[88] A.V. Roşca and I. Pop, "Flow and heat transfer over a vertical permeable stretching/shrinking sheet with a second order slip," *International Journal of Heat and Mass Transfer*, vol. 60, pp. 355-364, May 2013, doi: 10.1016/j.ijheatmasstransfer.2012.12.028.

[89] B.Takabi and S. Salehi, "Augmentation of the heat transfer performance of a sinusoidal corrugated enclosure by employing hybrid nanofluid," *Advances in Mechanical Engineering*, vol. 6, p. 147059, Jan. 2014, doi: 10.1155/2014/147059.

[90] H. F. Oztop and E. Abu-Nada, "Numerical study of natural convection in partially heated rectangular enclosures filled with nanofluids," *International Journal of Heat and Fluid Flow*, vol. 29, no. 5, pp. 1326-1336, Oct. 2008, doi: 10.1016/j.ijheatfluidflow.2008.04.009.